

Scientific Advisory Board

Ayşegül Akgün,

Ege University, Medical School, Department of Nuclear Medicine, İzmir, Turkey

Esma Akin,

The George Washington University, Medical School, Department of Diagnostic Radiology, Washington DC, USA

Claudine Als,

Hopitaux Robert Schuman Zitha Klinik, Médecine Nucléaire, Luxembourg

Vera Artiko,

Clinical Center of Serbia, Center for Nuclear Medicine, Belgrade, Serbia

Nuri Arslan,

Helat Sciences University, Gülhane Medical School, Gülhane Training and Research Hospital, Clinic of Nuclear Medicine, Ankara, Turkey

Marika Bajc,

Lund University Hospital, Clinic of Clinical Physiology, Lund, Sweden

Lorenzo Biassoni,

Great Ormond Street Hospital for Children NHS Foundation Trust, Department of Radiology, London, United Kingdom

Hans Jürgen Biersack,

University of Bonn, Department of Nuclear Medicine, Clinic of Radiology, Bonn, Germany

M. Donald Blafox,

Albert Einstein College of Medicine, Department of Radiology, Division of Nuclear Medicine, New York, USA.

Patrick Bourguet,

Centre Eugène Marquis, Department of Nuclear Medicine, Clinic of Radiology, Rennes, France

A. Cahid Civelek,

NIH Clinical Center, Division of Nuclear Medicine, Bethesda, USA

Arturo Chiti,

Humanitas University, Department of Biomedical Sciences; Humanitas Clinical and Research Center, Clinic of Nuclear Medicine, Milan, Italy

Josep Martin Comin,

Hospital Universitari de Bellvitge, Department of Nuclear Medicine, Barcelona, Spain

Alberto Cuocolo,

University of Naples Federico II, Department of Advanced Biomedical Sciences, Napoli, Italy

Tevfik Fikret Çermik,

Health Sciences University, İstanbul Training and Research Hospital, Clinic of Nuclear Medicine, İstanbul, Turkey

Angelika Bischof Delaloye,

University Hospital of Lausanne, Department of Radiology, Lausanne, Switzerland

Mustafa Demir,

İstanbul University, Cerrahpaşa Medical School, Department of Nuclear Medicine, İstanbul, Turkey

Hakan Demir,

Kocaeli University Medical School, Department of Nuclear Medicine, Kocaeli, Turkey

Peter Josef Ell,

University College Hospital, Institute of Nuclear Medicine, London, United Kingdom

Tanju Yusuf Erdil,

Marmara University, Pendik Training and Research Hospital, Clinic of Nuclear Medicine, İstanbul, Turkey

Türkan Ertay,

Dokuz Eylül University, Medical School, Department of Nuclear Medicine, İzmir, Turkey

Jure Feticich,

University Medical Centre Ljubljana, Department for Nuclear Medicine, Ljubljana, Slovenia

Christiane Franzius,

Klinikum Bremen Mitte Center, Center for Modern Diagnostics, Bremen, Germany

Lars Friberg,

University of Copenhagen Bispebjerg Hospital, Department of Nuclear Medicine, Copenhagen, Denmark

Jørgen Frøkiær,

Aarhus University Hospital, Clinic of Nuclear Medicine and PET, Aarhus, Denmark

■ The Owner on Behalf of Turkish Society of Nuclear Medicine

Prof. Gamze Çapa Kaya, MD.

Dokuz Eylül University, Medical School, Department of Nuclear Medicine, İzmir, Turkey

■ Publishing Manager

Prof. Zehra Özcan, MD.

Ege University, Medical School, Department of Nuclear Medicine, İzmir, Turkey

E-mail: zehra.ozcan@yahoo.com

■ Editor in Chief

Prof. Zehra Özcan, MD.

Ege University, Medical School, Department of Nuclear Medicine, İzmir, Turkey

E-mail: zehra.ozcan@yahoo.com

ORCID ID: 0000-0002-6942-4704

■ Associate Editor

Associate Prof. Murat Fani Bozkurt, MD. Hacettepe University, Medical School, Department of Nuclear Medicine, Ankara, Turkey

E-mail: fanibozkurt@gmail.com

ORCID ID: 0000-0003-2016-2624

Prof. Tanju Yusuf Erdil, MD. Marmara University Medical School, Department of Nuclear Medicine, İstanbul, Turkey

E-mail: yerdil@marmara.edu.tr

ORCID ID: 0000-0002-5811-4321

Associate Prof. Nalan Selçuk, MD. Yeditepe University, Medical School, Department of Nuclear Medicine, İstanbul, Turkey

E-mail: nalanselcuk@yeditepe.edu.tr

ORCID ID: 0000-0002-3738-6491

■ Statistics Editors

Prof. Gül Ergör, MD.

Dokuz Eylül University, Medical School, Department of Public Health, İzmir, Turkey

E-mail: gulergor@deu.edu.tr

Prof. Sadettin Kılıçkap, MD.

Hacettepe University, Medical School, Department of Preventive Oncology, Ankara, Turkey

E-mail: skilickap@yahoo.com

■ English Language Editor

Murat Mert Atmaca, MD.

Şanlıurfa, Turkey

Maria Lya Georgosopoulou,

University of Athens, 1st Department of Radiology, Aretaieion Hospital, Radiation Physics Unit, Athens, Greece

Gevorg Gevorgyan,

The National Academy of Sciences of Armenia, H. Buniatian Institute of Biochemistry, Yerevan, Armenia

Seza Güleç,

Florida International University Herbert Wertheim College of Medicine, Departments of Surgery and Nuclear Medicine, Miami, USA

Liselotte Højgaard,

University of Copenhagen, Department of Clinical Physiology, Nuclear Medicine and PET, Rigshospitalet, Copenhagen, Denmark

Ora Israel,

Tel Aviv University Sackler Medical School, Assaf Harofeh Medical Center, Clinic of Otolaryngology-Head and Neck Surgery, Haifa, Israel

Csaba Juhász,

Wayne State University Medical School, Children's Hospital of Michigan, PET Center and Translational Imaging Laboratory, Detroit, USA

Gamze Çapa Kaya,

Dokuz Eylül University, Medical School, Department of Nuclear Medicine, İzmir, Turkey

Metin Kır,

Ankara University, Medical School, Department of Nuclear Medicine, Ankara, Turkey

Irena Dimitrova Kostadinova,

Alexandrovska University Hospital, Clinic of Nuclear Medicine, Sofia, Bulgaria

Lale Kostakoğlu,

The Mount Sinai Hospital, Clinic of Nuclear Medicine, New York, USA

Rakesh Kumar,

All India Institute of Medical Sciences, Department of Nuclear Medicine, New Delhi, India

Georgios S. Limouris,

Athens University, Medical School, Department of Nuclear Medicine, Athens, Greece

Luigi Mansi,

Second University of Naples, Medical School, Department of Nuclear Medicine, Naples, Italy

Yusuf Menda,

University of Iowa Health Care, Carver College of Medicine, Department of Radiology, Iowa City, USA

Vladimir Obradović,

University of Belgrade, Faculty of Organizational Sciences, Department of Human Development Theory, Business Administration, Organizational Studies, Belgrade, Serbia

Yekta Özer,

Hacettepe University, Faculty of Pharmacy, Department of Radiopharmaceutical, Ankara, Turkey

Francesca Pons,

Hospital Clinic, Clinic of Nuclear Medicine, Barcelona, Spain

Monica Rossleigh,

Sydney Children's Hospital, Clinic of Nuclear Medicine, Sydney, Australia

Dragana Sobic Saranovic,

University of Belgrade, Medical School, Departments of Radiology, Oncology and Cardiology, Belgrade, Serbia

Mike Satheke,

University of Pretoria, Steve Biko Academic Hospital, Department of Nuclear Medicine, Pretoria, South Africa

Kerim Sönmezoğlu,

İstanbul University, Cerrahpaşa Medical School, Department of Nuclear Medicine, İstanbul, Turkey

Zsolt Szabo,

The Johns Hopkins Hospital, Divisions of Radiology and Radiological Science, Baltimore, USA

Istvan Szilvasi,

Semmelweis University, Medical School, Department of Nuclear Medicine, Budapest, Hungary

Berna Okudan Tekin,

Ankara Numune Training and Research Hospital, Clinic of Nuclear Medicine, Ankara, Turkey

Mathew L. Thakur,

Thomas Jefferson University, Department of Radiology, Pennsylvania, USA

Bülent Turgut,

Cumhuriyet University, Medical School, Department of Nuclear Medicine, Sivas, Turkey

Turgut Turoğlu,

Marmara University, Medical School, Department of Nuclear Medicine, İstanbul, Turkey

Gülin Uçmak,

Health Sciences University, Ankara Oncology Training and Research Hospital, Clinic of Nuclear Medicine, Ankara, Turkey

Doğangün Yüksel,

Pamukkale University, Medical School, Department of Nuclear Medicine, Denizli, Turkey

Turkish Society of Nuclear Medicine

Cinnah Caddesi Pilot Sokak No: 10/12 Çankaya 06650 Ankara, Turkey Phone: +90 312 441 00 45 Fax: +90 312 441 12 95 Web: www.tsnm.org E-mail: dernekmerkezi@tsnm.org

"Formerly Turkish Journal of Nuclear Medicine"

Reviewing the articles' conformity to the publishing standards of the Journal, typesetting, reviewing and editing the manuscripts and abstracts in English, creating links to source data, and publishing process are realized by Galenos.

**Galenos Publishing House
Owner and Publisher**

Derya Mor
Erkan Mor

Publication Coordinator

Burak Sever

Web Coordinators

Fuat Hocalar
Turgay Akpınar

Graphics Department

Ayda Alaca
Çiğdem Birinci
Gülşah Özgül

Project Coordinators

Duygu Yıldırım
Hatice Sever
Gamze Aksoy
Melike Eren
Saliha Tuğçe Evin

Project Assistants

Pınar Akpınar

Research&Development

Mert Can Köse
Mevlûde Özlem Akgüneş

Finance Coordinator

Sevinç Çakmak

Publisher Contact

Address: Molla Gürani Mah. Kaçamak Sk. No: 21/1

34093 İstanbul, Turkey

Phone: +90 (212) 621 99 25 Fax: +90 (212) 621 99 27

E-mail: info@galenos.com.tr/yayin@galenos.com.tr

Web: www.galenos.com.tr

Publisher Certificate Number: 14521

Publication Date: February 2020

ISSN: 2146-1414 E-ISSN: 2147-1959

International scientific journal published quarterly.



Molecular Imaging and Radionuclide Therapy (formerly Turkish Journal of Nuclear Medicine) is the official publication of Turkish Society of Nuclear Medicine.

Focus and Scope

Molecular Imaging and Radionuclide Therapy (Mol Imaging Radionucl Ther, MIRT) is a double-blind peer-review journal published in English language. It publishes original research articles, invited reviews, editorials, short communications, letters, consensus statements, guidelines and case reports with a literature review on the topic, interesting images in the field of molecular imaging, multimodality imaging, nuclear medicine, radionuclide therapy, radiopharmacy, medical physics, dosimetry and radiobiology. MIRT is published three times a year (February, June, October). Audience: Nuclear medicine physicians, medical physicists, radiopharmaceutical scientists, radiobiologists.

The editorial policies are based on the "Recommendations for the Conduct, Reporting, Editing, and Publication of Scholarly Work in Medical Journals (ICMJE Recommendations)" by the International Committee of Medical Journal Editors (2016, archived at <http://www.icmje.org/>) rules.

Open Access Policy

This journal provides immediate open access to its content on the principle that making research freely available to the public supports a greater global exchange of knowledge.

Open Access Policy is based on rules of Budapest Open Access Initiative (BOAI) (<http://www.budapestopenaccessinitiative.org/>). By "open access" to [peer-reviewed research literature], we mean its free availability on the public internet, permitting any users to read, download, copy, distribute, print, search, or link to the full texts of these articles, crawl them for indexing, pass them as data to software, or use them for any other lawful purpose, without financial, legal, or technical barriers other than those inseparable from gaining access to the internet itself. The only constraint on reproduction and distribution, and the only role for copyright in this domain, should be to give authors control over the integrity of their work and the right to be properly acknowledged and cited.

This journal is licensed under a Creative Commons 3.0 International License.

Permission Requests

Permission required for use any published under CC-BY-NC license with commercial purposes (selling, etc.) to protect copyright owner and author rights). Republication and reproduction of images or tables in any published material should be done with proper citation of source providing authors names; article title; journal title; year (volume) and page of publication; copyright year of the article.

Instructions for Authors

Instructions for authors are published in the journal and on the website <http://mirt.tsnmjournals.org>

Manuscripts can only be submitted electronically through the Journal Agent website (<http://www.journalagent.com/mirt/?plng=eng>) after creating an account. This system allows online submission and review.

All published volumes in full text can be reached free of charge through the website <http://mirt.tsnmjournals.org>

Material Disclaimer

Scientific and legal responsibilities pertaining to the papers belong to the authors. Contents of the manuscripts and accuracy of references are also the author's responsibility. The Turkish Society of Nuclear Medicine, the Editor, the Editorial Board or the publisher do not accept any responsibility for opinions expressed in articles.

Financial expenses of the journal are covered by Turkish Society of Nuclear Medicine.

Correspondence Address

Editor-in-Chief, Prof. Zehra Özcan, MD,

Ege University, Medical School, Department of Nuclear Medicine, İzmir, Turkey

Phone: +90 312 441 00 45

Fax: +90 312 441 12 97

E-mail: editor@tsnmjournals.org

Web page: <http://mirt.tsnmjournals.org>

Publisher Corresponding Address

Galenos Yayınevi Tic. Ltd. Şti.

Address: Molla Gürani Mah. Kaçamak Sk. No: 21/1 34093

Findıkzade, İstanbul, Turkey

Phone: +90 212 621 99 25

Fax: +90 212 621 99 27

E-mail: info@galenos.com.tr

INSTRUCTIONS TO AUTHORS

Molecular Imaging and Radionuclide Therapy (Mol Imaging Radionucl Ther, MIRT) publishes original research articles, short communications, invited reviews, editorials, case reports with a literature review on the topic, interesting images, consensus statements, guidelines, letters in the field of molecular imaging, multimodality imaging, nuclear medicine, radionuclide therapy, radiopharmacy, medical physics, dosimetry and radiobiology. MIRT is published by the Turkish Society of Nuclear Medicine three times a year (February, June, October).

Molecular Imaging and Radionuclide Therapy does not charge any article submission or processing fees.

GENERAL INFORMATION

MIRT commits to rigorous peer review, and stipulates freedom from commercial influence, and promotion of the highest ethical and scientific standards in published articles. Neither the Editor(s) nor the publisher guarantees, warrants or endorses any product or service advertised in this publication. All articles are subject to review by the editors and peer reviewers. If the article is accepted for publication, it may be subjected to editorial revisions to aid clarity and understanding without changing the data presented.

Manuscripts must be written in English and must meet the requirements of the journal. The journal is in compliance with the uniform requirements for manuscripts submitted to biomedical journals published by the International Committee of Medical Journal Editors (NEJM 1997; 336:309-315, updated 2016). Manuscripts that do not meet these requirements will be returned to the author for necessary revision before the review. Authors of manuscripts requiring modifications have a maximum of two months to resubmit the revised text. Manuscripts returned after this deadline will be treated as new submissions.

It is the authors' responsibility to prepare a manuscript that meets ethical criteria. The Journal adheres to the principles set forth in the Helsinki Declaration October 2013 (<https://www.wma.net/policies-post/wma-declaration-of-helsinki-ethical-principles-for-medical-research-involving-human-subjects/>) and holds that all reported research involving "Human beings" conducted in accordance with such principles.

Reports describing data obtained from research conducted in human participants must contain a statement in the MATERIALS AND METHODS section indicating approval by the ethical review board (including the approval number) and affirmation that INFORMED CONSENT was obtained from each participant.

All manuscripts reporting experiments using animals must include a statement in the MATERIALS AND METHODS section giving assurance that all animals have received humane care in compliance with the Guide for the Care and Use of Laboratory Animals (www.nap.edu) and indicating approval by the ethical review board.

If the study should have ethical approval, authors asked to provide ethical approval in order to proceed the review process. If they provide approval, review of the manuscript will continue.

In case report(s) and interesting image(s) a statement regarding the informed consent of the patients should be included in the manuscript and the identity of the patient(s) should be hidden.

Subjects must be identified only by number or letter, not by initials or names. Photographs of patients' faces should be included only if scientifically relevant. Authors must obtain written consent from the patient for use of such photographs. In cases of image media usage that potentially expose patients' identity requires

obtaining permission for publication from the patients or their parents/guardians. If the proposed publication concerns any commercial product, the author must include in the cover letter a statement indicating that the author(s) has (have) no financial or other interest with the product or explaining the nature of any relations (including consultancies) between the author(s) and editor the manufacturer or distributor of the product.

All submissions will be screened by Crossref Similarity Check powered by "iThenticate". Manuscripts with an overall similarity index of greater than 25%, or duplication rate at or higher than 5% with a single source will be returned back to authors.

MANUSCRIPT CATEGORIES

1. Original Articles
2. Short Communications are short descriptions of focused studies with important, but very straightforward results.
3. Reviews address important topics in the field. Authors considering the submission of uninvited reviews should contact the editor in advance to determine if the topic that they propose is of current potential interest to the Journal. Reviews will be considered for publication only if they are written by authors who have at least three published manuscripts in the international peer reviewed journals and these studies should be cited in the review. Otherwise only invited reviews will be considered for peer review from qualified experts in the area.
4. Editorials are usually written by invitation of the editor by the editors on current topics or by the reviewers involved in the evaluation of a submitted manuscript and published concurrently with that manuscript.
5. Case Report and Literature Reviews are descriptions of a case or small number of cases revealing a previously undocumented disease process, a unique unreported manifestation or treatment of a known disease process, unique unreported complications of treatment regimens or novel and important insights into a condition's pathogenesis, presentation, and/or management. The journal's policy is to accept case reports only if it is accompanied by a review of the literature on the related topic. They should include an adequate number of images and figures.
6. Interesting Image
One of the regular parts of Molecular Imaging and Radionuclide Therapy is a section devoted to interesting images. Interesting image(s) should describe case(s) which are unique and include interesting findings adding insights into the interpretation of patient images, a condition's pathogenesis, presentation, and/or management.
7. Consensus Statements or Guidelines may be submitted by professional societies. All such submissions will be subjected to peer review, must be modifiable in response to criticisms, and will be published only if they meet the Journal's usual editorial standards.
8. Letters to the Editor may be submitted in response to work that has been published in the Journal. Letters should be short commentaries related to specific points of agreement or disagreement with the published work.

Note on Prior Publication

Articles are accepted for publication on the condition that they are original, are not under consideration by another journal, or have not been previously published. Direct quotations, tables, or illustrations that have appeared in

INSTRUCTIONS TO AUTHORS

copyrighted material must be accompanied by written permission for their use from the copyright owner and authors. Materials previously published in whole or in part shall not be considered for publication. At the time of submission, authors must report that the manuscript has not been published elsewhere. Abstracts or posters displayed at scientific meetings need not be reported.

MANUSCRIPT SUBMISSION PROCEDURES

MIRT only accepts electronic manuscript submission at the web site <http://www.journalagent.com/mirt/>. After logging on to the website Click the 'online manuscript submission' icon. All corresponding authors should be provided with a password and a username after entering the information required. If you already have an account from a previous submission, enter your username and password to submit a new or revised manuscript. If you have forgotten your username and/or password, please send an e-mail to the editorial office for assistance. After logging on to the article submission system please read carefully the directions of the system to give all needed information and attach the manuscript, tables and figures and additional documents.

All Submissions Must Include:

1. Completed Copyright Assignment & Disclosure of Potential Conflict of Interest Form; This form should be downloaded from the website (provided in the author section), filled in thoroughly and uploaded to the website during the submission.
2. All manuscripts describing data obtained from research conducted in human participants must be accompanied with an approval document by the ethical review board.
3. All manuscripts reporting experiments using animals must include approval document by the animal ethical review board.
4. All submissions must include the authorship contribution form which is signed by all authors.

Authors must complete all online submission forms. If you are unable to successfully upload the files please contact the editorial office by e-mail.

MANUSCRIPT PREPARATION

General Format

The Journal requires that all submissions be submitted according to these guidelines:

- Text should be double spaced with 2.5 cm margins on both sides using 12-point type in Times Roman font.
- All tables and figures must be placed after the text and must be labeled.
- Each section (abstract, text, references, tables, figures) should start on a separate page.
- Manuscripts should be prepared as a word document (*.doc) or rich text format (*.rtf).
- Please make the tables using the table function in Word.
- Abbreviations should be defined in parenthesis where the word is first mentioned and used consistently thereafter.
- Results should be expressed in metric units. Statistical analysis should be done accurately and with precision. Please consult a statistician if necessary.
- Authors' names and institutions should not be included in the manuscript text and should be written only in the title page.

Title Page

The title page should be a separate form from the main text and should include the following:

- Full title (in English and in Turkish). Turkish title will be provided by the editorial office for the authors who are not Turkish speakers.
- Authors' names and institutions.
- Short title of not more than 40 characters for page headings.
- At least three and maximum eight keywords. (in English and in Turkish). Do not use abbreviations in the keywords. Turkish keywords will be provided by the editorial office for the authors who are not Turkish speakers. If you are not a native Turkish speaker, please reenter your English keywords to the area provided for the Turkish keywords. English keywords should be provided from <http://www.nlm.nih.gov/mesh> (Medical Subject Headings) while Turkish keywords should be provided from <http://www.bilimterimleri.com>.
- Word count (excluding abstract, figure legends and references).
- Corresponding author's e-mail and address, telephone and fax numbers.
- Name and address of person to whom reprint requests should be addressed.

Original Articles

Authors are required to state in their manuscripts that ethical approval from an appropriate committee and informed consents of the patients were obtained.

Original Articles should be submitted with a structured abstract of no more than 250 words. All information reported in the abstract must appear in the manuscript. The abstract should not include references. Please use complete sentences for all sections of the abstract. Structured abstract should include background, objective, methods, results and conclusions. Turkish abstract will be provided by the editorial office for the authors who are not Turkish speakers. If you are not a native Turkish speaker, please reenter your English abstract to the area provided for the Turkish abstract.

- Introduction
- Materials and Methods
- Results
- Discussion
- Study Limitations
- Conclusion

May be given for contributors who are not listed as authors, or for grant support of the research.

References should be cited in numerical order (in parentheses) in the text and listed in the same numerical order at the end of the manuscript on a separate page or pages. The author is responsible for the accuracy of references. Examples of the reference style are given below. Further examples will be found in the articles describing the Uniform Requirements for Manuscripts Submitted to Biomedical Journals (Ann Intern Med.1988; 208:258-265, Br Med J. 1988; 296:401-405). The titles of journals should be abbreviated according to the style used in the Index Medicus. Journal Articles and Abstracts: Surnames and initials of author's name, title of the article, journal name, date, volume number, and pages. All authors should be listed regardless of number. The citation of unpublished papers, observations or personal communications is not permitted. Citing an abstract is not recommended. Books: Surnames and initials of author's names, chapter title, editor's name, book title, edition, city, publisher, date and pages.

INSTRUCTIONS TO AUTHORS

Sample References

Journal Article: Sayit E, Söylev M, Çapa G, Durak I, Ada E, Yılmaz M. The role of technetium-99m-HMPAO-labeled WBC scintigraphy in the diagnosis of orbital cellulitis. *Ann Nucl Med* 2001;15:41-44.

Erselcan T, Hasbek Z, Tandogan I, Gumus C, Akkurt I. Modification of Diet in Renal Disease equation in the risk stratification of contrast induced acute kidney injury in hospital inpatients. *Nefrologia* 2009 doi: 10.3265/Nefrologia.2009.29.5.5449.en.full.

Article in a journal published ahead of print: Ludbrook J. Musculo-venous pumps in the human lower limb. *Am Heart J* 2009;00:1-6. (accessed 20 February 2009).

Lang TF, Duryea J. Peripheral Bone Mineral Assessment of the Axial Skeleton: Technical Aspects. In: Orwoll ES, Bliziotes M (eds). *Osteoporosis: Pathophysiology and Clinical Management*. New Jersey, Humana Press Inc, 2003;83-104.

Books: Greenspan A. *Orthopaedic Radiology a Practical Approach*. 3th ed. Philadelphia, Lippincott Williams Wilkins 2000, 295-330.

Website: Smith JR. 'Choosing Your Reference Style', *Online Referencing* 2(3), <http://orj.sagepub.com> (2003, accessed October 2008).

- Tables

Tables must be constructed as simply as possible. Each table must have a concise heading and should be submitted on a separate page. Tables must not simply duplicate the text or figures. Number all tables in the order of their citation in the text. Include a title for each table (a brief phrase, preferably no longer than 10 to 15 words). Include all tables in a single file following the manuscript.

- Figure Legends

Figure legends should be submitted on a separate page and should be clear and informative.

- Figures

Number all figures (graphs, charts, photographs, and illustrations) in the order of their citation in the text. At submission, the following file formats are acceptable: AI, EMF, EPS, JPG, PDF, PPT, PSD, TIF. Figures may be embedded at the end of the manuscript text file or loaded as separate files for submission. All images MUST be at or above intended display size, with the following image resolutions: Line Art 800 dpi, Combination (Line Art + Halftone) 600 dpi, Halftone 300 dpi. Image files also must be cropped as close to the actual image as possible.

Short Communications:

Short communications should be submitted with a structured abstract of no more than 200 words. These manuscripts should be no longer than 2000 words, and include no more than two figures and tables and 20 references. Other rules which the authors are required to prepare and submit their manuscripts are the same as described above for the original articles.

Invited Review Articles:

- Title page (see above)

- Abstract: Maximum 250 words; without structural divisions; in English and in Turkish. Turkish abstract will be provided by the editorial office for the authors who are not Turkish speakers. If you are not a native Turkish speaker, please reenter your English abstract to the area provided for the Turkish abstract.

- Text

- Conclusion

- Acknowledgements (if any)

- References

Editorial:

- Title page (see above)

- Abstract: Maximum 250 words; without structural divisions; in English and in Turkish. Turkish abstract will be provided by the editorial office for the authors who are not Turkish speakers. If you are not a native Turkish speaker, please reenter your English abstract to the area provided for the Turkish abstract.

- Text

- References

Case Report and Literature Review

- Title page (see above)

- Abstract: Approximately 100-150 words; without structural divisions; in English and in Turkish. Turkish abstract will be provided by the editorial office for the authors who are not Turkish speakers. If you are not a native Turkish speaker, please re-enter your English abstract to the area provided for the Turkish abstract.

- Introduction

- Case report

- Literature Review and Discussion

- References

Interesting Image:

No manuscript text is required. Interesting Image submissions must include the following:

Title Page: (see Original article section)

Abstract: Approximately 100-150 words; without structural divisions; in English and in Turkish. Turkish abstract will be provided by the editorial office for the authors who are not Turkish speakers. If you are not a native Turkish speaker, please re-enter your English abstract to the area provided for the Turkish abstract. Image(s): The number of images is left to the discretion of the author. (See Original article section)

Figure Legend: Reference citations should appear in the legends, not in the abstract. Since there is no manuscript text, the legends for illustrations should be prepared in considerable detail but should be no more than 500 words total. The case should be presented and discussed in the Figure legend section.

References: Maximum eight references (see original article section).

Letters to the Editor:

- Title page (see above)

- Short comment to a published work, no longer than 500 words, no figures or tables.

- References no more than five.

Consensus Statements or Guidelines: These manuscripts should typically be no longer than 4000 words and include no more than six figures and tables and 120 references.

Proofs and Reprints

Proofs and a reprint orders are sent to the corresponding author. The author should designate by footnote on the title page of the manuscript the name and

INSTRUCTIONS TO AUTHORS

address of the person to whom reprint requests should be directed. The manuscript when published will become the property of the journal.

Archiving

The editorial office will retain all manuscripts and related documentation (correspondence, reviews, etc.) for 12 months following the date of publication or rejection.

Submission Preparation Checklist

As part of the submission process, authors are required to check off their submission's compliance with all of the following items, and submissions may be returned to authors that do not adhere to these guidelines.

1. The submission has not been previously published, nor is it before another journal for consideration (or an explanation has been provided in Comments to the Editor).
2. The submission file is in Microsoft Word, RTF, or WordPerfect document file format. The text is double-spaced; uses a 12-point font; employs italics, rather than underlining (except with URL addresses); and the location for all illustrations, figures, and tables should be marked within the text at the appropriate points.
3. Where available, URLs for the references will be provided.
4. All authors should be listed in the references, regardless of the number.
5. The text adheres to the stylistic and bibliographic requirements outlined in the Author Guidelines, which is found in About the Journal.
6. English keywords should be provided from [http://www.nlm.nih.gov/mesh\(Medical Subject Headings\)](http://www.nlm.nih.gov/mesh(Medical Subject Headings)), while Turkish keywords should be provided from <http://www.bilimterimleri.com>
7. The title page should be a separate document from the main text and should be uploaded separately.
8. The "Affirmation of Originality and Assignment of Copyright/The Disclosure Form for Potential Conflicts of Interest Form" and Authorship Contribution Form should be downloaded from the website, filled thoroughly and uploaded during the submission of the manuscript.

TO AUTHORS

Copyright Notice

The author(s) hereby affirms that the manuscript submitted is original, that all statement asserted as facts are based on author(s) careful investigation and research for accuracy, that the manuscript does not, in whole or part, infringe any copyright, that it has not been published in total or in part and is not being submitted or considered for publication in total or in part elsewhere. Completed

Copyright Assignment & Affirmation of Originality Form will be uploaded during submission. By signing this form;

1. Each author acknowledges that he/she participated in the work in a substantive way and is prepared to take public responsibility for the work.
2. Each author further affirms that he or she has read and understands the "Ethical Guidelines for Publication of Research".
3. The author(s), in consideration of the acceptance of the manuscript for publication, does hereby assign and transfer to the Molecular Imaging and Radionuclide Therapy all of the rights and interest in and the copyright of the work in its current form and in any form subsequently revised for publication and/or electronic dissemination.

Privacy Statement

The names and email addresses entered in this journal site will be used exclusively for the stated purposes of this journal and will not be made available for any other purpose or to any other party.

Peer Review Process

1. The manuscript is assigned to an editor, who reviews the manuscript and makes an initial decision based on manuscript quality and editorial priorities.
2. For those manuscripts sent for external peer review, the editor assigns at least two reviewers to the manuscript.
3. The reviewers review the manuscript.
4. The editor makes a final decision based on editorial priorities, manuscript quality, and reviewer recommendations.
5. The decision letter is sent to the author.

Contact Address

All correspondence should be directed to the Editorial Office:
Cinnah Caddesi Pilot Sokak No:10/12 06650 Çankaya / Ankara, Turkey
Phone: +90 312 441 00 45
Fax: +90 312 441 12 97
E-mail: info@tsnmjournals.org

Original Articles

- 1** Hepatopulmonary Syndrome with Right-to-left Shunt in Cirrhotic Patients Using Macro-aggregated Albumin Lung Perfusion Scan: Comparison with Contrast Echocardiography and Association with Clinical Data
Sirotik Hastalardaki Sağ-Sol Şant ile ilişkili Hepatopulmoner Sendromun Tanısında Makro-Agregant Albümin Akciğer Perfüzyon Sintigrafisinin Kontrast Ekokardiyografi ile Karşılaştırılması ve Klinik Veriler ile İlişkisi
Zeynab Alipour, Abbas Armin, Soudabeh Mohamadi, Seyed Masoud Tabib, Zahra Azizmohammadi, Ali Gholamrezanezhad, Majid Assadi; Bushehr, Tehran, Los Angeles, Iran, USA
- 7** Esophageal Clearance in Laryngopharyngeal Reflux Disease: Correlation of Reflux Scintigraphy and 24-hour Impedance/pH in a Cohort of Refractory Symptomatic Patients
Laringofarengal Reflü Hastalığında Özofagus Klirensi: Reflü Sintigrafisi ve 24 Saatlik İmpedans ve Ph Monitorizasyonunun Refrakter Semptomatik Hastalarda Korelasyonu
Leticia Burton, Gregory L. Falk, Karl Baumgart, John Beattie, Scott Simpson, Hans Van der Wall; Sydney, Australia
- 17** The Prognostic Value of ¹⁸F-FDG PET/CT and KRAS Mutation in Colorectal Cancers
Kolorektal Kanserlerde ¹⁸F-FDG PET/CT ve KRAS Mutasyonunun Prognostik Değeri
Esra Arslan, Tamer Aksoy, Rıza Umar Gürsu, Nevra Dursun, Ekrem Çakar, Tevfik Fikret Çermik; İstanbul, Turkey
- 25** Metabolic Characteristics and Diagnostic Contribution of ¹⁸F-FDG PET/CT in Gastric Carcinomas
Mide Kanserinin Metabolik Özellikleri ve ¹⁸F-FDG PET / CT'nin Tanısal Katkısı
Esra Arslan, Tamer Aksoy, Cihan Gündoğan, Çiğdem Şen, Selda Yılmaz Tatar, Nevra Dursun, Tevfik Fikret Çermik; İstanbul, Turkey
- #### Interesting Images
- 33** Four Atypical Parathyroid Adenomas Detected by Dual Phase Tc-99m MIBI SPECT
Dört Atipik Paratiroid Adenomunun Dual Faz Tc-99m MIBI SPECT ile Saptanması
Mine Araz, Derya Çayır, Fatma Fulya Köybaşıoğlu, Harun Karabacak, Erman Çakal; Ankara, Turkey
- 37** Amyloidosis Associated Kidney Failure with Gross Hypermetabolic Intra-abdominal Mass
Böbrek Yetmezliği ile Birlikte Dev Hipermetabolik İntraabdominal Kitle Olan Hastada Amiloidosis
Zehra Pınar Koç, Pınar Pelin Özcan, Kenan Turgutalp, Kaan Esen, Tuğba Kara; Mersin, Turkey
- 41** ¹⁸F-NaF PET/CT and Extraordinary Involvement: Non-calcific Brain Involvement in a Prostate Cancer Case
¹⁸F-NaF PET/CT'de Sıra Dışı Tutulumlar: Prostat Kanserli Bir Olguda Kalsifiye Olmayan Beyin Tutulumu
Ulku Korkmaz, Funda Ustun; Edirne, Turkey
- 45** Increased Bone Marrow ¹⁸F-Choline Uptake in a Patient with Hepatocellular Carcinoma and Thalassemia Intermedia
Hepatosellüler Karsinom ve Talasemi Intermedia Tanılı Bir Hastada Artmış Kemik İliği ¹⁸F-Kolin Tutulumu
Luca Filippi; Latina, Italy



Hepatopulmonary Syndrome with Right-to-left Shunt in Cirrhotic Patients Using Macro-Aggregated Albumin Lung Perfusion Scan: Comparison with Contrast Echocardiography and Association with Clinical Data

Sirotik Hastalardaki Sağ-Sol Şant ile İlişkili Hepatopulmoner Sendromun Tanısında Makro-Agregant Albümin Akciğer Perfüzyon Sintigrafisinin Kontrast Ekokardiyografi ile Karşılaştırılması ve Klinik Veriler ile İlişkisi

© Zeynab Alipour¹, © Abbas Armin¹, © Sudabeh Mohamadi², © Seyed Masoud Tabib¹, © Zahra Azizmohammadi³, © Ali Gholamrezanezhad⁴, © Majid Assadi⁵

¹Bushehr University of Medical Sciences, Bushehr Medical Center Hospital, Department of Internal Medicine, Division of Gastroenterology, Bushehr, Iran

²Bushehr University of Medical Sciences, Faculty of Medicine, Department of Community Medicine, Bushehr, Iran

³Shahid Beheshti University of Medical Sciences, Imam Hossein Hospital, Department of Nuclear Medicine, Tehran, Iran

⁴University of Southern California, Keck School of Medicine, Department of Diagnostic Radiology, Los Angeles, USA

⁵Bushehr University of Medical Sciences, Bushehr Medical University Hospital, The Persian Gulf Nuclear Medicine Research Center, Department of Molecular Imaging and Radionuclide Therapy (MIRT), Bushehr, Iran

Abstract

Objectives: The diagnosis of hepatopulmonary syndrome (HPS) which is a common complication in cirrhotic patients is still subject to debate. This study investigated the association of clinical findings with HPS in cirrhotic patients using macro-aggregated albumin lung perfusion scan (^{99m}Tc-MAA lung scintigraphy). In addition, comparison between ^{99m}Tc-MAA lung scintigraphy and contrast echocardiography (CEE) in detection of HPS was also performed.

Methods: In this study, 27 patients with cirrhosis underwent ^{99m}Tc-MAA lung scintigraphy and contrast echocardiography comparison CEE and the frequency of HPS was assessed in them and also was compared across the other variables.

Results: The ^{99m}Tc-MAA lung scintigraphy showed HPS in 13 patients (48.1%) while CEE demonstrated HPS in 5 patients with cirrhosis (18.51%). HPS was mild in 40.74% (11/27) of the patients, and severe in only 2 patients. There was no relationship between gender, disease duration, having diagnosis of disease previously, pulmonary symptoms and Child-Pugh score variations and HPS (p>0.05). Comparison of hemodynamic indices, arterial blood gas analysis and laboratory indices between patients with and without HPS was also non-significant (p value >0.05). Among coagulation factors assessed in cirrhotic patients, we found only significant correlation between HPS and prothrombin time (p<0.05).

Conclusion: HPS, particularly its mild form, is noted in a great number of patients with cirrhosis using ^{99m}Tc-MAA lung scintigraphy. Because of its technical ease, and possibility to obtain objective quantitative information, ^{99m}Tc-MAA lung scintigraphy can be complementary to other diagnostic methods in the evaluation of HPS assessment, although additional studies are needed.

Keywords: Hepatopulmonary syndrome, cirrhosis, macro-aggregated albumin lung perfusion scan, contrast echocardiography

Öz

Amaç: Sirotik hastalarda sık görülen bir komplikasyon olan hepatopulmoner sendromun (HPS) tanısı halen tartışmaya açıktır. Bu çalışmada, makroagregat albümin akciğer perfüzyon sintigrafisi (^{99m}Tc-MAA akciğer sintigrafisi) kullanılarak sirotik hastalarda klinik bulgularla HPS'nin ilişkisi araştırılmıştır. Ayrıca, HPS'nin saptanmasında ^{99m}Tc-MAA akciğer sintigrafisi ile kontrast ekokardiyografi (KE) karşılaştırılmıştır.

Address for Correspondence: Majid Assadi MD, Bushehr University of Medical Sciences, Bushehr Medical University Hospital, The Persian Gulf Nuclear Medicine Research Center, Clinic of Molecular Imaging and Radionuclide Therapy (MIRT), Bushehr, Iran

Phone: +987712541828 **E-mail:** assadipoya@yahoo.com **ORCID ID:** orcid.org/0000-0003-3862-9472 **Received:** 31.03.2019 **Accepted:** 14.11.2019

©Copyright 2020 by Turkish Society of Nuclear Medicine
Molecular Imaging and Radionuclide Therapy published by Galenos Yayınevi.

Yöntem: Bu çalışmada, sirozlu 27 hastada ^{99m}Tc -MAA akciğer sintigrafisi ve KE karşılaştırıldı ve HPS sıklığı değerlendirildi. Ayrıca HPS'nin sıklığı ile diğer değişkenler arasındaki ilişki araştırıldı.

Bulgular: ^{99m}Tc -MAA akciğer sintigrafisi 13 sirozlu hastada (%48,1) HPS'nin varlığını gösterirken, KE 5 sirozlu hastada (%18,51) gösterdi. HPS hastaların %40,74'inde (11/27) hafif, sadece 2 hastada şiddetliydi. Cinsiyet, hastalık süresi, hastalık geçmişi, akciğer semptomları ve Child skoru ile HPS arasında herhangi bir ilişki yoktu ($p>0,05$). Hemodinamik indeksler, arteriyel kan gazı analizi ve laboratuvar indeksleri açısından HPS'li hastalar ve HPS'li olmayan hastalar arasında fark görülmedi ($p>0,05$). Sirotik hastalarda değerlendirilen koagülasyon faktörleri arasında, sadece HPS ve protrombin zamanı arasında anlamlı bir korelasyon bulundu ($p<0,05$).

Sonuç: ^{99m}Tc -MAA akciğer sintigrafisi ile çok sayıda sirozlu hastada HPS'nin özellikle hafif formu saptandı. Teknik kolaylığı ve objektif kantitatif bilgi edinme olasılığı nedeniyle, ^{99m}Tc -MAA akciğer sintigrafisi HPS'nin değerlendirilmesinde diğer yöntemlerini tamamlayıcı olabilir, ancak ek çalışmalara ihtiyaç vardır.

Anahtar kelimeler: Hepatopulmoner sendrom, siroz, makroagregat albümin akciğer perfüzyon sintigrafisi, kontrast ekokardiyografisi

Introduction

Cirrhosis is a pathologic process in which normal liver structure is substituted by scar tissue. Cirrhotic patients are vulnerable to many side effects that reduce their lifetime. One of these side effects is hypoxia resulting from hepatopulmonary syndrome (HPS) (1,2,3).

HPS, which can influence patient's prognosis, is described by a clinical triad entailing being of late stage liver disease, gas exchange disorders, eventually leading to hypoxemia and the occurrence of intrapulmonary vascular dilatations (IPVD), without being of intrinsic pulmonary disease (4).

Many conditions can influence the gas exchange in lungs (5). Ascites, pleural effusion, hepatomegaly and basal lung lobes atelectasis are the most common identified causes and can disturb oxygen exchange in a restrictive manner. On the other hand, some side effects of cirrhosis such as HPS or portopulmonary hypertension may not be diagnosed by physical examination, pulmonary imaging modalities or pulmonary function tests (6).

In addition, increased mortality rate of cirrhotic patients due to HPS is reported (6).

The only method to cure this status is liver transplantation, so, early diagnosis of this status carries important clinically significance (6).

The term HPS was coined by Kennedy and Knudson in 1977 (7,8). Signs of HPS are dyspnea, platypnea and orthodeoxia and HPS is diagnosed with a clinical triad including chronic liver disease, increased alveolar-arterial gradient of O₂ [$p(A-a)O_2$] ≥ 15 mmHg (≥ 20 mmHg for patients over 64 years) and the presence of intrapulmonary right to left shunt (9,10,11).

The prevalence of this syndrome has not been completely understood because figures depend on the manner used for the identification and the characteristics of the population investigated (12,13).

The intrapulmonary arteriovenous shunt can be diagnosed by contrast enhanced echocardiography (CEE) and ^{99m}Tc -labelled macro aggregated albumin scintigraphy (^{99m}Tc -MAA).

Contrast CEE is considered the standard technique (14) which in this method, a liquid with bubbles is injected into a peripheral vein and the liquid entering the left cavities is observed with saline bubble test.

In ^{99m}Tc -labelled macro aggregated albumin scintigraphy (^{99m}Tc -MAA), ^{99m}Tc labelled albumin particles are injected into a peripheral vein and then are capable to reach extra pulmonary sites like brain or kidneys parenchyma due to the presence of IPVD and intra pulmonary arteriovenous shunt (14,15,16) however, there is a doubt that in view of predisposing vasoconstriction in brain and kidney of cirrhotic patients, ^{99m}Tc -MAA scan may not be reliable in this setting (17).

In current study, we evaluated cirrhotic patients to find the frequency of HPS in these patients with assistance of clinical and paraclinical methods.

Materials and Methods

In this study, we evaluated 27 cirrhotic patients referred to the Department of Nuclear Medicine of a University Affiliated Hospital between 2017-2018.

Patients were divided into three groups based on Child-pugh and Meld scoring systems. The Child-pugh score employs five clinical measures (including total serum bilirubin, serum albumin, prothrombin time (PTT), ascites and hepatic encephalopathy) of liver disease. Each measure is scored 1-3, with 3 indicating most severe derangement. These three groups were as follow: group A (5-7), group B (8-9) and group C (10-15).

The Meld score is also calculated using a mathematical formula that is based on three laboratory results including total serum bilirubin, INR and SCR.

MELD formula= $3.78 \times \ln [\text{serum bilirubin (mg/dL)}] + 11.2 \times \ln (\text{INR}) + 9.57 \times \ln [\text{serum creatinine (mg/dL)}] + 6.43$.

Furthermore, we collected each patient's clinical history of dyspnea and other pulmonary symptoms and we accepted the presence of intrapulmonary arterio venous shunt >6% as abnormal finding and used it for HPS diagnosis.

During the admission time, lung perfusion scintigraphy, echocardiography or spirometry, and laboratory tests including arterial blood gas (ABG), complete blood count and liver function tests were carried out and above mentioned results were compared with patient's age, arterio venous shunt presence and severity of pulmonary failure. As mentioned above, HPS abundance was calculated in these cirrhotic patients.

The radionuclide study was carried out by injecting 1-4 mCi ^{99m}Tc -MAA intravenously. In cases of intrapulmonary shunting as in HPS, some amount of radiotracers goes through the lungs into the systemic circulation like brain, kidneys and thyroid along with the lung. The pulmonary shunt percent is calculated by applying the geometric mean (GM) of brain and lung counts in the formula:

$(\text{GM brain}) / (\text{GM brain} + \text{GM lung}) * 100$ (normal <6%)

Contrast enhanced bubble CEE was done by agitating a small amount of air with saline to produce bubbles using a three-way stopcock, when administered into the venous circulation. Appearing of even one bubble in the left side of the heart has been considered as a criterion of right-to left shunting.

Moreover, all eligible participants signed an inform consent. This study complies with the Declaration of Helsinki, and it was confirmed by the Ethics Committee of Bushehr University of Medical Sciences.

Statistical Analysis

Categorical variables were analyzed using chi-square test and continuous variables using Student's t-test. Categorical values were expressed as percentage and continuous values were expressed as mean value \pm standard deviation. Linear regression analysis was used to determine whether there was a correlation between above mentioned findings and HPS. P value <0.05 was considered as statically significant for all statistical tests. Statistical analysis was performed with the use of the SPSS statistical package (version 24).

Results

Our studied cirrhotic population consisted of 18 males (66.6%) and 9 females (33.3%), with mean age of

52.3 \pm 17.28 years. From this population, 13 patients (10 males and 3 females) had HPS due to the results of ^{99m}Tc -MAA scintigraphy, therefore, 48.15% had HPS and 51.85% did not have HPS. HPS was mild in 40.74% (11/27) of the patients, and severe in only 2 patients.

In comparison, CEE demonstrated five positive shunts (18.51%) and the remaining did not have shunt.

The average age of the patients with HPS was 45.5 \pm 13.43 years and it was 58.7 \pm 18.46 years in the patients without HPS. There was no statistically significant difference between groups in terms of age ($p > 0.05$).

There was no relationship between gender, disease duration, having diagnosis of disease previously, pulmonary symptoms (dyspnea, ortodeoxia, plathypnea and orthopnea) Child-pugh score variations and HPS ($p > 0.05$).

Comparison of hemodynamic indices, ABG analysis and laboratory indices between patients with and without HPS was also non-significant ($p > 0.05$) (Table 2,3,4).

Among coagulation factors assessed in cirrhotic patients, we found only significant ($p < 0.05$) correlation between HPS and PTT (Table 5).

Two images of positive and negative scans for HPS are illustrated in Figure 1 and 2.

Table 1. Comparison between gender, disease duration, having diagnosis of disease previously, pulmonary symptoms (dyspnea, ortodeoxia, plathypnea and orthopnea) and child score variations in two groups of patients with and without hepatopulmonary syndrome

Variation		HPS ⁺	HPS ⁻	p value
Gender	Male	44.4%	55.6%	0.695
	Female	55.6%	44.4%	
Disease duration	<1 year	50%	50%	1.000
	>1 year	44.4%	55.6%	
Having diagnosis of disease previously	Yes	41.2%	58.8%	0.440
	No	60%	40%	
Dyspnea	Yes	43.5%	56.5%	0.326
	No	75%	25%	
Orthodeoxia	Yes	50%	50%	1.000
	No	-	100%	
Plathypnea	Yes	50%	50%	1.000
	No	-	100%	
Orthopnea	Yes	45.8%	54.2%	0.596
	No	66.7%	33.3%	
Child-pugh score	A	35.7%	64.3%	0.180
	B,C	61.5%	38.5%	

Table 2. Comparison of hemodynamic indices between patients with and without hepatopulmonary syndrome

Variable	HPS	Average	SD	p value
SBP mmHg	Yes	124.6	26.8	0.57
	No	120	14.3	
DBP mmHg	Yes	73.9	16.8	0.70
	No	76	11.3	
PR bpm	Yes	78	11.3	0.26
	No	87.8	10.4	
RR bpm	Yes	15.9	1.65	0.33
	No	16.7	2.43	

SBP: Systolic blood pressure, DBP: Diastolic blood pressure, PR: Pulse rate, RR: Respiratory rate

Table 3. Comparison of arterial blood gas analysis between patients with and without hepatopulmonary syndrome

Variable	HPS	Average	SD	p value
O ₂ Sat (%)	Yes	96.5	1.3	0.96
	No	96.5	2.7	
PO ₂ mmHg	Yes	81.5	2.3	0.49
	No	80.7	3.2	
PH	Yes	7.37	0.038	0.47
	No	7.38	0.025	
PCO ₂ mmHg	Yes	45.6	6.3	0.22
	No	42.6	4.8	
HCO ₃	Yes	26.6	5.2	0.38
	No	25.1	2.5	

Discussion

HPS is one of the most important problems in cirrhotic patients. In this study, 13 (48.1%) cases with established HPS were detected. Moreover, there was significant correlation between PTT and HPS in current study ($p < 0.05$).

Surasi et al. (14) concluded that the ^{99m}Tc-MAA lung perfusion scintigraphy was helpful and could diagnose HPS in cirrhotic patients by finding the intrapulmonary arteriovenous shunt.

El-Shabrawi et al. (15) compared the findings of contrast CEE and ^{99m}Tc-MAA lung perfusion scintigraphy in 40 children with chronic liver disease and showed that lung perfusion scintigraphy with ^{99m}Tc-MAA was more sensitive than contrast CEE for determining intrapulmonary arteriovenous shunt in the patients with chronic hepatic failure. The result of that study was the same as with current study, in which a statistically significant difference between these two methods was noted.

Table 4. Comparison of laboratory indices between patients with and without hepatopulmonary syndrome

Variable	HPS	Average	SD	p value
Hb g/dl	Yes	11.2	2.7	0.86
	No	11.2	2.3	
Albūmin g/L	Yes	3.5	0.7	0.98
	No	3.5	0.6	
AST U/l	Yes	49.5	32.4	0.64
	No	57.5	53.1	
ALT U/l	Yes	39.8	36.2	0.92
	No	41.3	37.2	
ALP U/l	Yes	267.1	92.2	0.72
	No	295.4	193.7	
Na ⁺ mEq/L	Yes	138.5	2.4	1.00
	No	138.5	2.3	
Bilirubin mg/dL	Yes	2.2	0.8	0.76
	No	1.9	0.5	
Serum creatinine mg/dL	Yes	1.1	0.5	0.63
	No	1.04	0.3	

HPS: Hepatopulmonary syndrome, Hb: Hemoglobin, SD: Standard deviation, AST: Aspartat aminotransferaz, Alb: Albumin

Table 5. Comparison of coagulation factors between patients with and without hepatopulmonary syndrome

Variable	HPS	Average	SD	P value
Platelet count	Yes	117.4	64.5	0.77
	No	124.7	65.1	
PT seconds	Yes	13.2	1.3	0.09
	No	16.5	6.8	
PTT seconds	Yes	33.8	12.8	0.04
	No	53.2	28.1	
INR	Yes	1.2	0.2	0.07
	No	1.5	0.5	

PTT: Partial thromboplastin time, PT: Prothrombin time, INR: International normalized ratio, SD: Standard deviation, SD: Standard deviation

In the current report seven patients (48.15%) demonstrated right to left intrapulmonary shunts shown by lung perfusion scintigraphy. HPS was mild in 40.74% (11/27) of the patients, and severe in only 2 patients. This may be most likely due to the point that perfusion scintigraphy is able to identify trivial shunts using quantitative analysis, so CEE might fail to detect small shunts. Furthermore, CEE is also operator reliant.

In contrary, there are a few reports showing that CEE is more sensitive than lung perfusion scintigraphy for the diagnosis of

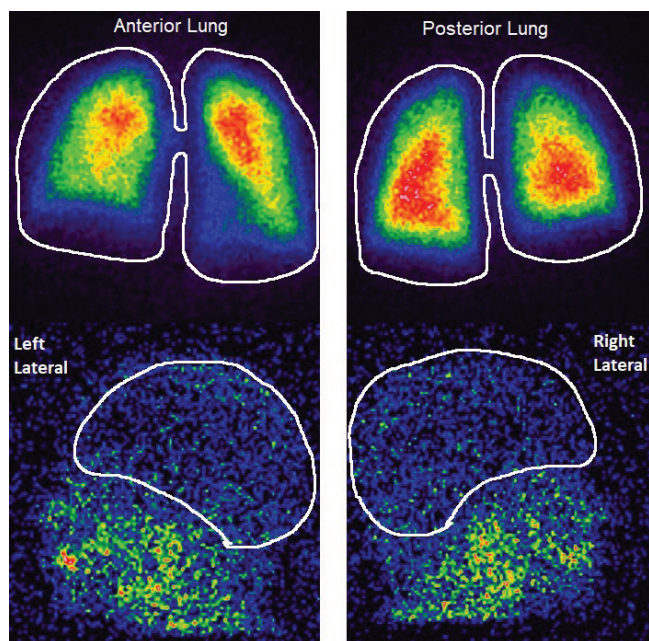


Figure 1. Normal scanning: ^{99m}Tc -MAA is only accumulated in the lungs (shunt=1%)

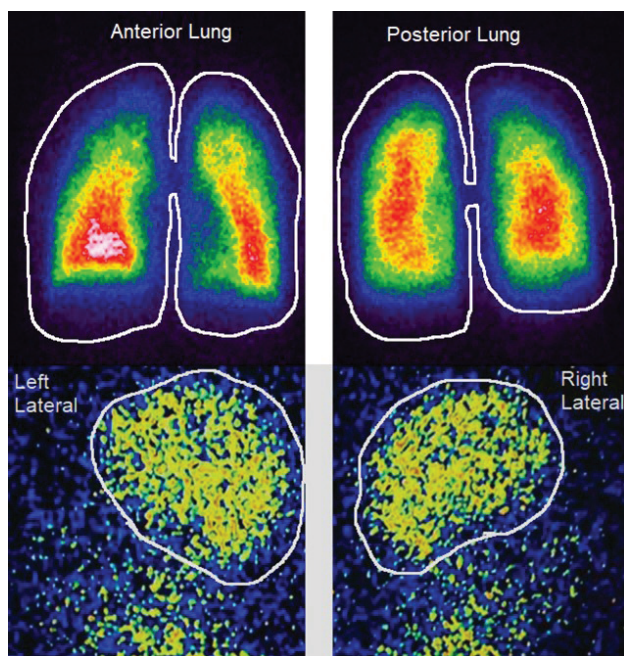


Figure 2. Hepatopulmonary syndrome: ^{99m}Tc -MAA is accumulated in the lungs, and brain (shunt=26%)

intrapulmonary shunting (9). In addition, CEE can be done as a part of standard echocardiographic screening for pulmonary hypertension and the European Respiratory Society Task Force on Pulmonary-hepatic vascular diseases has advised CEE as the first step method in screening of HPS (8).

In another study done by Grimon et al. (17), 135 children with chronic hepatic failure were evaluated and they delineated that ^{99m}Tc -MAA scintigraphy was more accurate than ABG analysis in detection of intrapulmonary arteriovenous shunt. Although we found the same result, there was no correlation between ABG indices and HPS.

Likewise, Fatemi et al. (18) worked on 54 cirrhotic patients and showed that 10 patients had the clinical criteria of HPS and 7 patients had sub-clinical criteria of HPS. Their rate was less than our rate of 48%. In their study, the most prevalent clinical signs were dyspnea and cyanosis. Dyspnea had high sensitivity and achropachy had high specificity in cirrhotic patients with HPS.

On the other hand, $\text{PO}_2 < 70$ and alveolar-arterial gradient had the highest sensitivity in this era (19) however, we did not find any relationship between these laboratory indices and HPS.

Fragaki et al. (20) assessed HPS in cirrhotic patients using ^{99m}Tc -MAA lung scintigraphy and correlated the results with clinical data. In total, 94 out of 102 included patients had complete scintigraphic data. Overall, 24 (26%) patients had HPS and 95.8% of them had mild-to-moderate HPS. There was no significant difference in terms of HPS between decompensated (24.6%) and compensated cirrhosis (27.3%). In the multivariate analysis, only the quantitative index was noteworthy for the identification of HPS. They concluded that mild-to moderate HPS had no substantial effect on survival of cirrhotic patients. Also in our study, most of the detected HPS was mild (40.74%).

In contrast to our finding, Grilo et al. (21) who assessed ^{99m}Tc -MAA lung perfusion scan in 115 cirrhotic subjects with HPS candidates for liver transplantation, demonstrated that the ^{99m}Tc -MAA had a low sensitivity for the diagnosis of HPS.

However, it should be noted that ^{99m}Tc -MAA lung scintigraphy as compared with CEE, has disadvantages of underestimation of intrapulmonary shunt fraction in advanced liver disease because of renal and cerebral arterial vasoconstriction occurring in patients with cirrhosis which increases with progression of the liver disease (16). In addition, ^{99m}Tc -MAA lung scintigraphy depicts total value of right to left shunt, which may be due to cardiac problem in origin, so performance of CEE can assess one-stop shop.

This study suffered from some demerits; the most important ones were a small overall sample of participating patients, and lack of follow up to assess the survival analysis. Therefore, further research necessitates a larger number of patients split into more categories of HPS to find the best clinical outcomes.

Conclusion

HPS, particularly its mild form is noted in a great number of patients with cirrhosis using ^{99m}Tc -MAA lung scintigraphy. Because of its technical ease, and possibility to obtain objective quantitative information, ^{99m}Tc -MAA lung scintigraphy can be complementary to other diagnostic methods in the evaluation of HPS assessment, although additional studies are needed.

Acknowledgments

This study was the postgraduate thesis of Dr. Abbas Armin, and was supported by the Bushehr University of Medical Sciences. We thank to colleagues at our institutes for helping in data gathering.

Ethics

Ethics Committee Approval: The study was approved by the Institutional Ethics Committee of Bushehr University of Medical Sciences (registration no: 123).

Informed Consent: Consent forms were filled out by all participants.

Peer-review: Externally and internally peer-reviewed.

Authorship Contributions

Surgical and Medical Practices: Z.A., A.A., S.M.T., M.A., Concept: Z.A., M.A., Design: Z.A., A.A., S.M.T., M.A., S.M., Data Collection or Processing: Z.A., A.A., S.M.T., Analysis or Interpretation: S.M., M.A., A.G., Literature Search: Z.A., S.M., A.A., Writing: Z.A., A.G., M.A.

Conflict of Interest: No conflict of interest was declared by the authors.

Financial Disclosure: This investigation was supported by the deputy of research at Bushehr University of Medical Sciences.

References

- Lima BL, França AV, Pazin-Filho A, Araújo WM, Martinez JA, Maciel BC, Simões MV, Terra-Filho J, Martinelli AL. Frequency, clinical characteristics, and respiratory parameter of hepatopulmonary Syndrome. *Mayo Clin Proc* 2004;79:42-48.
- Schen KP, Falmaann V, Madl C, Funk G, Lehr S, Kandel O, Müller C. Hepatopulmonary syndrome: prevalence and predictive value of various cut off for arterial oxygenation and their clinical consequences. *Gut* 2002;51:853-859.
- Hira HS, Kumaj T, Tyagi SK, Jain SK. A study of hepatopulmonary syndrome among patient of cirrhosis of liver and portal hypertension. *Indian J Chest Dis Allied Sci* 2003;45:165-171.
- Anond AC, Malcheryee D, Rao KS, Seth AK. Hepatopulmonary syndrome: prevalence and clinical profile. *Indian J Gastroenterol* 2001;20:24-27.
- Fallon MB, Abrams GA. Pulmonary dysfunction in chronic disease. *Hepatology* 2000;32:859-865.
- Przybyowski T, Krenke R, Fangrat A, Nasilowski J, Grabczak EM, Styczynsk G, Pruszczyk P, Krawczyk M, Chazan R. Gas exchange abnormalities in patients listed for liver transplantation. *J Physiol Pharmacol* 2006;57 Suppl 4:313-323.
- Flukiger M. Occurrence of club-shaped finger phalanges without chronic changes in the lungs or heart. *Wien Med Wochenschr* 1884;34:1457-1458.
- Rodriguez-Roisin R, Krowka MJ, Herve P, Fallon MB. Pulmonary hepatic vascular disorders (PHD). *Eur Respir J* 2004; 24:861-80.
- Abrams GA, Jaffe CC, Hoffer PB, Binder HJ, Fallon MB. Diagnostic utility of contrast echocardiography and lung perfusion scan in patients with hepatopulmonary syndrome. *Gastroenterology* 1995;109:1283-1288.
- Abrams GA, Nanda NC, Dubovsky EV, Krowka MJ, Fallon MB. Use of macro-aggregated albumin lung perfusion scan to diagnose hepatopulmonary syndrome: a new approach. *Gastroenterology* 1998;114:305-310.
- Gupta NA, Abramowsky C, Pillen T, Redd D, Fasola C, Heffron T, Romero R. Pediatric hepatopulmonary Syndrome is seen with polysplenia/interrupted inferior vena cava and without cirrhosis. *Liver Transpl* 2007;13:680-686.
- Swanson KL, Wiesner RH, Krowka MJ. Natural history of hepatopulmonary syndrome: impact of liver transplantation. *Hepatology* 2005;41:1122-1129.
- Noli K, Solomon M, Golding F, Charron F, Ling SC. Prevalence of hepatopulmonary syndrome in children. *Pediatrics* 2008;121:522-527.
- Surasi DS, Manapragada P, Bhambhani P. Lung perfusion imaging in hepatopulmonary syndrome using (^{99m}Tc) macroaggregated albumin. *J Nucl Cardiol* 2015;22:586-588.
- El-Shabrawi MH, Omran S, Wageeh S, Isa M, Okasha S, Mohsen NA, Zekry O, E-Bartan G, El-Karaksy HM. (^{99m}Tc)Technetium-macroaggregated albumin perfusion lung scan versus contrast enhanced echocardiography in the diagnosis of the hepatopulmonary syndrome in children with chronic liver disease. *Eur J Gastroenterol Hepatol* 2010;22:1006-1012.
- Kalambokis G, Tsianos EV. Lung perfusion scan is not superior to contrast-enhanced echocardiography for the diagnosis of the hepatopulmonary syndrome in chronic liver disease. *Eur J Gastroenterol Hepatol* 2010;22:1387-1388.
- Grimon G, André L, Bernard O, Raffestin B, Desgrez A. Early radionuclide detection of intrapulmonary shunts in children with liver disease. *J Nucl Med* 1994;35:1328-1332.
- Fatemi R, Alizadeh AM, Mirzaei V, Khoshbaten M, Talebbipour B, Sharifian A, et al. Clinical and diagnostic characteristics of hepatopulmonary syndrome among Iranian patients with cirrhosis. *Research in Medicine*. 2005;29:175-178.
- Fauci A, Kasper D, Hauser S, Longo D, Jameson L, Loscalzo J. *Harrison's Principles of Internal medicine*. 18th ed. New-York; McGraw Hill; 2012. p.1891-1999.
- Fragaki M, Sifaki-Pistolla D, Samonakis DN, Koulentaki M, Koukouraki S, Stathaki M, Kouroumalis E. Screening for Hepatopulmonary Syndrome in Cirrhotic Patients Using Technetium 99m -macroaggregated Albumin Perfusion Lung Scan (Tc-MAA): Diagnostic Approach and Clinical Correlations. *J Clin Gastroenterol* 2018;52:828-834
- Grilo I, Pascasio JM, Tirado JL, López-Pardo FJ, Ortega-Ruiz F, Sousa JM, Rodriguez-Puras MJ, Ferrer MT, Gómez-Bravo MÁ, Grilo Reina A. The utility of the macro-aggregated albumin lung perfusion scan in the diagnosis and prognosis of hepatopulmonary syndrome in cirrhotic patients candidates for liver transplantation. *Rev Esp Enferm Dig* 2017;109:335-343.



Esophageal Clearance in Laryngopharyngeal Reflux Disease: Correlation of Reflux Scintigraphy and 24-hour Impedance/pH in a Cohort of Refractory Symptomatic Patients

Laringofarengal Reflü Hastalığında Özofagus Klirensi: Reflü Sintigrafisi ve 24 Saatlik Empedans ve Ph Monitorizasyonunun Refrakter Semptomatik Hastalarda Korelasyonu

✉ Leticia Burton¹, ✉ Gregory L. Falk², ✉ Karl Baumgart³, ✉ John Beattie⁴, ✉ Scott Simpson⁵, ✉ Hans Van der Wall¹

¹University of Notre Dame, CNI Molecular Imaging, Sydney, Australia

²Concord Hospital and University of Sydney, Sydney Heartburn Clinic, Sydney, Australia

³North Shore Medical Centre, Sydney, Australia

⁴Ryde Medical Centre, Sydney, Australia

⁵Sydney Adventist Hospital and University of Sydney, Sydney, Australia

Abstract

Objectives: The role of gastroesophageal reflux disease (GERD) in the aetiology of laryngopharyngeal reflux (LPR) is poorly understood and remains a controversial issue. The 24-hour impedance monitoring has shown promise in the evaluation of LPR but is problematic in pharyngeal recording. We have shown the utility of scintigraphic studies in the detection of LPR and lung aspiration of refluxate. Correlative studies were obtained in patients with a strong history of LPR and severe GERD.

Methods: A highly selected sequential cohort of patients with a high pre-test probability of LPR/severe GERD who had failed maximal medical therapy were evaluated with 24-hour impedance/pH, manometry and scintigraphic reflux studies.

Results: The study group comprised 34 patients (15 M, 19 F) with a mean age of 56 years (range: 28-80 years). The majority had LPR symptoms (mainly cough) in 31 and severe GERD in 3. Impedance bolus clearance and pH studies were abnormal in all patients in the upright and supine position. A high rate of non-acid GERD was detected by impedance monitoring. LOS tone and ineffective oesophageal clearance were found in the majority of patients. Scintigraphic studies showed strong correlations with impedance, pH and manometric abnormalities, with 10 patients showing pulmonary aspiration.

Conclusion: Scintigraphic studies appear to be a good screening test for LPR and pulmonary aspiration as there is direct visualisation of tracer at these sites. Impedance studies highlight the importance of non-acidic reflux and bolus clearance in the causation of cough and may allow the development of a risk profile for pulmonary aspiration of refluxate.

Keywords: Gastroesophageal reflux disease, laryngopharyngeal reflux, reflux, impedance, pH, manometry, scintigraphy, pulmonary aspiration

Öz

Amaç: Laringofarengal reflü (LFR) etiolojisinde Gastroözofageal Reflü hastalığının (GÖRH) rolü tam olarak anlaşılamamıştır ve bu durum tartışmalı bir konu olmaya devam etmektedir. Yirmi dört saatlik empedans monitörizasyonu LFR'nin değerlendirilmesinde umut vaatetmektedir, ancak faringeal kayıtlamada sorun yaşanmaktadır. Biz, LFR'nin ve reflünün akciğer aspirasyonunun saptanmasında sintigrafik çalışmaların yararını göstermiştik. Şiddetli LFR ve GÖRH öyküsü olan hastalarda korelasyon çalışmaları yapılmıştır.

Yöntem: Maksimum medikal tedaviye yanıt vermeyen ve ön testte LFR/şiddetli GÖRH olasılığı yüksek saptanan seçilmiş bir hasta grubu; 24 saatlik empedans/pH monitörizasyonu, manometri ve sintigrafik reflü çalışmaları ile değerlendirildi.

Bulgular: Çalışma grubu, 15'i erkek, 19'u kadın olmak üzere 34 hastadan oluşmaktaydı ve yaş ortalaması 56 (28-80) idi. Hastaların 31'inde LFR semptomları (çoğunlukla öksürük) ve 3'ünde şiddetli GÖRH semptomları vardı. Empedans bolus klirensi ve pH çalışmaları, ayakta ve sırtüstü pozisyonda tüm hastalarda anormaldi. Empedans monitörizasyon ile yüksek oranda asidik olmayan GÖRH saptandı. Hastaların çoğunda düşük

Address for Correspondence: Hans Van der Wall MD, University of Notre Dame, CNI Molecular Imaging, Sydney, Australia

Phone: +61 2 9736 1040 **E-mail:** hvanderwall@gmail.com **ORCID ID:** orcid.org/000-0003-4184-3330

Received: 28.06.2019 **Accepted:** 06.10.2019

©Copyright 2020 by Turkish Society of Nuclear Medicine
Molecular Imaging and Radionuclide Therapy published by Galenos Yayınevi.

özofageal sfinkter tonusu ve inefektif özofageal klirens saptandı. Sintigrafik çalışmalar pulmoner aspirasyon gelişen 10 hastada; empedans, pH ve manometrideki anormalliklerle yüksek korelasyon gösterdi.

Sonuç: Sintigrafik çalışmalar, LFR ve pulmoner aspirasyon için iyi bir tarama testi gibi görünmektedir, çünkü bu bölgelerde tracerin doğrudan gösterilmesi mümkündür. Empedans çalışmaları, öksürüğün nedeni olarak asidik olmayan reflü ve bolus klirensinin önemini vurgulamaktadır ve reflünün pulmoner aspirasyonu için bir risk profilinin geliştirilmesinde kullanılabilir.

Anahtar kelimeler: Gastroözofageal Reflü hastalığı, larengofarengeal reflü, reflü, empedans, pH, manometri, sintigrafi, pulmoner aspirasyon

Introduction

The pathophysiology of proximal gastroesophageal reflux disease (GERD) causing laryngopharyngeal reflux (LPR) is poorly understood (1,2). It is an important consideration in the aetiology of chronic cough which remains undiagnosed after eight weeks of specialist investigation (1,2,3,4). The pathophysiology of reflux-induced cough is poorly described and the disease remains in dispute (1,2). Various disease processes may be generators of laryngeal and pharyngeal symptoms including proximal GERD. These may manifest as pharyngeal reflux, laryngeal contamination and pulmonary aspiration as well as acid reflex-mediated bronchospasm (5,6).

Response to proton pump inhibitor (PPI) therapy has been utilised as a diagnostic test (7,8) as there has been no accurate diagnostic test for LPR by which to make the initial diagnosis and to interrogate the success of treatment. A high placebo response in treatment of cough makes the matter more complex when evaluating therapy (7). Investigation of this situation by 24-hour pH reflux testing has been bedevilled by artefacts in the pharynx (9), leading to attempts to modify instrumentation to increase accuracy and reproducibility. The newer technology of reflux impedance monitoring has shown potential to identify non-acidic and slightly acidic reflux episodes as well as pharyngeal contamination (9,10). Intra-observer variability however has been a problem for accuracy of pharyngeal readings (10,11). Identifying reflux high in the oesophagus where observations are more accurate than in the pharynx does not necessarily predict pharyngeal exposure, as the upper oesophageal sphincter separates the chambers. The issue of an episode of reflux changing acidity during ascent in the oesophagus confounds proximal pH measurements, as does the recognition of symptoms associated with non-acid reflux (10,12).

Reflux scintigraphy has been utilised in children and to a variable extent in adults to evaluate pharyngeal contamination and pulmonary aspiration of refluxate (13,14,15). There have however been multiple technical difficulties and a lack of standardisation between studies with variable and sometimes contradictory results (13,16,17,18). We have developed and validated a

consistent scintigraphic technique for the detection of GERD and LPR with good correlations with pH monitoring and manometry (19,20).

We hypothesised that scintigraphic reflux studies could provide additional information and complement 24-hour pH and impedance studies in patients with GERD and suspected LPR. A secondary purpose of the study was to evaluate impedance reflux studies in prediction of proximal reflux disease causing LPR symptoms and lung aspiration of refluxate.

Materials and Methods

Clinical

Consecutive patients failing adequate medical investigation and management, with a high pre-test probability of proximal GERD with LPR symptoms were referred to a tertiary anti-reflux surgical service in the past 3 years. Patients underwent standard symptom pro-forma interview with regard to LPR symptoms including amongst others, cough, sore throat, voice change, and dyspnoea. Patients had previously undergone gastroscopy and laryngoscopy for symptoms of GERD/LPR. Alternative causes of LPR symptoms had been excluded by multi-disciplinary investigations.

Manometry, 24-hour dual channel pH and impedance reflux and scintigraphic reflux studies were obtained in all patients while off PPI therapy.

Hiatus hernia was diagnosed by endoscopy.

Oesophageal manometry was performed under topical nasal anaesthesia using a dent sleeve 4 mm trans-nasal 6 lumen catheter placed by identification of the lower oesophageal sphincter (LOS) by pull through and placement of the sleeve in the LOS. Wet swallows (10) of 2.5 mL water were performed by stationary technique using the dent mark 2 infusion pump (Dentsleeve International Ltd., Mississauga, Ontario, Canada). Studies were performed in the supine position. The swallows were assessed for peristaltic efficacy (21) and sphincter characteristics were determined. A lesser sub-group of motility disturbance was created for 20-30% ineffective oesophageal motility (IEM) which would previously have been included in the normal

group. Resting pressure of the sphincter and nadir pressure were reported from the mid-end expiratory pressure.

Twenty four-hour impedance reflux study with two channel 24-hour pH was performed after cessation of all anti-acid therapy for 48 hours. Patients were prepared with local anaesthetic prior to insertion of a trans-nasal catheter consisting of 2 level impedance rings and 2 level pH electrodes connected to an external monitoring device. Standard calibration was carried out. Impedance rings were placed at 5 and 15 cm above the upper border of the LOS (Zephyr device, catheter ZAI-BD31, Sandhill Co, Highlands Ranch, Colorado, USA). There were no dietary restrictions during the testing period other than ingestions of acidic beverages. Catheter placement was ascertained by measurements taken at manometry with the lower pH electrode 5 cm above the upper border of the LOS, the upper, 15 mm higher. The patient returned the following day when the assembly was removed. Meal-times were included in the reporting analysis. Reports of 24-hour pH and 24-hour impedance reflux were then generated using autoscan and manual review. Events which were considered not to be reflux or indeterminate were excised from the report. The categories of reflux were classified according to the consensus on impedance and pH monitoring (22). Briefly, it was based on oesophageal pH during reflux detected by impedance monitoring. Acid reflux was a fall in pH below 4, weakly acid reflux was a fall in pH which was ≥ 4 but < 7 and non-acid reflux where oesophageal pH increases ≥ 7 or remained ≥ 7 during reflux. Liquid bolus entry was the time when the 50% fall in impedance from baseline during liquid reflux was reached. Bolus duration was the time from liquid bolus entry to liquid bolus clearance (impedance increasing for > 5 seconds).

Scintigraphy

Patients were fasted for 12 hours and medications were ceased for the 24-hours prior to the test. While upright, patients were positioned in front of a Hawkeye 4 gamma camera (General Electric, Milwaukee, USA) with markers placed on the mandible and over the stomach to ensure the regions of interest were within the field of view of the camera. Patients swallowed 100-150 mL of water with 40-60 MBq of ^{99m}Tc diethylenetriamine penta-acetic acid followed by flushing with 50 mL of water to clear the mouth and oesophagus of radioactivity. Dynamic images of the pharynx, oesophagus and stomach were obtained for 5 minutes at 15 secs per frame into a 64x64 matrix. A second 30-minute dynamic image was obtained in the supine position immediately following the upright study utilising 30 sec frames (Figure 1). Following acquisition of the supine study, the patients were given a further 50 mL

of water with 60 MBq of ^{99m}Tc phytate (colloid) followed by 50 mL of water as a flush. Delayed images were obtained at 2 hours to assess the presence of aspiration of tracer activity into the lungs. Images were analysed by time activity curves over the pharynx, upper and lower half of the oesophagus and a background region over the right side of the chest, away from the stomach and oesophagus (Figure 2). Delayed images were analysed by a line profile over the lungs. Time activity curves were graded as showing no GERD, a falling curve, flat or rising curves. Area under the curve and maximal amplitude relative to background were estimated. A liquid gastric emptying half-time was

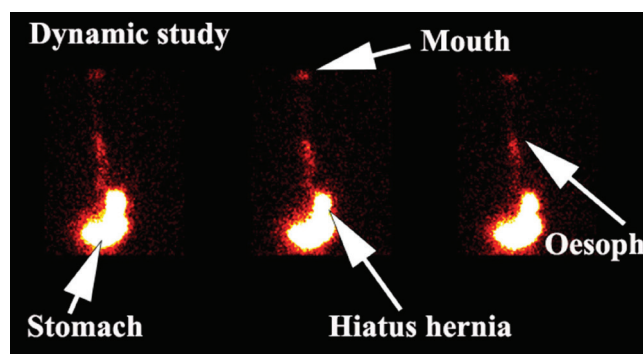


Figure 1. Dynamic scintigraphic study. The sequence of images demonstrates tracer activity in the stomach with evidence of a hiatus hernia and gastro-oesophageal reflux to the level of the oropharynx. Note the progressive accumulation of tracer in the region of the oropharynx (mouth)

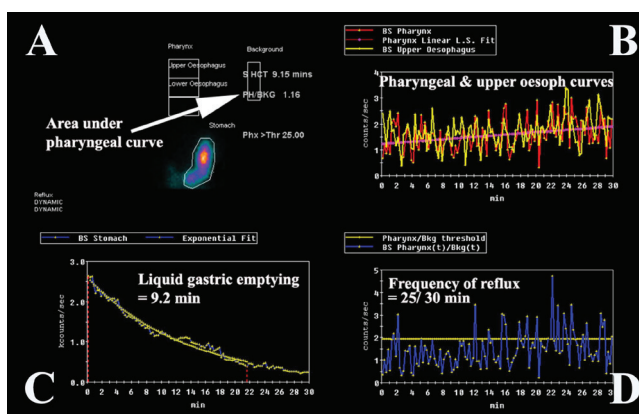


Figure 2. Graphical analysis of the dynamic study. (A) This panel demonstrates the regions of interest over the pharynx, upper and lower oesophagus with the background region of interest. It also indicates the area under the pharyngeal curve. Panel (B) illustrates the graphical output from the region of interest over the pharyngeal/laryngopharyngeal and upper oesophageal areas with the fitted pink curve demonstrating a rising pattern for the pharyngeal region. Panel (C) shows the analysis of the supine dynamic study of the liquid gastric emptying time. Panel (D) shows the frequency of reflux to the level of the pharynx/laryngopharynx with the fitted yellow line indicating the residual level after subtraction of background activity

determined from the 30-minute supine acquisition with a single exponential fit to the data.

Ethical Considerations

Patient data were extracted from a research database of either proven or suspected GERD which had been approved by the Institutional Ethics Committee of Concord Hospital (LNR/12CRGH/248). Patients gave written informed consent for the study under the Institutional Ethics Committee Guidelines.

Statistical Analysis

All statistics were calculated using the Statistical Package for the Social Sciences Version 24 (IBM, New York, USA). A proportion of the data was non-parametric in nature with ordinal responses such as the isotope time-activity curves for the pharynx and upper oesophagus (Grade 1-3) and lung aspiration of isotope (1=positive, 0=negative). All other variables were parametric or continuous. Spearman rank-order correlation was used for the non-parametric data and Pearson correlation co-efficient was used for the parametric data analysis. The paired t-test was utilised for comparison of test results in the same patient. Binary logistic regression and receiver operating characteristic (ROC) curves were utilised for determining best predictors of lung aspiration of refluxate.

Results

Clinical

Results were obtained from 34 consecutive patients undergoing impedance pH/manometric studies and compared with scintigraphic reflux studies. This comprised

15 males and 19 females (mean age: 56 years, range: 28-80 years). The dominant symptoms were of LPR (mainly cough) in 31 and severe typical GERD in 3 cases. The predominant symptom was cough which occurred in 27, other LPR symptoms were recorded in 4, heartburn and regurgitation in 3. Twenty patients were taking PPI, which were ceased for 48 hours prior to testing. No significant differences in results were recorded for the patients taking PPI and those not on PPIs.

A hiatus hernia was present in 16 patients. There was no significant correlation between hiatus hernia and impedance/pH results, manometric or scintigraphic parameters.

Impedance and pH

Impedance bolus clearance (Figure 3) when upright was a mean of 17.5 [range: 6-42, standard deviation (SD): 7.5] for this population. Results in normal volunteers have been reported as a median of 8 (95% value of 31) (23). Impedance bolus clearance for the 34 patients when supine was a mean of 25.1 (range: 0-214, SD: 34.4), compared to a values of 1-7 in normal volunteers (23). Impedance bolus clearance in total was a mean of 21.1 (range: 8-35, SD: 6.7).

pH results are provided in Tables 1 and 2. The means for acid, non-acid and total proximal reflux were significantly greater than has been reported in normal volunteers by Shay et al. (23). Even the relatively common occurrence of upright reflux in normal volunteers (mean: 1.2%) was significantly higher in this group (mean ~ 10% for acid and non-acid reflux). The frequency of supine reflux at the proximal and distal sites in the oesophagus was markedly

Table 1. Proximal reflux by pH monitoring

	Acid			Non-acid			Total reflux		
	Mean	Range	SD	Mean	Range	SD	Mean	Range	SD
Upright	9.4	0-44	11.6	11.8	0-45	10.3	22.4	2-79	15.1
Supine	1.4	0-10	2.4	1.5	0-14	2.7	2.9	0-24	4.6
All reflux	10.6	0-44	12.2	13.3	2-47	11.7	23.9	2-83	17.2

SD: Standard deviation

Table 2. Distal reflux by pH monitoring

	Acid			Non-acid			Total reflux		
	Mean	Range	SD	Mean	Range	SD	Mean	Range	SD
Upright	17.4	0-70	21.0	20.5	0-90	22.6	40.2	9-117	25.1
Supine	4.6	0-72	13.6	3.1	0-16	4.0	8.9	0-74	13.8
All reflux	22.0	0-127	29.2	28.7	4-102	25.6	49.1	10-131	31.7

SD: Standard deviation

greater by an order of magnitude than in normal volunteers (24).

There was no significant difference between proximal acid event frequency and proximal non-acid event frequency in either the upright or supine position by the paired t-test. There was no correlation between any markers of distal pH and either LPR or lung aspiration in the scintigraphic studies.

Manometric Characteristics of the Group

The LOS pressure was a mean of 2.0 mmHg (range: 0-12, SD: 2.8) compared with a normal sphincter pressures ranging from 18 to 25 mmHg. Thirty patients in this group had a hypotensive LOS. Sphincter pressure was not recorded in 4 patients due to technical difficulty: One patient could not tolerate it and we were unable to traverse the sphincter region in 3 others. Normal oesophageal body motility was present in 4 patients, 9 had a mild non-specific IEM, 4 had moderate IEM and 17 severe IEM according to our modification of the Kahrilas classification (21), where we separated mildly abnormal from normal patients which were included under the normal umbrella in that study.

Scintigraphy

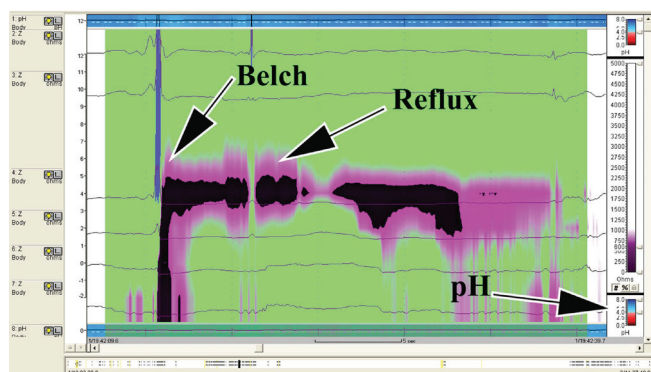


Figure 3. Impedance study demonstrating significant gastro-oesophageal reflux following a belch and the rapid fall in pH and impedance as acid/fluid enters the oesophagus. There is prolongation in clearance of the acid/fluid from the oesophagus (reflux). The pink colour is a marker of the acidity as shown in the colour bar (pH)

Dominant symptom profile	Curve analysis for pharynx/laryngopharynx			
	Grade 1	Grade 2	Grade 3	Aspiration
GERD upright	0	2	1	1
GERD supine	0	2	1	
LPR upright	5	10	16	9
LPR supine	4	5	22	

GERD: Gastro-oesophageal reflux disease, LPR: Laryngopharyngeal reflux

All 34 patients showed scintigraphic evidence of gastroesophageal regurgitation events and nasopharyngeal contamination in either the upright or supine position or both. A rising or flat time-activity curve was apparent for the pharynx in 30/34 and for the upper oesophagus in 25/34 cases (Table 3). The mean amplitude of activity in the pharynx when compared to background activity of the right upper lung and expressed as a ratio was 4.4 [95% confidence interval (CI): 3.7-5.1].

Pulmonary aspiration of refluxate was apparent in 10 of 34 cases. Of these, 9 patients had atypical histories and 1 had a typical history of heartburn and regurgitation. The most common symptoms associated with aspiration were cough, choking and recurrent throat clearing.

Liquid gastric emptying was abnormal in 12/34 cases (T1/2>16 min). Mean of the abnormal cases was 30 min (95% CI: 15-45 min). There was no significant relationship between liquid gastric emptying and any other scintigraphic results including LPR or lung aspiration of refluxate.

Statistical Correlations

Impedance and scintigraphy Table 4.

Clearance of refluxate from the oesophagus (impedance bolus clearance) was inversely correlated with the isotope pharyngeal time-activity curves. The longer time to clear the oesophagus of refluxate and return impedance to normal was associated with an increased likelihood of scintigraphic pharyngeal contamination by refluxate and a rising level of refluxate activity in the pharynx in the upright and supine positions (Spearman correlation coefficient -0.38, p<0.05): Similarly, impaired clearance was strongly associated with increased isotope identification in the upper oesophagus (Spearman correlation coefficient 0.60, p<0.05). Abnormal gastric emptying appeared to have no association with abnormal oesophageal clearance. There was a strong positive association of all measures of increasing bolus clearance duration and findings of isotope pulmonary aspiration (Spearman correlation coefficient 0.38-0.60, p<0.05).

Binary logistic regression analysis of pulmonary aspiration found that the best predictor of pulmonary aspiration was the delay in impedance bolus clearance when upright (wald 4.25, p=0.039). Other findings in pH, manometry and scintigraphy did not predict pulmonary aspiration (Table 4).

The best predictor of aspiration of refluxate into the lungs are the upright bolus clearance and total bolus clearance in the impedance studies. This is shown in the receiver operating characteristic curve in Figure 4.

pH and Scintigraphy

Isotope amplitude in the pharynx was positively correlated with non-acid proximal reflux when supine (Pearson correlation co-efficient 0.35, p=0.04) and all proximal supine

reflux (Pearson correlation co-efficient 0.38, p=0.03). A rising curve for the upper oesophagus was associated with significant proximal oesophageal acid exposure. Non-acid proximal reflux when supine was positively correlated with pulmonary aspiration in the scintigraphic studies (Spearman correlation co-efficient 0.36, p=0.04). Proximal acid reflux in the upright or supine position did not correlate with either scintigraphic pharyngeal exposure or lung aspiration of refluxate.

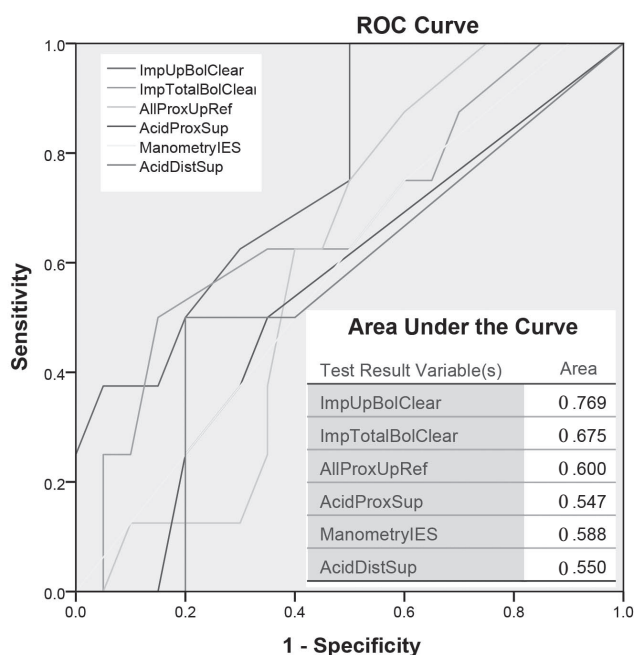


Figure 4. Receiver operating characteristic curve. The curve examines the best predictor of lung aspiration of refluxate amongst the standard testing methods of impedance, manometry and pH studies. The value is based on the comparison of areas under the curve in the interplay between sensitivity and specificity. In this instance, the best predictor of aspiration of refluxate into the lungs are the upright bolus clearance and total bolus clearance in the impedance studies. Note that the least useful value is the acid exposure of the proximal and distal oesophagus in the supine position

ROC: Receiver operating characteristic

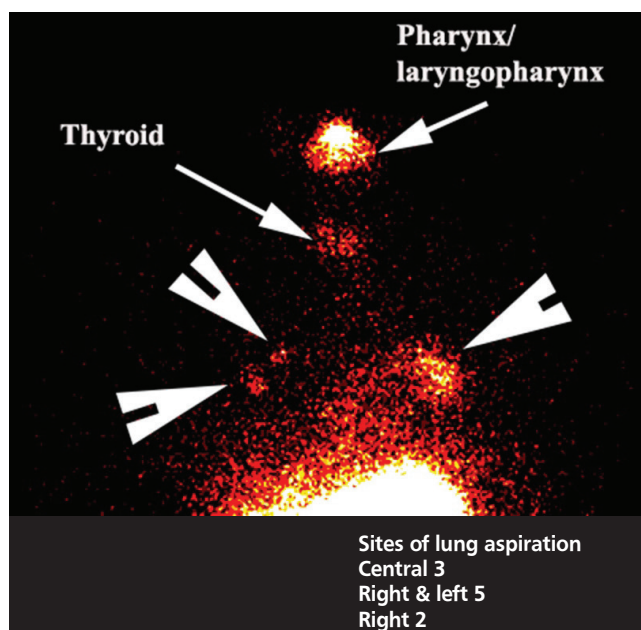


Figure 5. Bilateral lung aspiration. The arrowheads show sites of lung aspiration of refluxate into the main airways in both lungs. Note activity in the pharynx/laryngopharynx and some breakdown of the phytate with free pertechnetate uptake in the thyroid gland (arrows). The Table shows the sites of aspiration which are invariably in the central aspects of both lungs rather than in the lung bases

Significant correlations	p	Corr	No significant correlations	p	Corr
Isotope amplitude/supine prox non-acid reflux	0.041	0.35 PCC	Isotope pharyngeal curve/total prox reflux	>0.05	-0.18 Spear
Isotope amplitude/supine total prox reflux	0.029	0.38 PCC	Isotope pharyngeal curve/supine total prox reflux	>0.05	-0.23 Spear
Isotope pharyngeal curve/upright Imp bolus clear	<0.05	-0.36 Spear	Isotope pharyngeal curve/supine Imp bolus clear	0.05	-0.13 Spear
Isotope pharyngeal curve/total Imp bolus clear	0.00	-0.42 Spear	Isotope amplitude/total Imp bolus clearance	0.88	0.028 PCC
Isotope aspiration/upright Imp bolus clear	<0.05	0.38 Spear	Isotope aspiration/total Imp bolus clear	>0.05	0.27 Spear
Upper oesophageal curve/total Imp bolus clearance	<0.05	-0.60 Spear	Upper oesophageal curve/supine Imp bolus curve	>0.05	-0.046 Spear

p: p value, PCC: Pearson correlation, Spear: Spearman, Corr: Correlation, Imp: Impedance

Figure 4 shows that acid exposure in the upper oesophagus was not a good predictor of aspiration of refluxate in the lungs.

Manometry and Impedance/pH (Reflux/Clearance)

LOS pressure correlated with decreased impedance bolus clearance in the upright position (Pearson correlation coefficient 0.36, $p=0.04$) but not in the supine position or with total bolus clearance (Table 5).

A strong correlation was found between decreased manometric LOS pressure and increase in total proximal supine reflux event frequency (Pearson correlation coefficient 0.58, $p=0.001$). Total proximal upright reflux event frequency was also correlated with worsening ineffective oesophageal clearance by manometry (Pearson correlation coefficient 0.40, $p=0.02$). No significant difference was found between patients with normal oesophageal clearance and those with mild clearance abnormalities and this may be due to inadequate numbers of patients with normal clearance ($n=4$) leading to a type 1 error.

Manometry and Scintigraphy

LOS pressure was inversely correlated with isotope amplitude in the laryngopharynx (Pearson correlation coefficient -0.37, $p=0.04$) but not with any other scintigraphic variable such as lung aspiration (Table 5).

Discussion

It is important to state from the outset that the population in this study had severe established gastro-oesophageal reflux disease which was referred to a tertiary centre for consideration of laparoscopic fundoplication, largely after exclusion of other diseases by multiple other disciplines. Nearly all patients had both symptoms and investigative findings consistent with LPR disease. This group was characterized by the failure of response to high-dose PPI therapy. Approximately half the patients had hiatus hernias and the majority, abnormalities of LOS pressures. There was clearly a high susceptibility to high-grade reflux disease in this group of patients as has been reported previously (20).

Patients were studied with impedance/pH, manometry and scintigraphic reflux studies. The principal purpose of the studies was assessment for surgery, but these studies have enabled evaluation of the relative contributions of impedance monitoring and standard pH monitoring to predict LPR and lung aspiration of reflux detected by scintigraphic studies, which we have validated in previous work (19,20).

The most outstanding findings in the standard manometric studies was the LOS pressure which was a mean of 2 mmHg compared with a normal range of 18-25 mmHg. Only 4 of 34 patients had normal oesophageal motility underlining the degree of oesophageal clearance abnormalities in this population.

Impedance/pH studies allowed the evaluation of total reflux events (acid + non-acid) in the upper and lower oesophagus in a group of patients in whom PPI and other antacid therapy had been ceased prior to the study. Total proximal reflux measured by the impedance studies was found to be significantly different from both acid (measured by pH probe) and non-acid reflux (measured by impedance probe), reflecting the inadequacy of isolated pH monitoring as a tool for detection of proximal reflux. This is particularly problematic for detection of proximal non-acid reflux which may be significantly more common than acidic reflux (25), given that there is progressive neutralisation of gastric contents as refluxate ascends the oesophagus to its proximal extent or that primary reflux may be non-acidic or even alkaline in patients on maintenance PPI therapy (26,27).

All patients in this study were tested while off PPI therapy. In the study by Mainie et al. (27) on patients with symptoms refractory to PPI therapy ($n=144$), it was shown that non-acid reflux occurred in 37% and acid reflux in 11% utilising impedance/pH monitoring while still on PPI therapy. In line with these findings was the inverse correlation between LOS pressure and bolus clearance when the patient was upright. It indicates that the severity of abnormal dynamics in the oesophagus cannot be overcome by even favourable

Table 5. Correlations: Manometry and scintigraphy/Impedance-pH

Significant correlations	p	Corr	No significant correlations	p	Corr
Manometric lower oesophageal sphincter pressure/isotope amplitude	0.0042	0.37 PCC	Manometric lower oesophageal sphincter pressure Isotope pharyngeal curve	<0.05	-0.21 Spear
Manometric lower oesophageal sphincter pressure/supine proximal total reflux	0.001	0.58 PCC	Manometric lower oesophageal sphincter pressure/isotope aspiration	<0.05	-0.11 Spear
Manometric ineffective oesophageal clearance/upright total proximal reflux	0.02	0.40 PCC	Manometric ineffective oesophageal clearance/total proximal reflux	0.20	0.25 PCC

p: p value, PCC: Pearson correlation, Spear: Spearman, Corr: Correlation

gravitational circumstances. A strong positive correlation was also found between total proximal supine reflux event frequency (by impedance probe) and ineffective oesophageal clearance. Not only does the LOS pressure allow free reflux by a mechanical dysfunction but the associated motility disturbance fails to clear the refluxate from the oesophagus. There is a wealth of literature supporting this observation (28,29,30). Impedance bolus transit abnormalities parallel the severity of GERD (31) and in our study showed a significant correlation with a rising upper oesophageal scintigraphic time-activity curve. Under normal circumstances, clearance occurs as a function of gravity and peristalsis with neutralisation of acid by swallowed saliva (30).

The importance of non-acid GERD triggering symptoms has been a vexed issue which has been directly addressed by impedance studies. As the study of Mainie et al. (27) has shown, non-acidic reflux remains a cause of symptoms in patients on high-dose twice daily PPI therapy. Not all patients with non-acidic GERD have symptoms, even patients with established LPR and lung aspiration of refluxate may not have symptoms (20). The lack of symptoms implies a clinically silent but potentially damaging phenomenon and raises the question of appropriate therapy. A number of strategies have been advocated including agents that inhibit transient relaxation of the LOS (32) and experimental endoscopic therapies (26). Ultimately, surgical treatment with laparoscopic fundoplication has efficacy that has been established in numerous studies (19,33,34,35) on the basis of pH monitoring alone and more recently, impedance/pH monitoring in patients with non-acid but symptomatic GERD (36,37).

What additional value does the scintigraphic reflux study contribute to such a group of patients? Impedance and pH studies interrogate both the distal and proximal oesophagus for significant gastro-oesophageal reflux, be it acidic or non-acidic. Distal single-channel 24-hour pH does not show proximal reflux disease as has been shown in this study and dual-channel 24-hour pH is confounded by neutralisation of reflux during ascent of the oesophagus. The combined study assesses the severity and frequency of reflux, forming the basis of principles for treatment. However, the relatively uninterpretable areas that are not reproducibly identified in pharyngeal recording by the combined technique are the laryngopharynx and aspiration of refluxate into the lungs. While there has been some evidence of the utility of impedance studies in the detection of LPR, issues of reproducibility in the pharynx are a significant problem with the current generation of

instruments (11). The newer generation of impedance instruments may overcome this problem.

Scintigraphic studies allow direct visualisation of the entry of refluxate into the nasopharyngeal region as a dynamic study in cine format in the upright and supine position (Figure 1). It illustrates whether such activity is rising, static or clearing (Figure 2). We have shown in previous work that a rising pharyngeal curve is highly predictive of lung aspiration of refluxate (19). The delayed study shows if there has been aspiration of tracer into the lungs, which are normally free of tracer activity.

Scintigraphic studies are a good screening tool but as the sampling time is approximately 33 minutes in total, do not give an actual idea of the overall frequency of GERD, as do the 24-hour recordings of impedance/pH (Figure 3) and manometry. It may well underestimate the frequency and extent of reflux. There is however the clear implication that if such activity is visualised in 30 minutes, under conditions that do not predispose to reflux such as stomach filling as occurs after meals, then it reflects a chronicity of recurrence. Aspiration is screened for at 2 hours (Figure 5). Previous experience with 12-24-hour screening has not added to the pick-up rate significantly and was thought not to justify the inconvenience of bringing patients back for a second time. The study has a low radiation dose, being less than a chest X-ray and is relatively non-invasive as the patient swallows approximately 100 mL of radioactive liquid (40-60 MBq). The study is non-invasive and relatively inexpensive to obtain.

All 34 patients showed scintigraphic evidence of pharyngeal contamination with approximately one third aspirating refluxate into the lungs (Figure 5). This is a consistent pattern that we have observed in a previous study of patients undergoing laparoscopic fundoplication for symptomatic GERD and LPR which was resistant to high-dose PPI therapy (19). Time activity curves for the lower pharynx/laryngopharynx and the area under the curve are obtained from a region of interest positioned below retained activity in the oropharynx from the initial swallow (Figure 2). These derived markers of reflux therefore reflect an integration of the volume of reflux and failure of adequate clearance and is an effective parallel of the impedance marker of bolus clearance. The time-activity curves for the region showed a good correlation with the impedance findings of delayed bolus clearance from the oesophagus. The greater the delay in bolus clearance, the more likely was a rising time-activity curve for the lower pharynx/laryngopharynx. Furthermore, the increasing delay in bolus clearance made the chance of pulmonary aspiration much higher. Logistic regression identified the

delay in upright bolus clearance as the only factor that predicted pulmonary aspiration of refluxate (Figure 4). This may be an underestimate of supine aspiration, given that aspiration scanning was performed after a period of upright delay, rather than after lying supine for a longer period, as would occur during sleep.

Isotope amplitude is a measure of the highest single reflux episode compared to background activity. It is not a manifestation of "noise" on the curve as it is consistently shown on the curve obtained from the mid/lower oesophagus region of interest in the same temporal sequence. Isotope amplitude for the degree of refluxate in the lower pharynx/laryngopharynx was inversely correlated with LOS pressure and rose with falling pressures. It was also strongly correlated with non-acidic reflux and all reflux in the supine position. Pulmonary aspiration of refluxate was strongly correlated with proximal non-acidic reflux when the patient was supine, suggesting that sleep or the lack of sensory stimulus of less acidic material may disable protective reflex mechanisms (38). Such findings will allow the derivation of a risk-profile that allows prediction of the likelihood of LPR and lung aspiration of refluxate. In contrast, proximal acid reflux did not correlate with either lower pharyngeal/laryngopharyngeal amplitude or aspiration of tracer, again underlining the inherent inability of pH studies in identifying a risk profile for LPR and lung aspiration of refluxate.

Conclusion

A surprising level of ineffective oesophageal clearance has been identified in this series suggesting that oesophageal body dysfunction is a factor in proximal progression of refluxate. The advent of impedance studies has changed the paradigm for screening patients for GERD. It has brought the issue of non-acidic reflux into focus and increased the understanding of how symptoms can persist while patients are on maintenance high-dose PPI therapy. Many of the findings of oesophageal clearance are well correlated with the scintigraphic reflux studies and allow the formulation of a risk profile for the occurrence of LPR and lung aspiration of refluxate. Scintigraphic reflux studies are a good screening tool for reflux as they also demonstrate extra-oesophageal manifestations in the head, neck and lungs which is spectacularly shown by single photon emission computed tomography fused with low-dose X-ray computed tomography. We have found that LPR and lung aspiration of refluxate can only be attenuated or ceased by surgical fundoplication. Our experience in over 50 cases on maximal medical therapy is that the symptoms may disappear, but LPR and lung aspiration do not.

Ethics

Ethics Committee Approval: Patient data were extracted from a research database of either proven or suspected GERD which had been approved by the Institutional Ethics Committee of Concord Hospital (LNR/12CRGH/248).

Informed Consent: Patients gave written informed consent for the study under the Institutional Ethics Committee Guidelines.

Peer-review: Externally peer-reviewed.

Authorship Contributions

Data Collection or Processing: L.B., G.L.F., Analysis or Interpretation: L.B., Literature Search: L.B., G.L.F., K.B., J.B., S.S., H.V.W., Writing: L.B.

Conflict of Interest: No conflict of interest was declared by the authors.

Financial Disclosure: The authors declared that this study received no financial support.

References

1. Navaratnam RM, Winslet MC. Gastro-oesophageal reflux: the disease of the millennium. *Hosp Med* 1998;59:646-649.
2. Spechler SJ. Laryngopharyngeal reflux: a cause of faulty phonation or a faulted, phony diagnosis? *Clin Gastroenterol Hepatol* 2006;4:431-432.
3. Vaezi MF. Review article: the role of pH monitoring in extraoesophageal gastro-oesophageal reflux disease. *Aliment Pharmacol Ther* 2006;23(Suppl 1):40-49.
4. Vaezi MF. Laryngeal manifestations of gastroesophageal reflux disease. *Curr Gastroenterol Rep* 2008;10:271-277.
5. Ing AJ. Cough and gastro-oesophageal reflux disease. *Pulm Pharmacol Ther* 2004;17:403-413.
6. Smith JA, Abdulqawi R, Houghton LA. GERD-related cough: pathophysiology and diagnostic approach. *Curr Gastroenterol Rep* 2011;13:247-256.
7. Faruqi S, Molyneux ID, Fathi H, Wright C, Thompson R, Morice AH. Chronic cough and esomeprazole: a double-blind placebo-controlled parallel study. *Respirology* 2011;16:1150-1156.
8. Shaheen NJ, Crockett SD, Bright SD, Madanick RD, Buckmire R, Couch M, Dellon ES, Galanko JA, Sharpless G, Morgan DR, Spacek MB, Heidt-Davis P, Henke D. Randomised clinical trial: high-dose acid suppression for chronic cough - a double-blind, placebo-controlled study. *Aliment Pharmacol Ther* 2011;33:225-234.
9. Hoppo T, Komatsu Y, Jobe BA. Antireflux surgery in patients with chronic cough and abnormal proximal exposure as measured by hypopharyngeal multichannel intraluminal impedance. *JAMA Surg* 2013;148:608-615.
10. Shay SS, Abreu SH, Tsuchida A. Scintigraphy in gastroesophageal reflux disease: a comparison to endoscopy, LESp, and 24-h pH score, as well as to simultaneous pH monitoring. *Am J Gastroenterol* 1992;87:1094-1101.
11. Zerbib F, Roman S, Bruley Des Varannes S, Gourcerol G, Coffin B, Ropert A, Lepicard P, Mion F; Groupe Français De Neuro-Gastroentérologie. Normal values of pharyngeal and esophageal 24-hour pH impedance in individuals on and off therapy and interobserver reproducibility. *Clin Gastroenterol Hepatol* 2013;11:366-372.
12. Vela MF. Non-acid reflux: detection by multichannel intraluminal impedance and pH, clinical significance and management. *Am J Gastroenterol* 2009;104:277-280.

13. Kjellen G, Brudin L, Hakansson HO. Is scintigraphy of value in the diagnosis of gastroesophageal reflux disease? *Scand J Gastroenterol* 1991;26:425-430.
14. Maurer AH, Parkman HP. Update on gastrointestinal scintigraphy. *Semin Nucl Med* 2006;36:110-118.
15. Ravelli AM, Panarotto MB, Verdoni L, Consolati V, Bolognini S. Pulmonary aspiration shown by scintigraphy in gastroesophageal reflux-related respiratory disease. *Chest* 2006;130:1520-1526.
16. Caglar M, Volkan B, Alpar R. Reliability of radionuclide gastroesophageal reflux studies using visual and time-activity curve analysis: inter-observer and intra-observer variation and description of minimum detectable reflux. *Nucl Med Commun* 2003;24:421-428.
17. Seymour JC, West JH, Drane WE. Sequential ten-second acquisitions for detection of gastroesophageal reflux. *J Nucl Med* 1993;34:658-660.
18. Tuncel M, Kiratli PO, Aksoy T, Bozkurt MF. Gastroesophageal reflux scintigraphy: interpretation methods and inter-reader agreement. *World J Pediatr* 2011;7:245-249.
19. Falk GL, Beattie J, Ing A, Falk SE, Magee M, Burton L, Van der Wall H. Scintigraphy in laryngopharyngeal and gastroesophageal reflux disease: a definitive diagnostic test? *World J Gastroenterol* 2015;21:3619-3627.
20. Falk M, Van der Wall H, Falk GL. Differences between scintigraphic reflux studies in gastrointestinal reflux disease and laryngopharyngeal reflux disease and correlation with symptoms. *Nucl Med Commun* 2015;36:625-630.
21. Kahrilas PJ, Dodds WJ, Hogan WJ, Kern M, Arndorfer RC, Reece A. Esophageal peristaltic dysfunction in peptic esophagitis. *Gastroenterol* 1986;91:897-904.
22. Sifrim D, Castell D, Dent J, Kahrilas PJ. Gastro-oesophageal reflux monitoring: review and consensus report on detection and definitions of acid, non-acid, and gas reflux. *Gut* 2004;53:1024-1031.
23. Shay S, Tutuian R, Sifrim D, Vela M, Wise J, Balaji N, Zhang X, Adhami T, Murray J, Peters J, Castell D. Twenty-four hour ambulatory simultaneous impedance and pH monitoring: a multicenter report of normal values from 60 healthy volunteers. *Am J Gastroenterol* 2004;99:1037-1043.
24. Sloan S, Rademaker AW, Kahrilas PJ. Determinants of Gastroesophageal Junction Incompetence: Hiatal Hernia, Lower Esophageal Sphincter, or Both? *Ann Intern Med* 1992;117:977-982.
25. Tolin Hernani M, Crespo Medina M, Luengo Herrero V, Martínez López C, Salcedo Posadas A, Alvarez Calatayud G, Morales Pérez JL, Sánchez Sánchez C. Comparison between conventional pH measurement and multichannel intraluminal esophageal impedance in children with respiratory disorders. *Ann Pediatr (Barc)* 2012;77:103-110.
26. Mainie I, Tutuian R, Castell DO. The limitations of pH monitoring for detecting gastroesophageal reflux. *Clin Gastroenterol Hepatol* 2006;4:1184.
27. Mainie I, Tutuian R, Shay S, Vela M, Zhang X, Sifrim D, Castell DO. Acid and non-acid reflux in patients with persistent symptoms despite acid suppressive therapy: a multicentre study using combined ambulatory impedance-pH monitoring. *Gut* 2006; 55:1398-1402.
28. Chen CL, Yi CH, Liu TT. Heterogeneity in oesophageal dysfunction among patients with different reflux symptoms. *Eur J Gastroenterol Hepatol* 2012;24:1059-1065.
29. Fornari F, Blondeau K, Durand L, Rey E, Diaz-Rubio M, De Meyer A, Tack J, Sifrim D. Relevance of mild ineffective oesophageal motility (IOM) and potential pharmacological reversibility of severe IOM in patients with gastro-oesophageal reflux disease. *Aliment Pharmacol Ther* 2007;26:1345-1354.
30. Simren M, Silny J, Holloway R, Tack J, Janssens J, Sifrim D. Relevance of ineffective oesophageal motility during oesophageal acid clearance. *Gut* 2003;52:784-790.
31. Savarino E, Gemignani L, Pohl D, Zentilin P, Dulbecco P, Assandri L, Marabotto E, Bonfanti D, Inferrera S, Fazio V, Malesci A, Tutuian R, Savarino V. Oesophageal motility and bolus transit abnormalities increase in parallel with the severity of gastro-oesophageal reflux disease. *Aliment Pharmacol Ther* 2011;34:476-486.
32. Vela MF, Tutuian R, Katz PO, Castell DO. Baclofen decreases acid and non-acid post-prandial gastro-oesophageal reflux measured by combined multichannel intraluminal impedance and pH. *Aliment Pharmacol Ther* 2003;17:243-251.
33. Bell RC, Hanna P, Brubaker S. Laparoscopic fundoplication for symptomatic but physiologic gastroesophageal reflux. *J Gastrointest Surg* 2001;5:462-467.
34. Chen RY, Thomas RJ. Results of laparoscopic fundoplication where atypical symptoms coexist with oesophageal reflux. *Aust N Z J Surg* 2000;70:840-842.
35. Pessaux P, Arnaud JP, Delattre JF, Meyer C, Baulieux J, Mosnier H. Laparoscopic antireflux surgery: five-year results and beyond in 1340 patients. *Arch Surg* 2005;140:946-951.
36. del Genio G, Tolone S, del Genio F, Aggarwal R, d'Alessandro A, Allaria A, Rossetti G, Bruscianno L, del Genio A. Prospective assessment of patient selection for antireflux surgery by combined multichannel intraluminal impedance pH monitoring. *J Gastrointest Surg* 2008;12:1491-1496.
37. Mainie I, Tutuian R, Agrawal A, Adams D, Castell DO. Combined multichannel intraluminal impedance-pH monitoring to select patients with persistent gastro-oesophageal reflux for laparoscopic Nissen fundoplication. *Br J Surg* 2006;93:1483-1487.
38. Smith J, Woodcock A, Houghton L. New developments in reflux-associated cough. *Lung* 2010;188(Suppl 1):81-86.



The Prognostic Value of ¹⁸F-FDG PET/CT and KRAS Mutation in Colorectal Cancers

Kolorektal Kanserlerde ¹⁸F-FDG PET/BT ve KRAS Mutasyonunun Prognostik Değeri

Esra Arslan¹, Tamer Aksoy¹, Rıza Umar Gürsu², Nevra Dursun³, Ekrem Çakar⁴, Tevfik Fikret Çermik¹

¹University of Health and Sciences, İstanbul Training and Research Hospital, Clinic of Nuclear Medicine, İstanbul, Turkey

²University of Health and Sciences, İstanbul Training and Research Hospital, Clinic of Medical Oncology, İstanbul, Turkey

³University of Health and Sciences, İstanbul Training and Research Hospital, Clinic of Pathology, İstanbul, Turkey

⁴University of Health and Sciences, İstanbul Training and Research Hospital, Clinic of Surgery, İstanbul, Turkey

Abstract

Objective: Prognostic effect of KRAS mutation and side of tumor in colorectal cancer is a highly controversial subject. Therefore, we evaluated the association between FDG uptake pattern in ¹⁸F-fluoro-2-deoxy-glucose positron emission tomography/computed tomography (¹⁸F-FDG PET/CT) imaging and KRAS mutation and tumor localization in patients with a diagnosis of colon cancer and assessed the effects of these three factors on prognosis and survival.

Methods: Eighty-three patients with colorectal cancer were retrospectively included in this study. ¹⁸F-FDG PET/CT study was performed for pretreatment staging. The maximum standardized uptake value (SUV_{max}) of the primary tumor and survival data of patients were compared between groups. KRAS mutations were detected with the help of real-time Polymerase Chain Reaction technique through genomic DNA extracted from paraffin-embedded tumor tissue blocks. Tumor lesions with potential KRAS mutations were classified as mutant KRAS and wild type.

Results: Twenty five patients were female while 58 were male. The mean age of the patients was 59.8±11.3 years. Mean follow-up was 35.5±18.9 months. Primary tumor was localized in the left colon in 83.1% of patients and in the right colon in 16.9%. KRAS mutation was detected in 54.2% (n=45) of patients. Mean SUV_{max} of patients with primary tumor was estimated to be 21.1±9.1 (range= 6.0-47.5). Mean tumor SUV_{max} of patients with a KRAS mutation (24.0±9.0) was found to be significantly higher than those without KRAS mutation (17.7±8.2) (p=0.001). Mean survival was significantly shorter in patients with locoregional nodal metastasis than in patients without locoregional nodal metastasis as well as in patients with distant nodal metastasis than in patients without distant nodal metastasis and in patients with organ metastasis in initial PET/CT than in patients without organ metastasis. Also, mean survival was nearly statistically-significantly shorter in patients with tumors located in left colon (34.2±19.4) than in right colon (43.2±14.6) (p=0.059). However, we found no significant impact of KRAS mutation on survival.

Conclusion: In our study, we found that tumor localization had no significant effect on prognosis in patients with colon cancer. On the other hand, FDG uptake was observed to be higher in the presence of KRAS mutation and it was concluded that coexistence of KRAS mutation with higher SUV_{max} is a negative prognostic factor.

Keywords: Colorectal cancer, KRAS mutation, ¹⁸F-fluoro-deoxy-glucose positron emission tomography/computerized tomography (¹⁸F-FDG PET/CT), prognosis

Öz

Amaç: Kolorektal kanserde KRAS mutasyonu ve tümörün lokalizasyonu ile ilişkili prognostik etki tartışmalı bir konudur. Bu nedenle ¹⁸F-floro-2-deoksi-glukoz pozitron emisyon tomografi/bilgisayarlı tomografi (¹⁸F-FDG PET/BT) görüntülemeye FDG tutulum paterni ile kolon kanseri tanısı almış hastalarda KRAS mutasyonu ve tümör lokalizasyonu arasındaki ilişkiyi değerlendirdik. Bu üç faktörün prognoz ve sağkalım üzerindeki etkileri değerlendirildi.

Yöntem: Kolorektal kanser tanılı 83 hasta retrospektif olarak bu çalışmaya dahil edildi. Tedavi öncesi evreleme için ¹⁸F-FDG PET/BT çalışması yapıldı. Primer tümöre ait ortalama standart tutulum değeri (SUV_{max}) ve sağkalım verileri gruplar arasında karşılaştırıldı. KRAS mutasyonları, parafine

Address for Correspondence: Esra Arslan MD, University of Health and Sciences, İstanbul Training and Research Hospital, Clinic of Nuclear Medicine, İstanbul, Turkey

Phone: +90 212 459 64 55 **E-mail:** dresraarslan@gmail.com **ORCID ID:** orcid.org/0000-0002-9222-8883

Received: 23.09.2019 **Accepted:** 11.11.2019

©Copyright 2020 by Turkish Society of Nuclear Medicine
Molecular Imaging and Radionuclide Therapy published by Galenos Yayınevi.

gömülü tümör dokusu bloklarından ekstrakte edilen genomik DNA ile gerçek zamanlı polimeraz zincir reaksiyonu tekniği ile tespit edildi. Potansiyel KRAS mutasyonları olan tümöral lezyonlar mutant KRAS ve wild tip olarak sınıflandırıldı.

Bulgular: Olguların 25'i kadın, 58'i erkekti. Hastaların yaş ortalaması 59,8±11,3 idi. Ortalama takip süresi 35,5±18,9 aydı. Primer tümör hastaların %83,1'inde sol kolonda ve %16,9'unda sağ kolonda lokalize idi. KRAS mutasyonu hastaların %54,2'sinde (n=45) tespit edildi. Primer tümörün ortalama SUV_{maks} değeri 21,1±9,1 (dağılım aralığı= 6,0-47,5) olarak hesaplandı. KRAS mutasyonu olan hastaların ortalama tümör SUV_{maks}'i (24,0±9,0), KRAS mutasyonu olmayanlara (17,7±8,2) göre anlamlı derecede yüksek bulundu (p=0,001). Ortalama sağkalım, lokorejyonel nodal metastazı olan hastalarda, lokorejyonel nodal metastazı olmayanlara göre, uzak nodal metastazı olan hastalarda, uzak nodal metastazı olmayanlara göre ve evreleme amaçlı PET/BT'de organ metastazı olanlarda, organ metastazı olmayanlara göre anlamlı olarak daha kısaydı. Ayrıca, ortalama sağkalım sol kolona lokalize tümörü bulunan hastalarda (34,2±19,4) sağ kolona lokalize tümörü bulunanlara göre (43,2±14,6) istatistiksel olarak anlamlı derecede kısaydı (p=0,059). Ancak KRAS mutasyonunun sağkalım üzerinde anlamlı bir etkisi olmadığı belirlendi.

Sonuç: Çalışmamızda, kolon tümörü lokalizasyonunun prognoz üzerinde anlamlı bir etkisinin olmadığını bulduk. Öte yandan, FDG tutulumunun KRAS mutasyonu varlığında daha yüksek olduğu gözlemlendi ve KRAS mutasyonunun yüksek SUV_{maks} ile birlikteliğinin negatif prognostik bir faktör olduğu sonucuna varıldı.

Anahtar kelimeler: Kolorektal kanser, KRAS mutasyonu, ¹⁸F-floro-2-deoksi-glukoz pozitron emisyon tomografi/bilgisayarlı tomografi (¹⁸F-FDG PET/BT), prognoz

Introduction

Colorectal cancer is the third most common malignancy in males and the second most common in females worldwide (1). The disease has high incidence and mortality rates in countries with strong economies while its incidence is reported to be rising in developing countries (2). Western diet is held responsible for this higher incidence. In the 2011 update, the American Institute for Cancer Research reported that red and processed meat is also associated with the increasing incidence of colon cancer (3,4).

Stage, grade, presence of obstruction and/or perforation and presence of vascular invasion, nodal and organ metastases alter the prognosis in colon cancer. In addition, RAS mutation, surgical intervention, radiation therapy and adjuvant chemotherapy methods are also prognostic factors (5,6). It is well known that a group of prominent genetic mutations along with the accumulation of environmental risk factors increase the transformation into colorectal cancers (5). The RAS gene family (KRAS, HRAS and NRAS) codes membrane-bound G proteins (p21^{RAS}) that regulate cell growth and apoptosis via endothelial growth factor receptor (7). KRAS is the most commonly mutated oncogene associated with pancreatic, colorectal and pulmonary malignancies. As a result of deleted KRAS allele, the mutant p21^{KRAS} is activated and induces cell proliferation. Therefore, studies have recently concentrated on KRAS-targeted therapies (8).

It is difficult to establish the association between prognosis and treatment options in patients with colorectal cancer. Heterogeneous survival data are reported even in patients with same pathological grade. Therefore, establishing the prognostic factors accurately is vital in determining high risk patients (9). However, certain contexts are

still controversial for prognosis. For example, there are contradictory prognosis and survival data published on right and left colon which arise from different anatomical and embryonic origins (10). The findings of studies that evaluate right and left colon difference along with the presence of RAS mutation are particularly limited and controversial (11). Therefore, in our study, we evaluated FDG uptake pattern in patients who were initially staged with ¹⁸F-fluoro-2-deoxy-glucose positron emission tomography/computed tomography (¹⁸F-FDG PET/CT) imaging, which is increasingly used in the diagnosis, staging and prognosis determination of various types of cancer, and the presence of KRAS mutation and the association of tumor localization with these two factors and questioned the prognostic power and survival impact of these associations.

Materials and Methods

Patients

Eighty-three patients with colorectal cancer who had staging and follow-up ¹⁸F-FDG PET/CT examinations and tumor specimen for mutation analysis between September 2012 and June 2018 were included in this retrospective study. Histopathologic diagnosis and ¹⁸F-FDG PET/CT imaging were obtained prior to surgical resection and/or chemotherapy/radiation therapy. The study was approved by the İstanbul Training and Research Hospital Local Ethics Committee (no: 2018/1228). The diagnosis and histopathologic analysis of primary colorectal cancer were verified with materials obtained by surgery or from the biopsy. Staging was performed according to Tumor, Node and Metastases (TNM) staging system for colon cancer in concordance with the American Joint Committee on Cancer Guidelines (12).

¹⁸F-FDG PET/CT Imaging

In our study, primary lesions were assessed according to the location (left or right colon), ¹⁸F-FDG uptake and the presence of lymph node and distant metastases in PET/CT. Patients whose blood glucose levels were below 150 mg/dL after six hours of fasting were suitable for the procedure. Sixty minutes after the intravenous injection of 3.7-5.2 MBq/kg ¹⁸F-FDG, PET/CT imaging was obtained from vertex to upper femur (Biograph mCT ultra HD LSO PET/CT; Siemens Molecular Imaging; Hoffman Estates, IL, USA). CT imaging for PET/CT was performed using a multi-detector scanner with 20 slices, at 80-140 kV, 20-266 mAs, 0.8 pitch and 512x512 matrix [personalized settings determined by automatic exposure control system; automatically defined by the software used by manufacturer (CareDose 4D) depending on the patient and region assessed]. CT imaging was performed between vertex and upper-thigh in craniocaudal direction with 5 mm of slice thickness and 0.5 seconds of rotation time. Then, PET imaging was performed in the same range through craniocaudal direction at 8 to 9 bed positions, 1.5 minutes for each PET bed using LSO PET scanner. Ultra HD images were acquired using time of flight (TOF) + true X algorithm at iteration 2 and subset 16 values for reconstruction.

Standardized uptake value (SUV_{max}) was calculated by drawing a region of interest (ROI) around the region with the highest ¹⁸F-FDG uptake. SUV_{max} was calculated automatically by the software using the following formula: maximum activity within ROI (MBq/mL) / injected ¹⁸F-FDG dose (MBq/kg).

Mutation Analysis

DNA, for the assessment of KRAS mutation test, was extracted from paraffin-embedded tumor tissue blocks (Qiagen, Hilden, Germany), which obtained from biopsy materials after primary tumor resection or biopsy. Polymerase chain reaction was performed via some extraction, incubation and amplifications cycles according to the manufacturer's instructions. Tumor lesions with potential KRAS mutations in

Codon 12;

- + ___ Gly12Asp (GGT>GAT)
- + ___ Gly12Val (GGT>GTT)
- + ___ Gly12Cys (GGT>TGT)
- + ___ Gly12Ser (GGT>AGT)
- + ___ Gly12Ala (GGT>GCT)
- + ___ Gly12 Arg (GGT>CGT)
- + ___ Codon 12 mutation, not otherwise specified,

Codon 13;

- + ___ Gly13Asp (GGC>GAC)
- + ___ Gly13Arg (GGC>CGC)
- + ___ Gly13Cys (GGC>TGC)
- + ___ Gly13Ala (GGC>GCC)
- + ___ Gly13Val (GGC>GTC)
- + ___ Codon 13 mutation, not otherwise specified,

Codon 59,

Codon 61;

- + ___ Gln61Leu (CAA>CTA)
- + ___ Gln61His (CAA>CAC)
- + ___ Codon 61 mutation, not otherwise specified,

Codon 117,

Codon 146;

- + ___ Ala146Thr (G436A) (GCA>ACA)
- + ___ Codon 146 mutation, not otherwise specified was detected.

Statistical Analysis

All data were analyzed using SPSS software for Windows (v21.0; IBM, Armonk, NY, USA). Data were expressed as mean and standard deviation, median (min-max), distribution frequencies and percentages, when appropriate. Normalization of data distribution was evaluated using Kolmogorov-Smirnov test. For variables that were not normally-distributed, comparison was performed using Mann-Whitney U and Kruskal-Wallis tests while correlation was evaluated using Pearson's test. Categorical variables were evaluated using chi-square test. Survival rates were evaluated with Kaplan-Meier analysis. P values <0.05 were considered statistically significant.

Results

Out of 83 subjects with a diagnosis of colorectal cancer, 25 (30.1%) were female and 58 (69.9%) were male. Mean age was 59.8±11.3 years (range=35-81). Sixty-nine (83.1%) tumoral lesions were located in the left colon while 14 (16.9%) were located in the right colon. KRAS mutation was found in 54.2% (n=45) of patients. Thirty-eight (84.4%) of KRAS mutant colorectal tumors were left-sided while 7 (15.6%) were right-sided. Also, ¹⁸F-FDG uptake was observed in all primary lesions (n=83) and mean SUV_{max} was estimated to be 21.1±9.2 (median=20.2, range=6.0-47.5). When clinical characteristics of the patients were considered along with ¹⁸F-FDG uptake, no statistically significant association was found between the mean SUV_{max} in the group with patients younger than 50

years (19.6±6.2) (n=18) and the mean SUV_{max} in the group with patients ≥50 years (21.5±9.8) (n=65) (p=0.436). Similarly, patient gender had no statistically significant impact on primary tumor mean SUV_{max} (p=0.452) (Table 1). When subjects were evaluated for tumor localization, there was no difference between left-sided (21.2±8.6) and right-sided (20.4±11.6) tumors in terms of mean SUV_{max} (p=0.768). Mean tumor SUV_{max} of patients with KRAS mutation was 24.0±9.0 (Figure 1) while this value was calculated as 17.7±8.2 (Figure 2) in patients without mutation (wild type). Therefore, mean SUV_{max} in subjects with KRAS mutation was significantly higher when compared to wild type (p=0.001) (Table 1).

According to the staging 1 patient had stage II, 13 patients had stage III, and 69 patients had stage IV disease according to The American Joint Committee on Cancer TNM classification and staging system. Sixty-eight (81.9%) subjects were found to have locoregional nodal metastases at the time of diagnosis; 54 (79%) of these tumors were left-sided and 14 (21%) were right-sided. Twenty-six (31.3%) subjects had distant nodal metastases, 20 (77%) of which were left-sided and 6 (23%) of which were right-sided colon tumors. There was no difference between subjects with locoregional or distant nodal metastases and subjects without nodal metastases in terms of mean tumor SUV_{max} (p=0.928 and 0.135, respectively) (Table 1). Initial PET/CT revealed organ metastases in 81.9% (n=68) of patients, while distant metastases developed later in follow-up in 18.1% (n=15). Similarly, there was no statistically significant difference between the group with distant metastases at diagnosis and the group with metastases developed in follow-up in terms of primary tumor mean SUV_{max} (p=0.323). Distant organ metastases

were most frequently observed in liver (47.0%, n=39), followed by lung (19.3%, n=16), peritoneum (8.4%, n=7) and liver + peritoneum (4.8%, n=4). Of patients, 20.5% (n=17) had multiorgan metastases.

Mean follow-up period of patients included was 35.5±18.9 months (range=3.8-73.4 months). Comparison of mean survival and clinical characteristics is presented in Table 2. According to this, mean survival time of patients with locoregional nodal metastasis and distant nodal metastasis (33.4±18.2 and 29.8±15.6 months, respectively) was significantly shorter than the survival time of patients

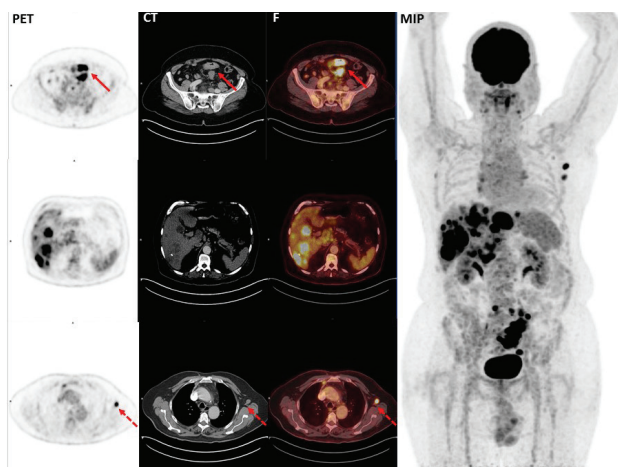


Figure 1. A 65-year-old male patient with mutant type adenocarcinoma localized to sigmoid colon positron emission tomography, computed tomography, fusion, maximum intensity projection. Red arrows show fluorodeoxyglucose uptake of the primary tumor, primary tumor: SUV_{max}: 31.5 with multiple liver metastases. Dotted red arrows show left axillary lymph node metastases. SUV_{max}: Maximum standardized uptake value, PET: Positron emission tomography, CT: Computed tomography, F: Fusion, MIP: Maximum intensity projection

Table 1. The association between mean SUV _{max} and clinical, histopathological features of patients				
	Clinical variables	n (%)	SUV _{max} (Mean ± SD)	p-value
KRAS mutations	Mutant	45 (54.2%)	24.0±9.0	0.001*
	Wild	38 (45.8%)	17.7±8.2	
Tumor localization	Left	69 (83.1%)	21.2±8.6	0.768
	Right	14 (16.9%)	20.4±11.6	
Gender	Female	25 (30.1%)	19.9±7.5	0.452
	Male	58 (69.9%)	21.6±9.7	
Age	<50	18 (21.7%)	19.6±6.2	0.436
	≥50	65 (78.3%)	21.5±9.8	
Locoregional nodal metastasis	Absent	15 (18.1%)	20.9±9.3	0.928
	Present	68 (81.9%)	21.1±9.1	
Distant nodal metastasis	Absent	57 (68.7%)	21.9±10.1	0.135
	Present	26 (31.3%)	19.2±6.3	
Distant organ metastasis	Initially	68 (81.9%)	20.6±9.1	0.323
	Subsequently	15 (18.1%)	23.2±9.1	

*= p<0.05 statistically significant, SUV_{max}: Maximum standardized uptake value, SD: Standard deviation

without locoregional nodal metastasis and distant nodal metastasis (33.4±18.2 and 29.8±15.6 months, respectively) (p=0.037 and 0.046, respectively) (log rank=0.020 and 0.001, respectively) (Graph 1, 2). Also, mean survival time of patients with organ metastasis at diagnosis (33.4±19.0 months) was observed to be significantly shorter than patients who developed distant metastasis during follow-up (44.7±16.1 month) (p=0.037, log rank=0.023) (Graph 3). Mean survival was nearly statistically-significantly shorter in patients with tumors located to left colon (34.2±19.4) than in right colon (43.2±14.6) (p=0.059). KRAS mutation, age and sex were found to have no statistically significant influence on mean survival (p=0.136, 0.224 and 0.257, respectively).

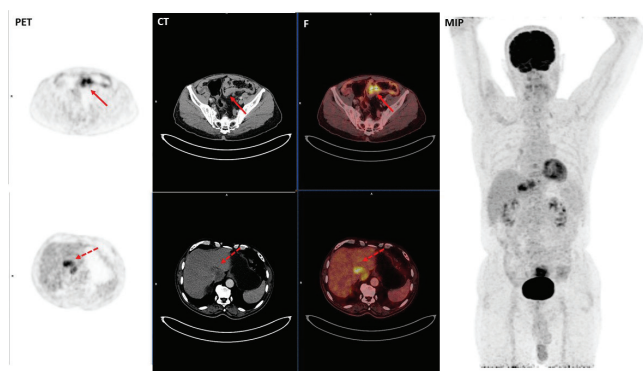
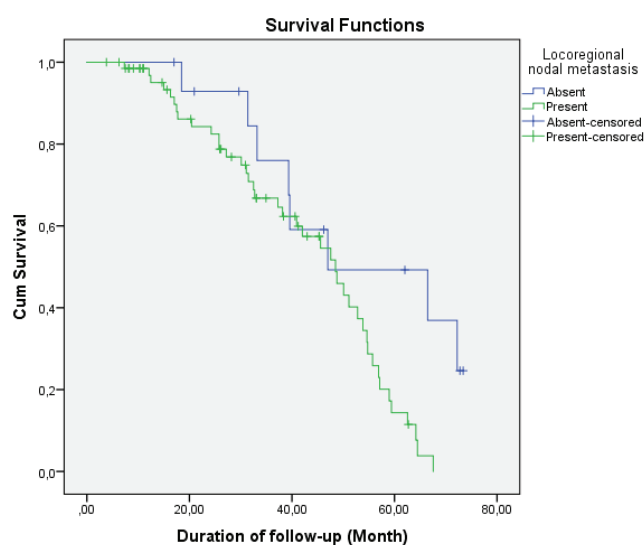


Figure 2. A 70-year-old male patient with wild type adenocarcinoma localized to sigmoid colon positron emission tomography, computed tomography, Fusion, maximum intensity projection. Red arrows show fluorodeoxyglucose uptake of the primary tumor. Primary tumor: SUV_{max}: 11.5 dotted red arrows show hepatic metastases
SUV_{max}: Maximum standardized uptake value, PET: Positron emission tomography, CT: Computed tomography, F: Fusion, MIP: Maximum intensity projection

Mean survival time after diagnosis was estimated to be 17.4±13.8 months (range=1.3-62.2 months). Mean overall survival after diagnosis of patients with KRAS-mutant and wild-type tumors was 18.3±16.3 and 16.7±11.5 months, respectively. Also, mean overall survival of patients with primary tumor located to left and right colon was 18.8±14.9 and 12.6±7.3 months, respectively with no statistically significant difference between groups (p values=0.818 and 0.391, respectively).

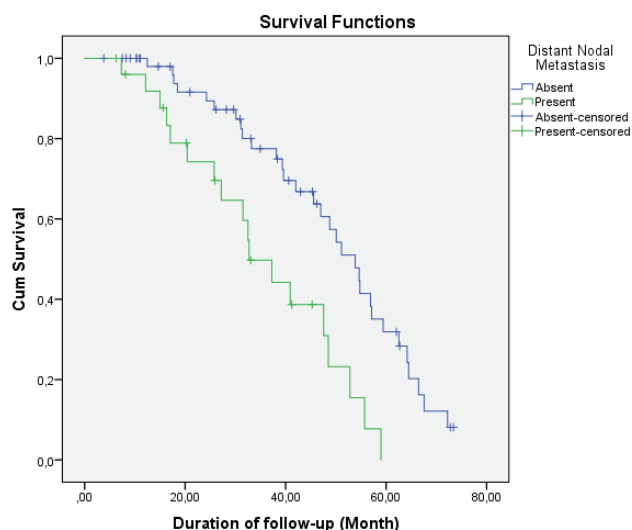
In our study, 52 patients (62.7%) received bevacizumab, 13 patients (15.7%) received cetuximab and 8 patients (9.6%) received panitumumab protocol as primary



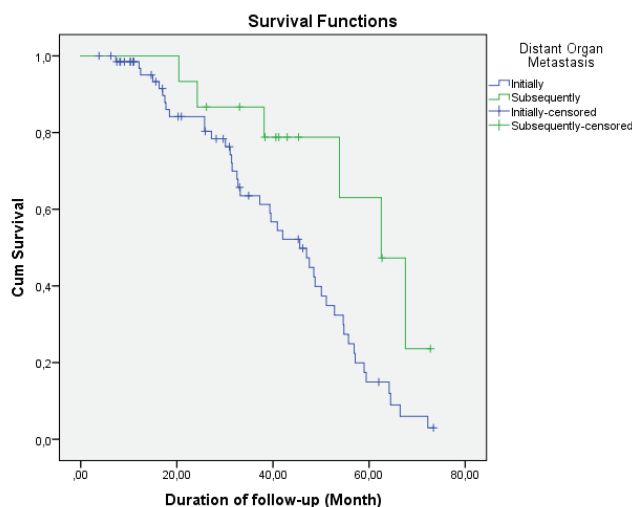
Graph 1. Survival chart according to locoregional nodal involvement (log rank=0.020)

Table 2. Comparison of patients' clinical/histopathological features and mean survival times				
	Clinical variables	n (%)	Survival (month) (Mean ± SD)	p-value
KRAS mutations	Mutant	45 (54.2%)	32.6±19.8	0.136
	Wild	38 (%45.8%)	38.8±17.5	
Tumor localization	Left	69 (%83.1%)	34.2±19.4	0.059
	Right	14 (%16.9%)	43.2±14.6	
Gender	Female	25 (%30.1%)	39.3±19.9	0.224
	Male	58 (%69.9%)	33.8±18.4	
Age	<50	18 (%21.7%)	40.0±21.1	0.257
	≥50	65 (%78.3%)	34.2±18.3	
Locoregional nodal metastasis	Absent	15 (%18.1%)	44.6±20.3	0.037*
	Present	68 (%81.9%)	33.4±18.2	
Distant nodal metastasis	Absent	57 (%68.7%)	38.0±19.9	0.046*
	Present	26 (%31.3%)	29.8±15.6	
Distant organ metastasis	Initially	68 (%81.9%)	33.4±19.0	0.037*
	Subsequently	15 (%18.1%)	44.7±16.1	

*= p<0.05 statistically significant, SD: Standard deviation



Graph 2. Survival chart according to distant nodal involvement (log rank=0.001)



Graph 3. Survival chart according to distant visceral organ metastasis (log rank=0.023)

treatment. Of patients 31.3% (n=26) showed progression and 6 of these (7.2%) received cetuximab, 17 (20.5%) received bevacizumab and 1 (1.2%) received aflibercept as second-line treatment. The presence of KRAS mutation and tumor localization were not significantly associated with progression ($p=0.603$ and 0.687 , respectively). At the end of follow-up period, 57.8% of patients (n=48) were deceased. Among survivors, 7 patients (8.4%) were in remission, 20 patients were refractory and 8 were lost to follow-up (9.6%). The presence of KRAS mutation and tumor localization were not significantly associated with mortality ($p=0.073$ and 0.563 , respectively).

Discussion

Despite the globally rising prevalence of colorectal cancers, recent developments in early diagnosis and treatment options have caused a decline in its incidence in especially advanced ages. However, the increase in the incidence of colorectal cancers in patients younger than 50 years is noteworthy (1,2,3,4). Because poor prognostic factors tend to accumulate in younger patients, predictive value of prognostic factors gain importance (9). Increased FDG uptake in ¹⁸F-FDG PET/CT imaging, which has been widely used in the diagnosis and staging of many malignancies including breast, gastric and lung carcinoma as well as colorectal cancer, is significantly associated with aggressive tumor pattern and poor prognosis (13,14,15,16). Bundschuh et al. (17) evaluated 27 patients with locally advanced rectal cancer and reported that ¹⁸F-FDG PET/CT imaging has significant prognostic advantage in evaluating disease progression and provides important data in assessing treatment response and determining patients with high risk. In their study with 67 patients with colorectal cancer, Petersen et al. (18) stated the importance of ¹⁸F-FDG PET/CT imaging in staging and underlined that it was possible to change treatment strategy in approximately 30% of patients with the contribution of ¹⁸F-FDG PET/CT imaging. Besides these, the most important factors determining the prognosis in colorectal cancers are certainly the presence of nodal metastases and distant organ metastases. However, there are also prognostic factors specific to colorectal cancers which are sometimes controversial. The leading is KRAS mutations (8,9). Roth et al. (19) evaluated the prognostic effects of KRAS and BRAF mutations by extracting DNA from 1321 of 1404 specimens of colon cancer. The researcher concluded that KRAS mutation had no major prognostic value in patients with stage II and III colon cancer and did not influence survival. Ogino et al. (20) found similar results and reported that KRAS mutation had no effect on prognosis or survival. On the contrary, Lee et al. (21) found that KRAS mutations had negative prognostic effects on 437 patients with stage II and III colon cancer. Vogelaar et al. (22) pointed out the association between the presence of KRAS mutation and shorter survival. Similarly, Ribeiro et al. (23) evaluated 58 patients with metastatic colon adenocarcinoma and reported that KRAS mutation was significantly associated with lymph node metastasis and organ metastasis when evaluated together with CD44 and CD166 expression. As the literature data indicate, findings about KRAS are quite contradictory. In our study, we observed that survival times shortened significantly with locoregional and distant nodal

metastasis and the presence of distant organ metastasis at diagnosis while KRAS mutation had no statistically significant effect on mean survival. Also, the presence of KRAS mutation was found to have no significant impact on patients who were deceased or showed progression after treatment. However, when KRAS mutation was assessed together with FDG uptake pattern, mean tumor SUV_{max} was observed to increase significantly in subjects with KRAS mutation. Therefore, considering that increased FDG uptake is associated with aggressive tumor characteristics and negative prognostic effect, increased SUV_{max} in the presence of KRAS mutations was interpreted as a poor prognostic factor.

Another controversial topic in prognostic factor assessment for colon cancer is tumor side. Embryologic, histological, genetic and immunological differences of the right and left colon provide basis for these discussion. Certain studies in the literature could not define any difference between the right and left colon that can affect survival, while others reported the left colon to be associated with higher survival (10). Karim et al. (24) evaluated 6365 patients who were diagnosed with early stage colon cancer between 2002 and 2008 and concluded that tumor side had no significant association with overall survival or cancer-specific survival. In contrast, Petrelli et al. (25) conducted a meta-analysis that includes 66 studies with 1.437.846 patients and reported that tumors localized to left colon had significantly lower risk of death and this was independent of stage, ethnicity and adjuvant chemotherapy. Similarly, in the study by Ulanja et al. (10) that included 163,986 patients with colon cancer with the help of the "Surveillance, Epidemiology, and End Results" database, the researchers reported that 52.3% of tumors were localized in the right colon and 47.7% were in the left colon while left colon cancer was significantly associated with better survival. In our study, 83.1% of tumoral lesions were left-sided while 16.9% were right-sided. We found no statistically significant difference between tumors localized to right or left colon both in terms of FDG uptake and survival. Also, tumor localization and the presence of KRAS mutation had no statistically significant impact on mortality. However, we think that our prognostic evaluation using both ¹⁸F-FDG PET/CT imaging modality and the presence of KRAS mutation may have a predictive value.

Conclusion

In conclusion, side of tumor in patients with colorectal cancer was not found to have significant impact on prognosis in our study. On the other hand, we observed an association between the presence of KRAS mutation and increased FDG uptake in the primary tumor. We think that this association may have a predictive value for poor prognosis and our data may contribute to patient management especially in this subgroup.

Ethics

Ethics Committee Approval: The study has been approved by the İstanbul Training and Research Hospital Local Ethics Committee (no: 2018/1228).

Informed Consent: Consent form was filled out by all participants.

Peer-review: Externally and internally peer-reviewed.

Authorship Contributions

Surgical and Medical Practices: E.Ç., N.D., Concept: E.A., T.A., T.F.Ç., Design: E.A., Data Collection or Processing: E.A., R.U.G., Analysis or Interpretation: E.A., T.F.Ç., Literature Search: T.A., E.A., Writing: E.A., T.A., T.F.Ç.

Conflict of Interest: No conflict of interest was declared by the authors.

Financial Disclosure: The authors declared that this study received no financial support.

References

1. Torre LA, Bray F, Siegel RL, Ferlay J, Lortet-Tieulent J, Jemal A. Global cancer statistics, 2012. *CA Cancer J Clin* 2015;65:87-108.
2. Stewart BW, WC. World cancer report 2014. Available at: <http://publications.iarc.fr/Non-Series-Publications/World-Cancer-Reports/World-Cancer-Report-2014>. Accessed June 8, 2019.
3. Pan P, Yu J, Wang LS. Colon cancer: what we eat. *Surg Oncol Clin N Am* 2018;27:243-267.
4. World Cancer Research Fund/American Institute for Cancer Research. Continuous update project report. Food, nutrition, physical activity, and the prevention of colorectal cancer. Available at: <http://www.aicr.org/continuousupdate-project/reports/Colorectal-Cancer-2011-Report.pdf>. Accessed July2, 2019.
5. Nakayama M, Oshima M. Mutant p53 in colon cancer. *J Mol Cell Biol*. 2018;11:267-276.
6. Amri R, Bordeianou LG, Sylla P, Berger DL. Impact of screening colonoscopy on outcomes in colon cancer surgery. *JAMA Surg* 2013;148:747-754.
7. Haigis KM, Kendall KR, Wang Y, Cheung A, Haigis MC, Glickman JN, Niwa-Kawakita M, Sweet-Cordero A, Sebolt-Leopold J, Shannon KM,

- Settleman J. Differential effects of oncogenic K-Ras and N-Ras on proliferation, differentiation and tumor progression in the colon. *Nat Genet* 2008;40:600-608.
8. Brito H, Martins AC, Lavrado J, Mendes E, Francisco AP, Santos SA, Ohnmacht SA, Kim NS, Rodrigues CM, Moreira R, Neidle S. Targeting KRAS oncogene in colon cancer cells with 7-carboxylate indolo [3, 2-b] quinoline tri-alkylamine derivatives. *PLoS One* 2015;10:e0126891.
 9. Graziosi L, Elisabetta M, Rebonato A, Donini A. Preoperative Serum Markers Prognostic Evaluation in Colon Cancer Patients. *J Cancer Sci Ther* 2018;10:22-26.
 10. Ulanja MB, Rishi M, Beutler BD, Sharma M, Patterson DR, Gullapalli N, Ambika S. Colon Cancer Sidedness, Presentation, and Survival at Different Stages. *J Oncol* 2019;2019:4315032.
 11. Venook AP, Niedzwiecki D, Innocenti F, Fruth B, Greene C, O'Neil BH, Shaw JE, Atkins JN, Horvath LE, Polite BN, Meyerhardt JA. Impact of primary (1^o) tumor location on overall survival (OS) and progression-free survival (PFS) in patients (pts) with metastatic colorectal cancer (mCRC): Analysis of CALGB / SWOG 80405 (Alliance). <http://meetinglibrary.asco.org/record/123617/abstract>. Presented June 25, 2016. Accessed May 26, 2017.
 12. Puppa G, Sonzogni A, Colombari R, Pelosi G. TNM staging system of colorectal carcinoma: a critical appraisal of challenging issues. *Arch Pathol Lab Med* 2010;134:837-852.
 13. Groheux D, Cochet A, Humbert O, et al. ¹⁸F-FDG PET/CT for staging and restaging of breast cancer. *J Nucl Med* 2016;57:17-26.
 14. Wu Z, Zhao J, Gao P et al. Prognostic value of pretreatment standardized uptake value of F-18- fluorodeoxyglucose PET in patients with gastric cancer: a meta-analysis. *BMC Cancer* 2017;17:275.
 15. Aogi K, Kadoya T, Sugawara Y, et al. Utility of ¹⁸F-FDG-PET/CT for predicting prognosis of luminal-type breast cancer. *Breast Cancer Res Treat* 2015;150:209-217.
 16. Ben-Haim S, Ell P. ¹⁸F-FDG PET and PET/CT in the evaluation of cancer treatment response. *J Nucl Med* 2009;50:88-99.
 17. Bundschuh RA, Dinges J, Neumann L, Seyfried M, Zsótér N, Papp L, Rosenberg R, Becker K, Astner ST, Henninger M, Herrmann K. Textural parameters of tumor heterogeneity in ¹⁸F-FDG PET/CT for therapy response assessment and prognosis in patients with locally advanced rectal cancer. *J Nucl Med* 2014;55:891-897.
 18. Petersen R.K, Hess S, Alavi A, Carlsen PFH. Clinical impact of FDG-PET/CT on colorectal cancer staging and treatment strategy. *Am J Nucl Med Mol Imaging* 2014;4(5):471-482.
 19. Roth AD, Tejpar S, Delorenzi M, Yan P, Fiocca R, Klingbiel D, Dietrich D, Biesmans B, Bodoky G, Barone C, Aranda E. Prognostic role of KRAS and BRAF in stage II and III resected colon cancer: results of the translational study on the PETACC-3, EORTC 40993, SAKK 60-00 trial. *J Clin Oncol* 2010;28:466-474.
 20. Ogino S, Meyerhardt JA, Irahara N, Niedzwiecki D, Hollis D, Saltz LB, Mayer RJ, Schaefer P, Whittom R, Hantel A, Benson AB. KRAS mutation in stage III colon cancer and clinical outcome following intergroup trial CALGB 89803. *Clin Cancer Res* 2009;15:7322-7329.
 21. Lee DW, Kim KJ, Han SW, Lee HJ, Rhee YY, Bae JM, Cho NY, Lee KH, Kim TY, Oh DY, Im SA. KRAS mutation is associated with worse prognosis in stage III or high-risk stage II colon cancer patients treated with adjuvant FOLFOX. *Ann Surg Oncol* 2015;22:187-194.
 22. Vogelaar FJ, van Erning FN, Reimers MS, van der Linden H, Pruijt H, van den Brule AJ, Bosscha K. The prognostic value of Microsatellite Instability, KRAS, BRAF and PIK3CA mutations in stage II colon cancer patients. *Mol Med* 2015;21:1038-1046.
 23. Ribeiro KB, da Silva Zanetti J, Ribeiro-Silva A, Rapatoni L, de Oliveira HF, da Cunha Tirapelli DP, Garcia SB, Feres O, da Rocha JJ, Peria FM. KRAS mutation associated with CD44/CD166 immunoreexpression as predictors of worse outcome in metastatic colon cancer. *Cancer Biomark* 2016;16:513-521.
 24. Karim S, Brennan K, Nanji S, Berry SR, Booth CM. Association between prognosis and tumor laterality in early-stage colon cancer. *JAMA Oncol* 2017;3:1386-1392.
 25. Petrelli F, Tomasello G, Borronovo K, Ghidini M, Turati L, Dallera P, Passalacqua R, Sgroi G, Barni S. Prognostic survival associated with left-sided vs right-sided colon cancer: a systematic review and meta-analysis. *JAMA Oncol* 2017;3:211-219.



Metabolic Characteristics and Diagnostic Contribution of ¹⁸F-FDG PET/CT in Gastric Carcinomas

Mide Kanserinin Metabolik Özellikleri ve ¹⁸F-FDG PET/CT'nin Tanısal Katkısı

Esra Arslan¹, Tamer Aksoy¹, Cihan Gündoğan¹, Çiğdem Şen¹, Selda Yılmaz Tatar², Nevra Dursun³, Tevfik Fikret Çermik¹

¹University of Health and Sciences, İstanbul Training and Research Hospital, Clinic of Nuclear Medicine, İstanbul, Turkey

²Yeniüzyıl University, Gaziosmanpaşa Hospital, Department of Nuclear Medicine, İstanbul, Turkey

³University of Health and Sciences, İstanbul Training and Research Hospital, Department of Pathology, İstanbul, Turkey

Abstract

Objectives: The aim of this study was to evaluate ¹⁸F-fluoro-2-deoxy-glucose (FDG) uptake patterns in primary tumors and metastatic lesions, and also to assess the diagnostic contribution of positron emission tomography/computed tomography (PET/CT) in the initial staging of gastric cancer (GC).

Methods: The total number of 341 patients with GC were included in this study. All ¹⁸F-FDG PET/CT imagings were performed for initial staging. The maximum standardized uptake value (SUV_{max}) of primary tumor, obtained from ¹⁸F-FDG PET/CT imaging was compared between subtypes of GC.

Results: Mean SUV_{max} of 339 patients' primary tumor was 12.9±8.6. The highest mean SUV_{max} was detected in patients with medullary subtype GC (17.8±9.9) while the lowest mean SUV_{max} (9.7±7.6) was seen in signet ring cell carcinoma (SRCC). The primary mean SUV_{max} was found statistically higher in adenocarcinoma (AC) group than SRCC group (p<0.001). Higher SUV_{max} values were found statistically significantly correlated with advanced age (aged ≥60) and increased tumor size (>3 cm) in patients with AC (p=0.03). Primary tumor SUV_{max} was found statistically higher in regional lymph node (RLN) positive patients than in RLN negative patients in AC and SRCC groups (p<0.001 and p=0.012, respectively). Also, in patients with SRCC, SUV_{max} was significantly higher in the distant metastatic group than in the group without metastasis (p=0.025).

Conclusion: Increased primary tumor SUV_{max} was associated with some of clinical parameters such as age and RLN metastasis in patients with AC. However, there was no relationship between distant metastatic state and primary tumor ¹⁸F-FDG uptake in AC. However, high SUV_{max} of primary tumor in SRCC was associated with regional and distant metastasis, and primary tumor ¹⁸F-FDG uptake may be a prognostic value for this subgroup.

Keywords: Gastric cancer, ¹⁸F-fluorodeoxyglucose positron emission tomography/computed tomography (¹⁸F-FDG PET/CT), adenocarcinomas

Öz

Amaç: Bu çalışmanın amacı primer tümörlerde ve metastatik lezyonlarda ¹⁸F-floro-2-deoksi-glukoz (¹⁸F-FDG) tutulum paternlerini değerlendirmek ve ayrıca mide kanserinin (MK) evrelemesinde pozitron emisyon tomografi/bilgisayarlı tomografi'nin (PET/CT) tanısal katkısını değerlendirmektir.

Yöntem: Çalışmaya toplam 341 MK hastası dahil edildi. Primer evreleme ¹⁸F-FDG PET/CT görüntüleme ile yapıldı. ¹⁸F-FDG PET/CT görüntülemenden elde edilen primer tümöre ait maksimum standart tutulum (SUV_{max}) MK alt tipleri arasında karşılaştırıldı.

Bulgular: Üç yüz otuz dokuz hastaya ait primer tümörün ortalama SUV_{max} değeri 12,9±8,6 idi. En yüksek ortalama SUV_{max} medüller alt tip MK'li hastalarda (17,8±9,9), en düşük ortalama SUV_{max} (9,7±7,6), taşlı yüzük hücreli mide kanserinde (TYHMK) görüldü. Ortalama SUV_{max} adenokarsinom (AK) grubunda TYHMK grubundan istatistiksel olarak daha yüksek bulundu (p<0,001).

Daha yüksek SUV_{max} değerleri, AK'li hastalarda ileri yaşla (yaş ≥60) ve artan tümör büyüklüğü (>3 cm) ile istatistiksel olarak anlamlı derecede ilişkili bulundu (p=0,03). Primer tümör SUV_{max} bölgesel lenf nodu (RLN) pozitif olan hastalarda AK ve TYHMK gruplarındaki RLN negatiflerden anlamlı

Address for Correspondence: Esra Arslan MD, University of Health and Sciences, İstanbul Training and Research Hospital, Clinic of Nuclear Medicine, İstanbul, Turkey

Phone: +90 212 459 64 55 **E-mail:** dresraarslan@gmail.com **ORCID ID:** orcid.org/0000-0002-9222-8883

Received: 19.11.2019 **Accepted:** 07.01.2020

©Copyright 2020 by Turkish Society of Nuclear Medicine
Molecular Imaging and Radionuclide Therapy published by Galenos Yayınevi.

olarak yüksek bulundu ($p<0,001$, $p=0,012$, sırasıyla). Ayrıca, TYHMK'li hastalarda, uzak metastatik grupta SUV_{max} , metastazı olmayan gruba göre anlamlı derecede yüksekti ($p=0,025$).

Sonuç: Primer tümör SUV_{max} 'ı yüksek AK'li hastalarda yaş ve RLN metastazı gibi bazı klinik parametrelerle ilişkilendirildi. Bununla birlikte, AK'de uzak metastatik durum ile primer tümör ¹⁸F-FDG tutulumu arasında ilişki bulunmadı. Bununla birlikte, TYHMK'deki primer tümörün yüksek SUV_{max} 'ı, bölgesel ve uzak metastaz ile ilişkiliydi ve primer tümörün ¹⁸F-FDG tutulumu, bu alt grup için prognostik bir değeri olabileceğini düşünmekteyiz.

Anahtar kelimeler: Mide kanseri, ¹⁸F-florodeoksiglukoz pozitron emisyon tomografisi/bilgisayarlı tomografi (¹⁸F-FDG PET/CT), adenokarsinomlar

Introduction

Gastric cancer (GC) is the fifth most common cancer worldwide with an estimated 900.000 new cases diagnosed annually (1). Adenocarcinomas (AC), the most prevalent GC subtype, is the third leading cause of cancer-related deaths (2). The main issue pointed out by reports is that GC typically constitutes higher proportion of new mortality/cases compared with more prevalent cancers (3). The majority of patients with GC (64%) are usually diagnosed when the disease is already in advanced or metastatic stages (4).

Recently, ¹⁸F-fluoro-2-deoxy-glucose positron emission tomography/computed tomography (¹⁸F-FDG PET/CT) has been demonstrated as a noninvasive, useful modality for diagnosis and staging of patients with cancer (5). The higher maximum standardized uptake value (SUV_{max}) levels were found significantly associated with the metastasis and poor prognosis in several types of cancer, including breast, esophagus and non-small cell lung cancers (6,7,8).

The role of ¹⁸F-FDG PET/CT in GC remains controversial, as reports indicate low sensitivity for staging and predicting prognosis (5). In contrast to limited sensitivity reports, several studies concluded an acceptable prognostic and clinical value of ¹⁸F-FDG PET/CT in GC staging (9,10).

In this study, we aimed to evaluate ¹⁸F-FDG uptake patterns in GC subtypes, not only in primary tumors but also in nodal and distant metastatic lesions, as well as to assess the diagnostic contribution of PET/CT to nodal involvement and distant metastasis in the initial staging of GC.

Materials and Methods

Patients

The total of 341 patients with GC [256 (75.1%) males, 85 (24.9%) females, mean age 62.2 ± 11.5 years (range: 23-90)], who were diagnosed as having primary GC with gastroscopy, histopathological examination and underwent ¹⁸F-FDG PET/CT for initial staging between May 2011 and July 2018 were included in this study. Patients who were previously diagnosed as having another malignancy were not included in the study.

Primary GC diagnosis and histopathological analysis have been based on tissue samples derived by endoscopic biopsies performed before ¹⁸F-FDG PET/CT imaging. ¹⁸F-FDG PET/CT imagings were performed preoperatively or before chemotherapy/radiotherapy for all patients. Staging was performed based on the TNM classification for carcinoma of the stomach according to the 8th edition of the American Joint Committee on Cancer guidelines (11). The staging system depends on extend of the tumor, regional lymph node (RLN) and distant metastasis. Also, other prognostic factors such as tumor diameter, histological grade, lymphovascular invasion, perineural invasion, surgical margins were evaluated pathologically on resection specimens. The histological classification proposed by the World Health Organization was used for pathological reporting (12). This retrospective study was approved by the local ethics committee (2017/1048). All patients included were asked for their verbal or written consent for the use of their individual clinical findings for research purposes.

¹⁸F-FDG PET/CT Imaging

Patients with blood glucose levels lower than 150 mg/dL after at least six hours of fasting were admitted for the procedure. Standard 3.7-5.2 MBq/kg (0.1-0.2 mCi/kg) ¹⁸F-FDG intravenous injection was administered to the patients. Sixty minutes after 4 injection of ¹⁸F-FDG, whole body PET/CT imaging was obtained including the area from vertex to upper femur at supine position (first 42 imagings were performed by Biograph 6 HD LSO, and subsequent 299 imagings were performed by mCT 20 ultra HD LSO PET/CT), (Siemens molecular imaging, Hoffmann Estates, Illinois, USA). A solution containing 75 cc mannitol and 2 grams of locust bean gum was added to 1.5 liters of water for all patients to drink as negative oral contrast agent during the time period between injection and image acquisition. CT imaging for PET/CT was performed using a multi-detector scanner with 6 and 20 slices, at 80-140 kV, 20-266 mAs, 0.8 pitch and 512x512 matrix [personalized settings determined by automatic exposure control system; automatically defined by the software used by manufacturer (CareDose 4D) depending on the patient and region assessed]. CT imaging was performed

between vertex and upper-thigh in craniocaudal direction with 5 mm of slice thickness and 0.5 seconds of rotation time. Then, PET imaging was performed in the same range through craniocaudal direction at 8 to 9 bed positions, 1.5 minutes for each PET bed using Siemens mCT 20 ultra HD LSO PET-CT scanner. Ultra HD images were acquired using Time of flight + True X algorithm for Siemens mCT 20 ultra HD LSO PET-CT at iteration 2 and subset 16 values for reconstruction. 3D imaging was performed using Siemens Biograph 6 HD LSO PET-CT scanner at 6 to 8 bed positions for 2.5 minutes per bed. HD images were acquired using True X algorithm for Siemens Biograph 6 HD LSO PET-CT.

Interpretation of PET/CT Images

Images acquired from all patients were evaluated by at least two senior nuclear medicine physicians, at the workstation both visually and semi-quantitatively in axial, coronal and sagittal planes. ¹⁸F-FDG PET/CT image evaluation was done unaware of previous imaging results of subjects. For visual evaluation, foci of increased ¹⁸F-FDG uptake compared to background and CT findings were evaluated in conjunction. For semi-quantitative analysis, SUV_{max} was measured by placing the "volume-of-interest" around the ¹⁸F-FDG positive primary and nodal metastatic lesions in visual evaluation. Focal FDG uptakes with an abnormal soft tissue mass or a lymph node on CT counterpart was considered significant for malignancy. For SUV_{max} calculation, "regions of interest" (ROI) which included the location of highest uptake was drawn on PET cross-sections. SUV_{max} was calculated according to the following formula: Maximum activity inside the ROI (MBq/gr) /injected ¹⁸F-FDG dosage (MBq/kg body mass). Maximum tumor diameter and wall thickness were measured from the axial CT scan of the PET/CT imaging.

Statistical Analysis

All the data were analyzed with SPSS software for Windows (v21.0; IBM, Armonk, NY, USA). Individual and aggregate data were summarized using descriptive statistics including mean, standart deviations, medians (minimum-maximum), frequency distributions and percentages. Normality of data distribution was verified by Kolmogorov-Smirnov test. Comparison of the variables with normal distribution was made with Student t-test. Evaluation of categorical variables was performed by chi-square test. The kappa statistic was calculated to evaluate the agreement. P values of <0.05 were considered statistically significant.

Results

In our study group, the prevalence was highest in the patients' seventh decade of life (37.2%), followed by

the sixth decade (25.9%). In PET/CT imaging, 22.0% (n=75) of the lesions were detected in the proximal part (cardioesophageal junction or cardia), 29.6% (n=101) in the middle part (fundus and corpus), 38.7% (n=132) in the distal part (antral or pyloric) and 9.7% (n=33) of the lesions were diffuse in the stomach.

The final histopathologic diagnosis was obtained in 70.0% of patients (n=239) only by endoscopic biopsy. These patients were directed to non-surgical treatments due to inoperability. In this subgroup, the findings obtained by the second PET/CT were used as the gold standard in the following three or six months after diagnosis. Remaining 102 patients underwent gastrectomy and nodal staging was performed together with detailed histopathological analysis in these patients. AC was the most common histological subtype, accounting for 62.7% (n=214) of total patients, followed by signet ring cell carcinoma (SRCC) (26.9%) (n=92), mucinous carcinoma (5.6%) (n=19), neuroendocrine carcinoma (1.5%) (n=5), adenosquamous carcinoma (0.9%) (n=3), medullary carcinoma (0.9%) (n=3) and other subtypes (1.5%) (n=5) in our study (Table 1). Histological subtypes of patients who underwent surgical resection were as follows: AC in 57 (55.9%) patients, SRCC in 21 (20.6%) patients, mucinous carcinoma in 17 (16.6%) patients, neuroendocrine carcinoma in 4 (3.9%) patients, medullary carcinoma in 2 (2%) patients and adenosquamous carcinoma 1 (1%) patient.

Primary tumor FDG uptake was observed in all the subjects except 2 patients with SRCC. Therefore, the analysis was performed according to semiquantitative analysis instead of visual evaluation. Mean ± standard deviation SUV_{max} obtained from 339 patients with ¹⁸F-FDG accumulation in primary tumor was 12.9±8.6 in PET/CT imaging. The

Table 1. Incidences and comparison of SUV_{max} according to histopathological subtypes of GC

	n (%)	SUV _{max} (Mean ± SD)	p values
Adenocarcinoma	214 (62.7)	14.5±8.8	0.00
Signet ring cell carcinoma	92 (26.9)	9.7±7.6	0.00
Mucinous carcinoma	19 (5.6)	10.9±7.1	0.022
Neuroendocrine carcinoma	5 (1.5)	10.6±5.5	0.200
Adenosquamous carcinoma	3 (0.9)	11.0±5.3	0.138
Medullary carcinoma	3 (0.9)	17.8±10.0	0.532
Other	5 (1.5)	15.8±9.1	0.200

p<0.05 statistically significant, p*: General linear model-univariate analysis, GC: Gastric cancer, SUV_{max}: Maximum standardized uptake value, SD: Standard deviation

highest SUV_{max} was detected in patients with medullary subtype GC (17.8±9.9) while the lowest SUV_{max} (9.7±7.6) was seen in SRCC. A statistically significant difference was documented among all histological types based on ¹⁸F-FDG uptakes (p<0.001), and the primary tumor SUV_{max} was found statistically higher in patients with AC (14.5±8.8) than in patients with SRCC (p<0.001) (Table 1) (Figure 1 and 2).

The SUV_{max} measured in group aged 60 years or over (n=147) was found to be statistically higher than in group aged lower than 60 years (n=67) in patients with AC (p=0.03). When the primary tumor size was taken into consideration, the SUV_{max} of RLN positive group in PET/CT (n=168) was found significantly higher than RLN negative group (n=46) (15.9±8.8 and 8.7±5.9, respectively) (p<0.001). There were no statistically significant differences in terms of SUV_{max} among the different anatomic locations of the lesions in stomach (p=0.274), and different tumor differentiation grades in patients with AC (p=0.102) (Table 2).

The primary tumor SUV_{max} of RLN positive group (n=62) was found significantly higher than RLN negative group (n=30) (11.0±8.5 and 6.9±3.8, respectively) in patients with SRCC (p=0.012). Similarly, the primary tumor SUV_{max} of the group with distant organ metastasis (n=11) was significantly higher than the group without distant organ metastasis (n=81) (14.1±8.2 and 9.7±7.3, respectively) in patients with SRCC (p=0.025). In patients with SRCC, there were no statistically significant differences in terms of primary tumor SUV_{max} among the different anatomic locations (p=0.284), and different tumor differentiation grades (p=0.946) (Table 3). In SRCC group, primary tumor FDG uptake was increased in the presence of distant nodal and distant organ metastasis. There was a similar tendency for distant nodal metastasis in the AC group, but this was not true for distant organ metastasis in our study group (Table 2).

In our study, 102 patients underwent surgical resection. Postoperative histopathological analysis was accepted as gold standard for detection of RLN metastatic involvement and sensitivity and specificity for PET/CT were calculated according to postoperative histopathological analysis results. The sensitivity and specificity of PET/CT were found to be 78.2% and 58.3% in the detection of RLN, respectively. Positive predictive value (PPV) and net present value (NPV) of the PET/CT imaging were 89.5% and 45.2% for RLN metastasis, respectively. On the other hand, primary tumors' SUV_{max} was found statistically higher in patients with positive RLN (14.6±8.9) than in patients with negative RLN (8.2±5.3) (p<0.001). The SUV_{max} of RLN was found significantly higher in patients with AC than in patients with SRCC (SUV_{max}=8.8±8.4 and 5.8±7.1, respectively; p=0.001) (Table 4).

Distant organ metastasis was found in 91 (26.7%) patients. Forty two patients with distant metastasis had AC, 11 had SRCC and 38 remaining patients had other subtypes of GC. In our study group, the most common organ with metastasis

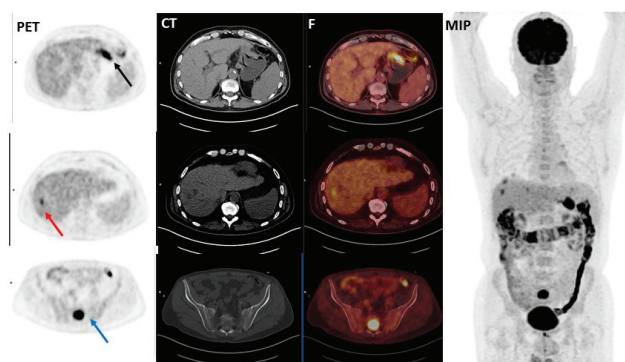


Figure 1. A 68-year old male patient with gastric adenocarcinoma. Axial PET (A), CT (B), and fusion (C) images showed high ¹⁸F-FDG uptake (SUV_{max}: 13.29) in primary tumor in the fundus of the stomach (black arrow). Liver metastasis showed increased ¹⁸F-FDG uptake (short axis diameter: 1.88 cm, SUV_{max}: 6.24) (red arrow). Additionally, bone metastasis was demonstrated in PET/CT images (SUV_{max}:16.29) (blue arrow)

¹⁸F-FDG: Fluorine-18-fluorodeoxyglucose, SUV_{max}: Maximum standardized uptake value, MIP: Maximum intensity projection image, PET: Positron emission tomography, CT: Computed tomography

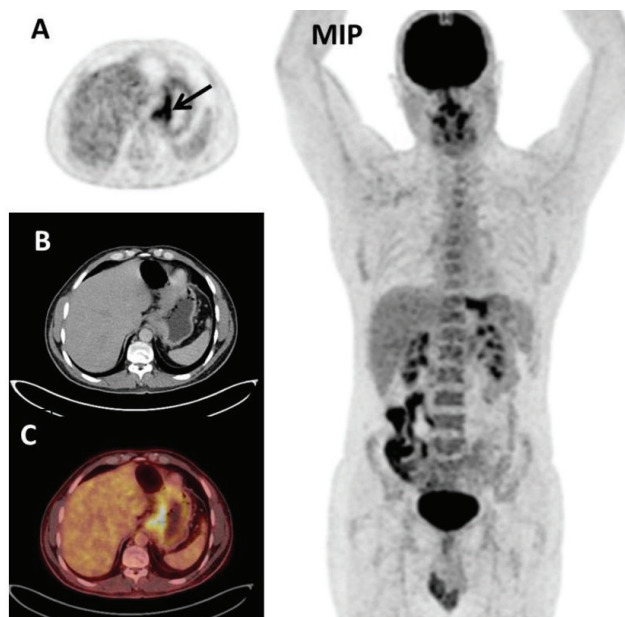


Figure 2. A 48-year-old male patient with SRCC. Axial PET (A), CT (B), and fusion (C) images showed ¹⁸F-FDG uptake (SUV_{max}: 7.9) in primary tumor in the cardia of the stomach (arrow). There was no locoregional lymph node or distant metastasis in PET/CT imaging

¹⁸F-FDG: Fluorine-18-fluorodeoxyglucose, SUV_{max}: Maximum standardized uptake value, MIP: Maximum intensity projection image, PET/CT: Positron emission tomography/computed tomography, SRCC: Signet ring cell carcinoma

was found as liver (64.8%, n=59). This was followed by bone-bone marrow (11%, n=10), multiple organs (9.9%, n=9), lungs (8%, n=7) and serosal metastasis (6.3%, n=6). There was no relation between distant organ metastatic state and primary tumor ¹⁸F-FDG uptake rate (p>0.05). Similarly, there was no statistically significant difference

between the distant lymph node metastasis positive or negative patients according to the primary tumor ¹⁸F-FDG uptake rate (p>0.05) (Table 2). The SUV_{max} of distant lymph node metastatic lesions was 11.0±7.0 and there was no statistically significant difference detected between AC (11.7±5.5) and SRCC groups (9.3±9.3) (p=0.264).

Table 2. Relation between primary tumor SUV_{max} and clinical and histopathological features of the AC-patients

	Clinical variables	n (%)	Primary tumor SUV _{max} (Mean ± SD)	p value
Age	<60 years	67 (31.0%)	13.2±11.0	0.030*
	≥60 years	147 (69.0%)	14.5±7.8	
Tumor size in PET/CT	≤3 cm	25 (11.7%)	11.0±5.3	0.070
	>3 cm	189 (88.3%)	15.4±9.8	
Tumor localization in PET/CT	Proximal	59 (27.6%)	14.8±8.0	0.274
	Middle	49 (22.9%)	16.2±11.6	
	Distal	89 (41.6%)	13.0±7.9	
	Diffuse	17 (7.9%)	15.1±5.5	
Differentiation grade after surgery	Well differentiated AC	15 (22.4%)	13.2±7.8	0.102
	Moderately differentiated AC	28 (41.8%)	12.4±6.8	
	Poorly differentiated AC	24 (35.8%)	18.4±14.2	
RLN involvement in PET/CT	Negative	46 (21.5%)	8.7±5.9	0.001*
	Positive	168 (78.5%)	15.9±8.8	
Distant nodal involvement in PET/CT	Absent	158 (74.0%)	13.9±9.5	0.158
	Present	56 (26.0%)	15.4±7.3	
Distant organ metastasis in PET/CT	Absent	172 (80.4%)	14.5±9.3	0.788
	Present	42 (19.6%)	14.0±6.5	

*p<0.05 statistically significant, SUV_{max}: Maximum standardized uptake value, AC: Adenocarcinoma, SD: Standard deviation, PET/CT: Positron emission tomography/computed tomography, RLN: Regional lymph node

Table 3. Relation between primary tumor SUV_{max} and clinical and histopathological features of the SRCC-patients

	Clinical variables	n (%)	Primary tumor SUV _{max} (Mean ± SD)	p value
Age	<60 years	43 (47.0%)	7.9±4.2	0.074
	≥60 years	47 (53.0%)	10.2±5.6	
Tumor size in PET/CT	≤3 cm	9 (10%)	8.6±1.3	0.763
	>3 cm	83 (90 %)	11.9±9.7	
Tumor localization in PET/CT	Proximal	18 (19.6%)	10.8±6.4	0.284
	Middle	31 (33.7%)	10.0±5.7	
	Distal	31 (33.7%)	9.6±10.5	
	Diffuse	12 (13.0%)	7.1±3.2	
Differentiation grade after surgery	Well differentiated AC	1 (5.6%)	8.6	0.946
	Moderately differentiated AC	2 (11.1%)	7.9±1.1	
	Poorly differentiated AC	15 (83.3%)	8.5±4.3	
RLN involvement in PET/CT	Negative	30 (32.6%)	6.9±3.8	0.012*
	Positive	62 (67.4%)	11.0±8.5	
Distant nodal involvement in PET/CT	Absent	77 (84.0%)	8.8±9.8	0.061
	Present	15 (16.0%)	12.3±7.7	
Distant organ metastasis in PET/CT	Absent	81 (88.0%)	9.0±7.3	0.025*
	Present	11 (12.0%)	14.1±8.2	

*p<0.05 statistically significant, SUV_{max}: Maximum standardized uptake value, AC: Adenocarcinoma, SD: Standard deviation, PET/CT: Positron emission tomography/computed tomography, RLN: Regional lymph node, SRCC: Signet ring cell carcinoma

Table 4. Comparison of RLN diameter and SUV_{max} in histopathological subtypes

	RLN diameter (Mean ± SD)	SUV _{max} (Mean ± SD)	p value	p value
Adenocarcinoma (n=214)	1.8±1.3	8.8±8.0	0.001*	0.016 [#]
Signet ring cell carcinoma (n=92)	1.5±1.0	5.8±7.1		
Mucinous carcinoma (n=19)	0.9±0.5	2.6±2.9		

*: General linear model- Multivariate analysis: p-value for Primary SUV_{max}. [#]: General linear model- Multivariate analysis: p value for RLN diameter, p<0.05 statistically significant, SUV_{max}: Maximum standardized uptake value, RLN: Regional lymph node, SD: Standard deviation

Discussion

GC still has one of the highest mortality rates among all malignancies worldwide, although 5-year survival rates have markedly increased with currently available treatments (13). The GC typically emerges between the 6th and 7th decade of life. National Cancer Institute (NCI) documented a median age of 69 years at diagnosis and majority of cases (81.5%) were diagnosed at ages between 55 and 84 years (14). Liu et al. (15) reported that the mean age was 58 years and that 69.8% of the patients were male and that 30.2% were female. Of 75.1% our study group was consisted of males and 24.9% females and the mean age of patients was 62.2 years. The prevalence was highest in the patients' seventh decade of life (37.2%), followed by the sixth decade (25.9%) in this study. Advanced age and increased tumor size were described as independent prognostic risk factors in numerous published data (15,16). In a study conducted by Liu et al. (15), multivariate analysis demonstrated that age and tumor size were independent prognostic factors in both patients with SRCC and with non (N)-SRCC and also documented that the 5-year survival rates of SRCC and NSRCC group were significantly lower in patients ≥60 years old and in patients with increased size of tumor diameter. Chen et al. (16) found the mean SUV_{max} for the primary tumors significantly higher in patients ≥60 years old and increased tumor sizes. In our study, the mean SUV_{max} measured in group aged 60 years or over was found to be statistically higher than in the group aged lower than 60 years in patients with AC.

The affinity of the primary lesion to ¹⁸F-FDG may be low in some types of GC and PET/CT may be false negative due to low metabolic activity especially in early-stage tumors and SRCC. Wu et al. (5) demonstrated increased ¹⁸F-FDG uptake as an important prognostic factor in primary lesions of GC. Similarly, Kaneko et al. (10) noted that ¹⁸F-FDG PET/CT scoring system may contribute in the selection of the most effective treatment modality for patients with GC and they showed some significant predictors of ¹⁸F-FDG uptake in primary tumor such as large tumor size, NSRCC type, and GLUT 1 expression. Chen et al. (16) showed significantly higher SUV_{max} in AC than SRCC. In accordance

with all mentioned data, the lowest SUV_{max} was detected in patients with SRCC and the primary SUV_{max} was found statistically higher in AC than SRCC in our study. In our study, there was statistically significant difference between all histological types based on ¹⁸F-FDG uptake. The highest SUV_{max} was obtained from medullary carcinoma and AC groups in our study. On the other hand, Stahl et al. (17) showed that ¹⁸F-FDG uptake was not predictive of survival in GC.

There are some studies in the literature that investigate the relationship between primary tumor ¹⁸F-FDG uptake and differentiation grade in GC. Chen et al. (16) reported a higher SUV_{max} in poorly differentiated AC than well or moderately differentiated AC (9.579±6.474 vs. 5.452±3.722; p=0.014) in retrospective analysis of 64 patients with GC who had undergone ¹⁸F-FDG PET/CT. However, Yun (18) reported significantly higher mean SUV_{max} in well differentiated AC (10.4±7.3) and moderately differentiated AC (9.2±6.7) than in SRCC (4.4±1.8) in their study which included 126 patients with GC. In our study, there was no statistically significant difference in terms of differentiation grade in patients with AC and SRCC.

It is well known that presence of lymph node metastases is one of the most important prognostic factors in GC (19). According to the NCI statistics, the 5-year survival rates are significantly poor for patients diagnosed as having lymph node disease (29.9%) and metastatic disease (4.5%), particularly at advanced stages (14). ¹⁸F-FDG PET/CT is documented to have a prominent role for detection of unsuspected metastases and nodal involvement at staging (16,18). Mukai et al. (19) detected a significantly higher rates of nodal involvement (p=0.0035) in 62 patients with GC with ¹⁸F-FDG PET. In a meta-analysis, the sensitivity and specificity of ¹⁸F-FDG PET in lymph node involvement were reported between 85.7% to 97.0%, respectively (20). In our study, when RLN detection was taken into consideration in postoperative histopathological results of 102 patients; the sensitivity, specificity, PPV and NPV for PET/CT were found 78.2%, 58.3%, 89.5% and 45.2%, respectively. According to the results of previous studies, these rates were relatively low. Although PET/CT has low

sensitivity for RLN involvement, Song et al. (21) reported that preoperative lymph node ¹⁸F-FDG uptake in GC was an independent prognostic factor for progression and overall survival. Similarly, in a study by Kwon et al. (22) it was demonstrated that FDG uptake of lymph nodes was an independent factor contributing to recurrence free survival after curative resection in patients with advanced GC. Oh et al. (23) demonstrated that lymph node metastasis was significantly associated with primary tumor SUV_{max} (p<0.001). They described primary tumor SUV_{max} as an independent indicator of lymph node metastasis and also noted that they could not find any association between SUV_{max} and tumor location (23). Primary SUV_{max} was found statistically higher in patients with positive RLN than patients with negative RLN in our AC and SRCC groups. Moreover, the primary tumor SUV_{max} was found to be higher in the distant metastasis positive patients than the distant metastasis negative patients in SRCC group. This finding indicated that high FDG uptake could be a poor prognostic factor in the SRCC group. There were also no statistically significant differences according to the different anatomic locations of the lesions of stomach. Smyth et al. (24) reported that ¹⁸F-FDG PET/CT could only able to detect the distant unsuspected metastases in approximately 10% of patients with AC. Also, ¹⁸F-FDG PET/CT provided better diagnostic accuracy for the detection of lymph node and distant metastasis in patients with advanced GC (25,26).

Conclusion

In conclusion, metabolic differences among subtypes of GC were revealed with the results of this study. Increased primary tumor SUV_{max} was associated with some clinical variables such as age and RLN metastasis in AC. Unexpectedly, no relationship was found between distant metastatic state and primary tumor SUV_{max} in AC. However, higher SUV_{max} of primary tumor in SRCC was associated with regional, distant nodal and distant organ metastasis. Although ¹⁸F-FDG uptake in SRCC was lower than AC, we think that SUV_{max} of primary tumor may be a prognostic value for this subgroup. Unfortunately, satisfactory results could not be obtained with PET/CT in regional nodal staging in this study. However, increased ¹⁸F-FDG uptake in RLNs could be a reliable guide to detect nodal metastasis before surgery.

Ethics

Ethics Committee Approval: This retrospective study was approved by the local ethics committee (2017/1048).

Informed Consent: All patients included were asked for their verbal or written consent for the use of their individual clinical findings for research purposes.

Peer-review: Externally peer-reviewed.

Authorship Contributions

Surgical and Medical Practices: N.D., Concept: E.A., T.F.Ç., Design: E.A., T.F.Ç., T.A., Data Collection or Processing: E.A., S.Y.T., Ç.Ş., C.G., Analysis or Interpretation: E.A., S.Y.T., Literature Search: E.A., S.Y.T., Ç.Ş., C.G., Writing: E.A., S.Y.T.

Conflict of Interest: No conflict of interest was declared by the authors.

Financial Disclosure: The authors declared that this study received no financial support.

References

1. Luo G, Zhang Y, Guo P, Wang L, Huang Y, Li K. Global patterns and trends in stomach cancer incidence: Age, period and birth cohort analysis. *Int J Cancer* 2017;141:1333-1344.
2. Schumacher SE, Shim BY, Corso G, Ryu MH, Kang YK, Roviello F, Saksena G, Peng S, Shivdasani RA, Bass AJ, Beroukhir R. Somatic copy number alterations in gastric adenocarcinomas among Asian and Western patients. *PLoS One* 2017;12:e0176045.
3. GE4GAC group, Soares FA, Coimbra JFJ, Pelosof AG, Freitas HC, Begnami MD, Costa WL, Fannelli MF, Mello CAL, Amorim MG, Pizzi MP, Caramelo L, Ferreira EN, Barros BDF, Torrezan GT, Ramalho R, Carraro DM, Chulam T, Carvalho FS, Carvalho DD, Krepischki ACV, Santos ET, Coelho LGV, Sant'Ana RO, Burbano RR, Assumpção P, Setúbal JC, Thomas AM, Chinen LTD, Braun AC, Alves V, Cassinela EK, Oliveira GP, Landemberger MC, Valieris R, Drummond R, Silva IG, Cézar R, Calsavara VF, Nóbrega CR, Bobrovniticha IG, Bartelli TF, Baladão GPB, Pereira ACC, Gatti CM, Abrantes LLS, Martins VR, Nunes DN, Curado MP, Neto ED. Genomics and epidemiology for gastric adenocarcinomas. *Applied Cancer Research*, 2017;37:1-9.
4. Shah MA, Strong VE, Boughey JC. A new approach for advanced gastric cancer: Using PET scans as a biomarker of preoperative chemotherapy efficacy. *Bull Am Coll Surg* 2017;102:46-48.
5. Wu Z, Zhao J, Gao P, Song Y, Sun J, Chen X, Ma B, Wang Z. Prognostic value of pretreatment standardized uptake value of F-18- fluorodeoxyglucose PET in patients with gastric cancer: a meta-analysis. *BMC Cancer* 2017;17:275.
6. Groheux D, Cochet A, Humbert O, Alberini JL, Hindíe E, Mankoff D. ¹⁸F-FDG PET/CT for staging and restaging of breast cancer. *J Nucl Med* 2016;57:17-26.
7. Cerfolio RJ, Bryant AS. Maximum standardized uptake values on positron emission tomography of esophageal cancer predicts stage, tumor biology, and survival. *Ann Thorac Surg* 2006;82:391-395.
8. Lopez Guerra JL, Gladish G, Komaki R, Gomez D, Zhuang Y, Liao Z. Large decreases in standardized uptake values after definitive radiation are associated with better survival of patients with locally advanced non-small cell lung cancer. *J Nucl Med* 2012;53:225-233.
9. Filik M, Kir KM, Aksel B, Soyda Ç, Özkan E, Küçük ÖN, İbşi E, Akgül H. The role of ¹⁸F-FDG PET/CT in the primary staging of gastric cancer. *Mol Imaging Radionucl Ther* 2015;24:15-20.
10. Kaneko Y, Murray WK, Link E, Hicks RJ, Duong C. Improving patient selection for ¹⁸F-FDG PET scanning in the staging of gastric cancer. *J Nucl Med* 2015;56:523-529.

11. Amin MB, Edge SB, Greene FL, Brierley JD. AJCC cancer staging manual. 8th ed. New York: Springer; 2017.
12. Bosman FT, Carreiro F, Ralph H, Hruban, Teise N, eds. World Health Organization Classification of Tumours of the Digestive System. 4th ed. Geneva, Switzerland: WHO Press; 2010.
13. Lee JW, Lee SM, Lee MS, Shin HC. Role of 18 F-FDG PET/CT in the prediction of gastric cancer recurrence after curative surgical resection. *Eur J Nucl Med Mol Imaging* 2012;39:1425-1434.
14. SEER Cancer Statistics Factsheets: Stomach Cancer. National Cancer Institute. Bethesda, MD, Accessed in 21 Apr 2016. Available from: <http://seer.cancer.gov/statfacts/html/stomach.html>
15. Liu X, Cai H, Sheng W, Yu L, Long Z, Shi Y, Wang Y. Clinicopathological characteristics and survival outcomes of primary signet ring cell carcinoma in the stomach: retrospective analysis of single center database. *PLoS One* 2015;10:e0144420.
16. Chen R, Zhou X, Liu J, Huang G. Relationship between 18F-FDG PET/CT findings and HER2 expression in gastric cancer. *J Nucl Med* 2016;57:1040-1044.
17. Stahl A, Ott K, Weber WA, Becker K, Link T, Siewert JR, Schwaiger M, Fink U. FDG PET imaging of locally advanced gastric carcinomas: correlation with endoscopic and histopathological findings. *Eur J Nucl Med Mol Imaging* 2003;30:288–295.
18. Yun M. Imaging of Gastric Cancer Metabolism Using 18 F-FDG PET/CT. *J Gastric Cancer* 2014;14:1-6.
19. Mukai K, Ishida Y, Okajima K, Isozaki H, Morimoto T, Nishiyama S. Usefulness of preoperative FDG-PET for detection of gastric cancer. *Gastric Cancer* 2006;9:192-196.
20. Kim SK, Kang KW, Lee JS, Kim HK, Chang HJ, Choi JY, Lee JH, Ryu KW, Kim YW, Bae JM. Assessment of lymph node metastases using 18F-FDG PET in patients with advanced gastric cancer. *Eur J Nucl Med Mol Imaging* 2006;33:148-155.
21. Song BI, Kim HW, Won KS, Ryu SW, Sohn SS, Kang YN. Preoperative standardized uptake value of metastatic lymph nodes measured by 18F-FDG PET/CT improves the prediction of prognosis in gastric cancer. *Medicine (Baltimore)* 2015;94:e1037.
22. Kwon HW, An L, Kwon HR, Park S, Kim S. Preoperative Nodal (18)F-FDG Avidity Rather than Primary Tumor Avidity Determines the Prognosis of Patients with Advanced Gastric Cancer. *J Gastric Cancer* 2018;18:218-229.
23. Oh HH, Lee SE, Choi IS, Choi WJ, Yoon DS, Min HS, Ra YM, Moon JI, Kang YH. The peak standardized uptake value (P-SUV) by preoperative positron emission tomography computed tomography (PET-CT) is a useful indicator of lymph node metastasis in gastric cancer. *J Surg Oncol* 2011;104:530-533.
24. Smyth E, Schöder H, Strong VE, Capanu M, Kelsen DP, Coit DG, Shah MA. A prospective evaluation of the utility of 2-deoxy-2-[(18)F]fluoro-D-glucose positron emission tomography and computed tomography in staging locally advanced gastric cancer. *Cancer* 2012;118:5481-5488.
25. Kawanaka Y, Kitajima K, Fukushima K, Mouri M, Doi H, Oshima T, Niwa H, Kaibe N, Sasako M, Tomita T, Miwa H, Hirota S. Added value of pretreatment (18)F-FDG PET/CT for staging of advanced gastric cancer: comparison with contrast-enhanced MDCT. *Eur J Radiol* 2016;85:989-995.
26. Altini C, Niccoli Asabella A, Di Palo A, Fanelli M, Ferrari C, Moschetta M, Rubini G. 18F-FDG PET/CT role in staging of gastric carcinomas: comparison with conventional contrast enhancement computed tomography. *Medicine (Baltimore)* 2015;94:e864.



Four Atypical Parathyroid Adenomas Detected by Dual Phase Tc-99m MIBI SPECT

Dört Atipik Paratiroid Adenomunun Dual Faz Tc-99m MIBI SPECT ile Saptanması

© Mine Araz¹, © Derya Çayır¹, © Fatma Fulya Köybaşıoğlu², © Harun Karabacak³, © Erman Çakal⁴

¹University of Health Sciences, Dışkapı Yıldırım Beyazıt Training and Research Hospital, Clinic of Nuclear Medicine, Ankara, Turkey

²University of Health Sciences, Dışkapı Yıldırım Beyazıt Training and Research Hospital, Clinic of Pathology, Ankara, Turkey

³University of Health Sciences, Dışkapı Yıldırım Beyazıt Training and Research Hospital, Clinic of General Surgery, Ankara, Turkey

⁴University of Health Sciences, Dışkapı Yıldırım Beyazıt Training and Research Hospital, Clinic of Endocrinology and Metabolism Diseases, Ankara, Turkey

Abstract

We report a case of a 55-year-old female with tertiary hyperparathyroidism and osteoporosis who had end stage renal disease and a history of hemodialysis for 15 years. Patient's informed is taken. Neck ultrasonography showed multinodular goiter together with a hypoechoic lesion compatible with a parathyroid adenoma. Dual phase technetium (Tc) Tc-99m MIBI single photon emission computed tomography (SPECT) showed pathological uptake in four parathyroid gland locations. Total thyroidectomy and subtotal parathyroidectomy revealed nodular hyperplasia and atypical adenomas in four parathyroid glands. Atypical parathyroid adenoma is a rare clinical entity. Multiple atypical adenomas are even less frequent. A very rare condition, detection of atypical adenomas in four of the parathyroid glands by dual phase Tc-99m MIBI SPECT, is presented in this case.

Keywords: Parathyroid gland, parathyroid adenoma, Tc-99m sestamibi, single photon emission computed tomography

Öz

Son dönem böbrek hastalığı nedeni ile 15 yıldır hemodiyalize giren, tersiyer hiperparatiroidi ve osteoporozu bulunan 55 yaşında bir kadın hastayı sunuyoruz. Hastadan bilgilendirilmiş onam alınmıştır. Hastanın boyun ultrasonografisinde multinodüler guatr ve paratiroid adenomu ile uyumlu olan hipoekoik bir lezyon saptandı. Dual faz teknesyum (Tc) Tc-99m MIBI tek foton emisyonlu bilgisayarlı tomografi (SPECT), dört paratiroid bezi lokalizasyonunda patolojik tutulum gösterdi. Total tiroidektomi ve subtotal paratiroidektomi sonucu tiroid bezinde nodüler hiperplazi ve dört paratiroid bezinde atipik paratiroid adenomu ile uyumluydu. Atipik paratiroid adenomu nadir görülen bir klinik antitedir. Multipl atipik paratiroid adenomu daha da az sıklıkla görülür. Bu olguda, dört atipik paratiroid adenomunun dual faz Tc-99m MIBI SPECT ile saptandığı çok nadir bir durumu sunuyoruz.

Anahtar kelimeler: Paratiroid bezi, paratiroid adenomu, Tc-99m sestamibi, tek foton emisyonlu bilgisayarlı tomografi

Address for Correspondence: Mine Araz MD, University of Health Sciences, Dışkapı Yıldırım Beyazıt Training and Research Hospital, Clinic of Nuclear Medicine, Ankara, Turkey

Phone: +90 532 666 73 13 **E-mail:** minesoylu@yahoo.com **ORCID ID:** orcid.org/0000-0001-6467-618x

Received: 14.04.2018 **Accepted:** 07.02.2019

©Copyright 2020 by Turkish Society of Nuclear Medicine
Molecular Imaging and Radionuclide Therapy published by Galenos Yayınevi.

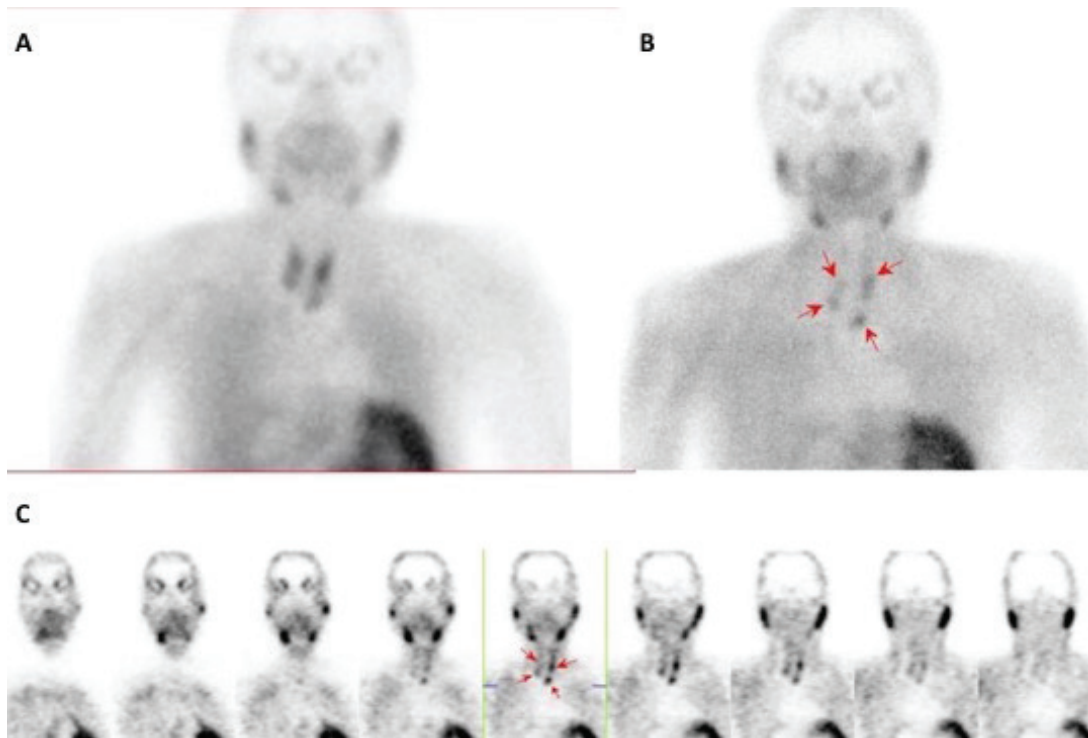


Figure 1. Dual phase technetium (Tc) Tc-99m MIBI planar imaging and single photon emission computed tomography (SPECT) (Figure 1A) were performed in nuclear medicine department. Following intravenous injection of 20 mCi Tc-99m MIBI, early (15 min after injection) (Figure 1B) and delayed (2 hours later) (Figure 1C) planar images of the neck and upper abdomen were obtained by a large field of view γ camera equipped with a low energy high resolution parallel hole collimator. SPECT study was performed 2 hours after radiopharmaceutical injection (images were acquired at 120 projections, 20 sec/projection, into 128x128 matrix) revealed focal activity retention in four different locations: Posterior neighbourhood of the middle portion and lower pole of the left lobe and posterior neighbourhood of the middle portion and lower pole of the right lobe. Scintigraphic findings were interpreted as supportive of parathyroid hyperplasia secondary to end stage renal disease.



Figure 2. Surgery involving total thyroidectomy and removal of 3 and a half of the parathyroid glands was performed. Macroscopic demonstration of the left inferior parathyroid gland is given.

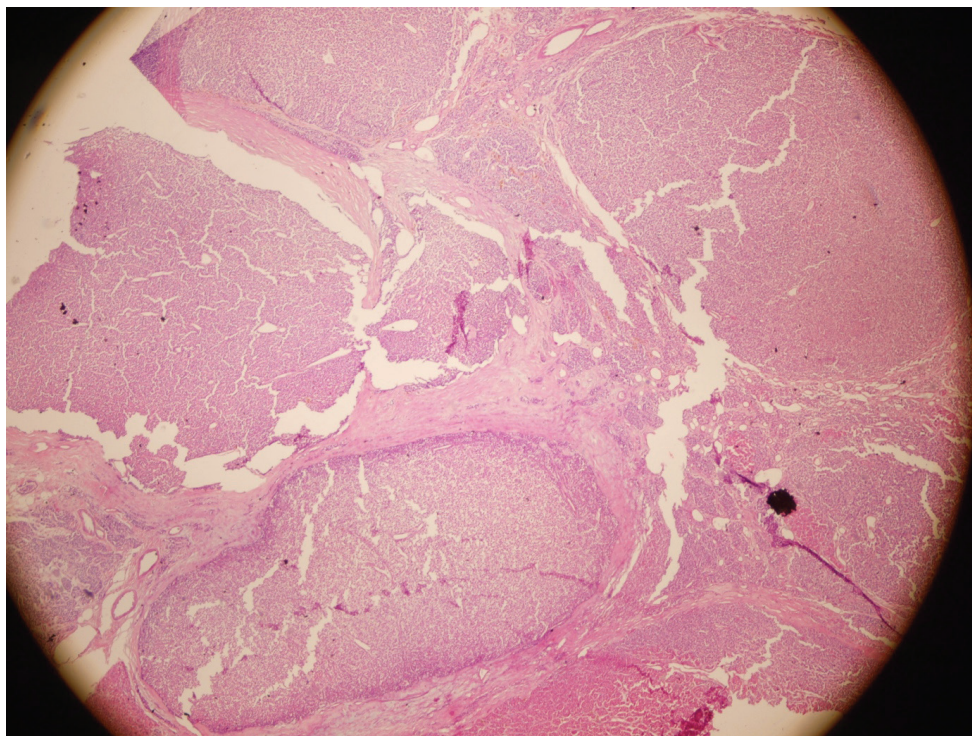


Figure 3. Histopathological examination revealed nodular hyperplasia of thyroid gland and atypical parathyroid adenomas of four glands. Nodular structures were separated by fibrous septae. No typical findings suggestive of parathyroid carcinoma like mitosis, atypia or vascular invasion were observed (hematoxylin and eosin, magnification x400).

Preoperatively, serum parathormone (PTH) was 1876 pg/mL, Ca was 10.14 mg/dL and P was 5.02 mg/dL. Following the operation, serum PTH level dropped to 99 pg/mL and serum Ca level was 9.7 mg/dL.

Tertiary hyperparathyroidism is mostly caused by hyperplasia and rarely by adenoma (1). Atypical parathyroid adenoma is a rare entity with borderline pathological characteristics, between adenoma and carcinoma (2). Parathyroid surgery is a relatively hard procedure as it necessitates surgical skill and experience. The use of Tc-99m MIBI scintigraphy is well established for patients undergoing reoperation for hyperparathyroidism. Some surgeons tend to skip preoperative imaging in secondary or tertiary hyperparathyroidism because bilateral neck exploration is needed anyway, but some studies suggested that parathyroid scintigraphy could be of value before initial parathyroidectomy (3,4). Tc-99m MIBI scintigraphy may help recognize an unexpected appearance of an ectopic or supernumerary parathyroid gland, as well as show the gland with the least radiotracer accumulation that can be autotransplanted. Protocol of parathyroid scan is argued to be important. Although dual isotope techniques are reported to be superior to dual phase imaging and SPECT/CT is recommended strongly to provide topographic anatomic information, in this case, both four pathological glands could still be identified by dual phase Tc-99m MIBI SPECT (5). Ultrasonography (USG) and Tc-99m MIBI scintigraphy are complementary in parathyroid imaging. The success of both modalities is similar in single gland disease. However, in case of multiglandular disease, frequently seen in secondary or tertiary hyperparathyroidism, they have been reported to have lower sensitivities. Thus, especially in these patients, combination of scintigraphic and sonographic imaging provides a more accurate approach in the preoperative evaluation (6).

In our case, MIBI was capable of detecting atypical adenomas in four parathyroid glands with respect to one gland demonstrated by USG. This report is interesting in the way that atypical adenomas of parathyroid gland were presented in all four of the glands in a patient with tertiary hyperparathyroidism and that the only preoperative method that could address multiglandular disease was Tc-99m MIBI SPECT.

Ethics

Informed Consent: Informed consent was taken.

Peer-review: Externally and internally peer-reviewed.

Authorship Contributions

Surgical and Medical Practices: H.K., E.Ç., F.F.K., Concept: M.A., Design: M.A., Data Collection or Processing: D.Ç., Analysis or Interpretation: M.A., Literature Search: D.Ç., Writing: M.A.

Conflict of Interest: No conflict of interest was declared by the authors.

Financial Disclosure: The authors declared that this study received no financial support.

References

1. Sheu-Grabellus SY, Schmid KW. Pathology of parathyroid glands: Practical aspects for routine pathological investigations. *Pathologie* 2015;36:229-236.

2. Carlson D. Parathyroid pathology: hyperparathyroidism and parathyroid tumors. *Arch Pathol Lab Med* 2010;134:1639-1644.
3. Piga M, Bolasco P, Satta L, Altieri P, Loi G, Nicolosi A, Tarquini A, Mariotti S. Double phase parathyroid technetium-99m- MIBI scintigraphy to identify functional anatomy in secondary hyperparathyroidism. *J Nucl Med* 1996;37:565-569.
4. Torregrosa JV, Fernández-Cruz L, Canalejo A, Vidal S, Astudillo E, Almaden Y, Pons F, Rodríguez M. (99m)Tc-sestamibi scintigraphy and cell cycle in parathyroid glands of secondary hyperparathyroidism. *World J Surg* 2000;24:1386-1390.
5. Taïeb D, Ureña-Torres P, Zanotti-Fregonara P, Rubello D, Ferretti A, Henter I, Henry JF, Schiavi F, Opocher G, Blickman JG, Colletti PM, Hindié E. Parathyroid scintigraphy in renal hyperparathyroidism: the added diagnostic value of SPECT and SPECT/CT. *Clin Nucl Med* 2013;38:630-635.
6. Ruda JM, Stack BC Jr, Hollenbeak CS. The cost-effectiveness of additional preoperative ultrasonography or sestamibi-SPECT in patients with primary hyperparathyroidism and negative findings on sestamibi scans. *Arch Otolaryngol Head Neck Surg* 2006;132:46-53.



Amyloidosis Associated Kidney Failure with Gross Hypermetabolic Intra-abdominal Mass

Böbrek Yetmezliği ile Birlikte Dev Hipermetabolik İntra-abdominal Kitesi Olan Hastada Amiloidozis

✉ Zehra Pınar Koç¹, ✉ Pınar Pelin Özcan¹, ✉ Kenan Turgutalp², ✉ Kaan Esen³, ✉ Tuğba Kara⁴

¹Mersin University Faculty of Medicine, Department of Nuclear Medicine, Mersin, Turkey

²Mersin University Faculty of Medicine, Department of Nephrology, Mersin, Turkey

³Mersin University Faculty of Medicine, Department of Radiology, Mersin, Turkey

⁴Mersin University Faculty of Medicine, Department of Pathology, Mersin, Turkey

Abstract

A 23-year-old male patient who presented with impaired kidney function tests attended to hospital for hemodialysis and underwent ¹⁸F-FDG positron emission tomography/computed tomography (PET/CT) examination for the metabolic characterization of the intra-abdominal mass which was found in the ultrasonography. ¹⁸F-FDG PET/CT revealed a mass lesion adjacent to the liver which was hypermetabolic and the pathology of the lesion was determined as amyloidosis. To the best of our knowledge, the case with ¹⁸F-FDG PET/CT images of a huge amyloid mass is the first in the literature.

Keywords: Amyloidosis, abdominal mass, ¹⁸F-FDG positron emission tomography/computed tomography

Öz

Yirmi üç yaşında erkek hasta böbrek yetmezliği ile diyaliz için hastanemize yönlendirilmiştir. Hastanın ultrasonografisinde tesadüfen saptanan intra-abdominal kitle lezyonunun metabolik karakterizasyonu için yapılan ¹⁸F-FDG pozitron emisyon tomografi/bilgisayarlı tomografi (PET/BT) çalışmasında hipermetabolik kitle izlenmiş olup kitlenin biyopsisi amiloidozis ile uyumlu olarak bulunmuştur. Bilgilerimize göre, bu olgu ile, dev amiloid kitesi ile başvuran bir hastanın ¹⁸F-FDG PET/BT görüntüleri literatürde ilk kez sunulmaktadır.

Anahtar kelimeler: Amiloidoz, abdominal kitle, ¹⁸F-FDG pozitron emisyon tomografi/bilgisayarlı tomografi

Address for Correspondence: Zehra Pınar Koç MD, Mersin University Faculty of Medicine, Department of Nuclear Medicine, Mersin, Turkey

Phone: +90 324 241 00 00 **E-mail:** zehrapinarkoc@gmail.com **ORCID ID:** orcid.org/0000-0002-3274-5790

Received: 04.05.2018 **Accepted:** 17.03.2019

©Copyright 2020 by Turkish Society of Nuclear Medicine
Molecular Imaging and Radionuclide Therapy published by Galenos Yayınevi.

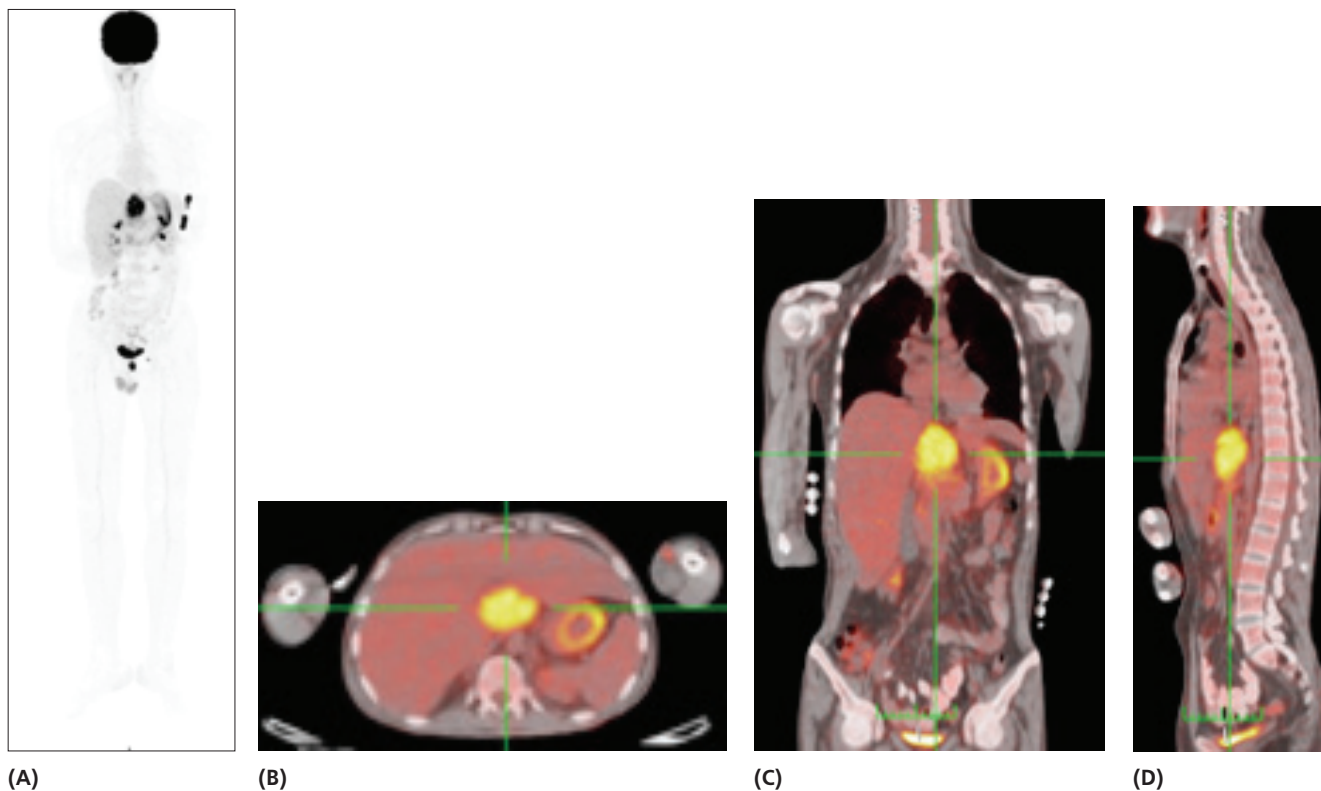


Figure 1. A) ^{18}F -FDG positron emission tomography/computerized tomography (PET/CT) maximum intensity projection image showing hypermetabolic intra-abdominal mass standardized uptake value (SUV_{max} : 5) adjacent to the liver, spleen and stomach and an additional hypermetabolic left servical lymph node (SUV_{max} : 3.6). **B, C, D)** Cross sectional images of the same intraabdominal mass in transaxial, coronal and sagittal projections. A 23-year-old male patient presented with sudden onset acute kidney failure and the patient was referred for hemodialysis. The abdominal ultrasonography revealed intra-abdominal mass adjacent to the liver and the patient was referred to the Nuclear Medicine Department with pre-diagnosis of plasmocytoma. ^{18}F -FDG PET/CT imaging showed hypermetabolic intra-abdominal mass and a mildly hypermetabolic left cervical lymph node which was thought to be sccondary to an infection. The hypermetabolic abdominal mass was diagnosed as amyloid deposition via true-cut biopsy.

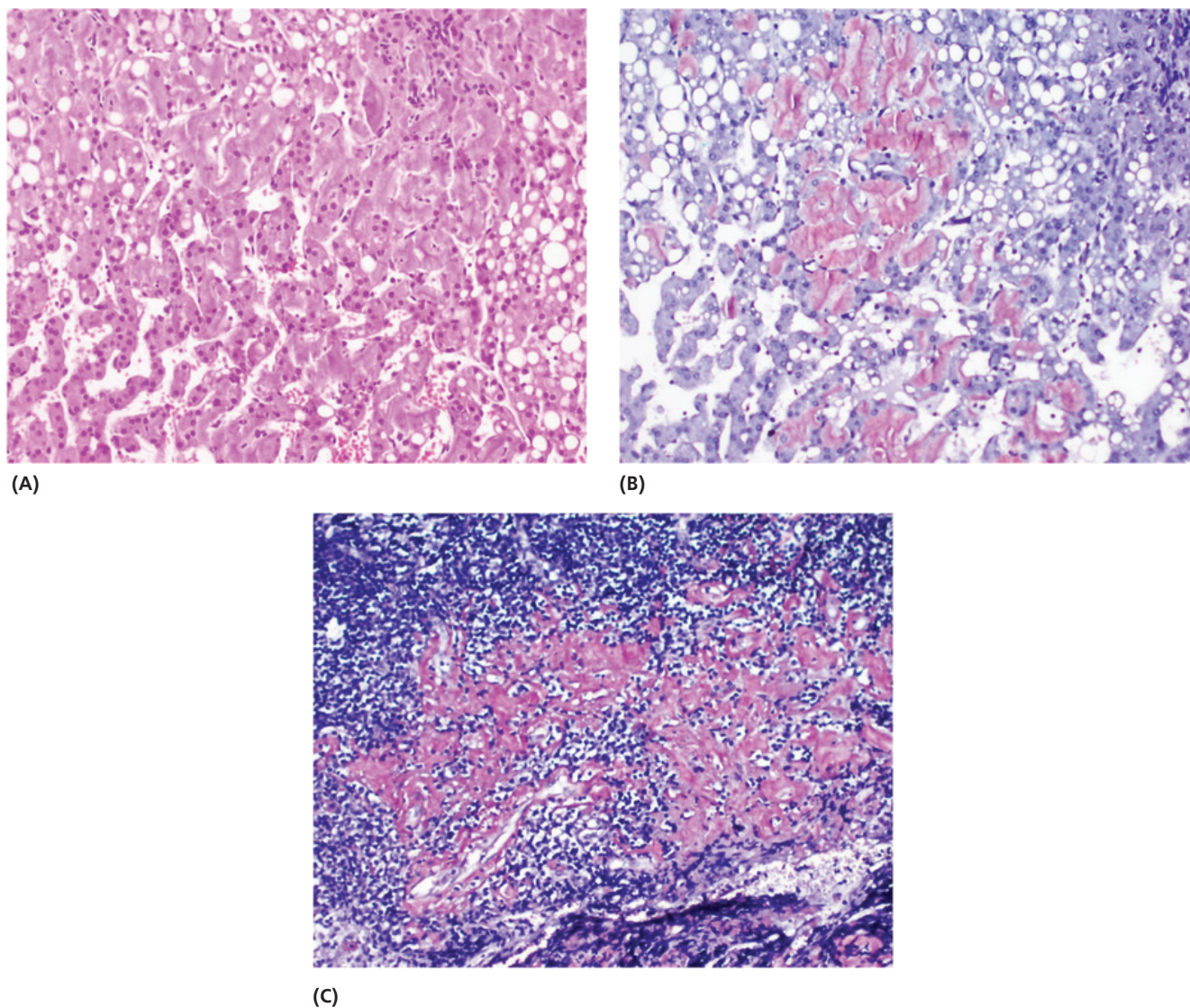


Figure 2. Abdominal lymph node biopsy and wedge resection from the liver parenchyma and adjacent lymph node were performed. The pathological result of the mass was found to be an amyloid deposition. Additionally, amyloid deposits were also found in the hepatocytes. **A)** Acellular, amorphous, eosinophilic amyloid deposits in hepatocyte cytoplasm (hematoxylin and eosin, x200), **B)** amyloid was stained brown to orange with Kongo Red dye in the hepatocyte cytoplasm (Kongo Red, x200), **C)** amyloid deposits in the lymph node parenchyma (Kongo Red, x200). In microscopic examination, acellular, amorphous, eosinophilic deposits were detected in the lymph node parenchyma and also in the hepatocyte cytoplasm and disse space in the liver parenchyma. Additionally depositions were shown in the vascular walls indicating systemic amyloidosis. The deposits were stained brown to orange with Kongo Red dye and also showed birefringence under polarized light, which was compatible with amyloidosis. To specify the type of amyloid proteins immunohistochemically, AA amyloid dye was applied to the biopsy materials and positive staining was observed. Primary amyloidosis presented with hepatic involvement is a rare disease that was previously reported in some cases with multiple myeloma (1). Additionally, there are case reports about ^{18}F -FDG accumulation of primary amyloidosis in the lungs (2). A previous case report showed diffuse increased liver ^{18}F -FDG uptake (3), however the series comparing systemic and localized amyloidosis indicate that systemic amyloidosis may not accumulate ^{18}F -FDG but localized amyloidosis does (4). The lesion in this report was located in close proximity to the liver, spleen and stomach but not in the any of these organs. The probable reason for the kidney impairment was amyloidosis as well. The prediagnosis of multiple myeloma or plasmocytoma was excluded by laboratory analysis. Kidney biopsy was not performed however amyloid deposition in the normal liver parenchyma was shown by pathology results demonstrating systemic amyloidosis. However the reason of this amyloidosis could not be determined. The patient also has some ^{18}F -FDG uptake in gastric region which was explained by gastritis. In the literature, this is the first case report with systemic and localized amyloidosis presented with kidney failure and gross abdominal mass showing high ^{18}F -FDG uptake.

Ethics

Informed Consent: Consent form was filled out by all participants.

Peer-review: Externally peer-reviewed.

Authorship Contributions

Surgical and Medical Practices: Z.P.K., P.P.Ö., K.T., K.E., T.K.,
Concept: Z.P.K., P.P.Ö., Design: Z.P.K., P.P.Ö., Data Collection
or Processing: Z.P.K., P.P.Ö., K.T., K.E., T.K., Analysis or
Interpretation: Z.P.K., P.P.Ö., K.T., K.E., T.K., Literature
Search: Z.P.K., P.P.Ö., Writing: Z.P.K., P.P.Ö.

References

1. Scott PP, Scott WW Jr, Siegelman SS. Amyloidosis: An overview. *Semin Roentgenol* 1986;21:103-112.
2. Seo JH, Lee SW, Ahn BC, Lee J. Pulmonary amyloidosis mimicking multiple metastatic lesions on F-18 FDG PET/CT. *Lung Cancer* 2010;67:376-379.
3. Son YM, Choi JY, Bak CH, Cheon M, Kim YE, Lee KH, Kim BT. 18F-FDG PET/CT in primary AL hepatic amyloidosis associated with multiple myeloma. *Korean J Radiol* 2011;12:634-637.
4. Glaudemans AW, Slart RH, Noordzij W, Dierckx RA, Hazenberg BP. Utility of 18F-FDG PET(/CT) in patients with systemic and localized amyloidosis. *Eur J Nucl Med Mol Imaging* 2013;40:1095-1101.



¹⁸F-NaF PET/CT and Extraordinary Involvement: Non-calcific Brain Involvement in a Prostate Cancer Case

¹⁸F-NaF PET/BT'de Sıra Dışı Tutulumlar: Prostat Kanseri Bir Olguda Kalsifiye Olmayan Beyin Tutulumu

Ulku Korkmaz, Funda Ustun

Trakya University Faculty of Medicine, Department of Nuclear Medicine, Edirne, Turkey

Abstract

With the increase in the diagnosis of the cancer, the frequency of using imaging methods for diagnosis and for staging is also increased. Because of the complex structure of cancer and tumor behavior, the assessment methods have been updated and metabolic imaging has gained weight. The most popular of these techniques is hybrid positron emission tomography/computed tomography (PET/CT) systems. Prostate cancer is the second most common cancer in the world, is the fifth common type in cancer-related male deaths. Estimation of prognosis and treatment planning of the patients are based on the TNM classification. Bone metastasis is a prognostic factor of morbidity and mortality in prostate cancer. Sodium fluoride (NaF) PET/CT is a promising imaging modality in evaluation of skeletal system. This article will review the involvement of ¹⁸F-NaF in extra-osseous tissues in the prostate cancer and reveal the fundamental differences between ¹⁸F-NaF imaging and ¹⁸F-FDG imaging in these areas.

Keywords: NaF, PET, brain, metastasis

Öz

Kanser tanısının artmasıyla birlikte tanı ve evreleme için görüntüleme yöntemlerinin kullanım sıklığı da artmaktadır. Kanser ve tümör davranışının karmaşık yapısından dolayı değerlendirme yöntemleri güncellenmiştir ve metabolik görüntüleme ağırlık kazanmıştır. Bu tekniklerin en popüler olanı hibrid pozitron emisyon tomografi/bilgisayarlı tomografi (PET/BT) sistemleridir. Prostat kanseri dünyada en sık görülen ikinci kanser ve erkeklerde kanserle ilgili ölüm nedenleri arasında beşinci en sık nedendir. Kemik metastazı, prostat kanserinde morbidite ve mortalite açısından prognostik bir faktördür. Sodyum florür (NaF) PET/BT, iskelet sisteminin değerlendirilmesinde umut verici bir görüntüleme yöntemidir. Bu makale ¹⁸F-NaF'nin prostat kanserinde kemik dışı dokulardaki tutulumunu gözden geçirerek bu alanlarda ¹⁸F-NaF görüntüleme ve ¹⁸F-FDG görüntülemenin temel farklılıklarını ortaya koyacaktır.

Anahtar kelimeler: NaF, PET, beyin, metastaz

Address for Correspondence: Ulku Korkmaz MD, Trakya University Faculty of Medicine, Department of Nuclear Medicine, Edirne, Turkey

Phone: +90 532 799 33 01 **E-mail:** korkmaz.ulku@gmail.com **ORCID ID:** orcid.org/0000-0002-7155-7610

Received: 29.06.2018 **Accepted:** 07.07.2019

©Copyright 2020 by Turkish Society of Nuclear Medicine
Molecular Imaging and Radionuclide Therapy published by Galenos Yayınevi.

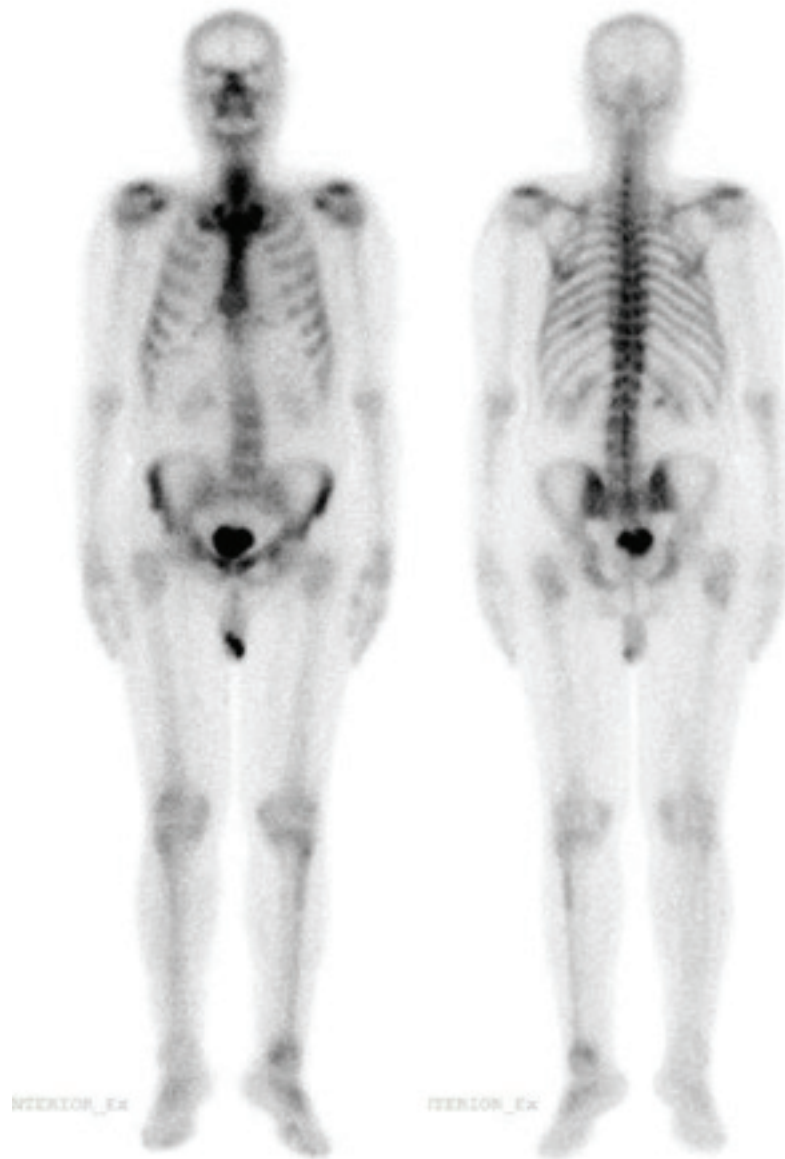
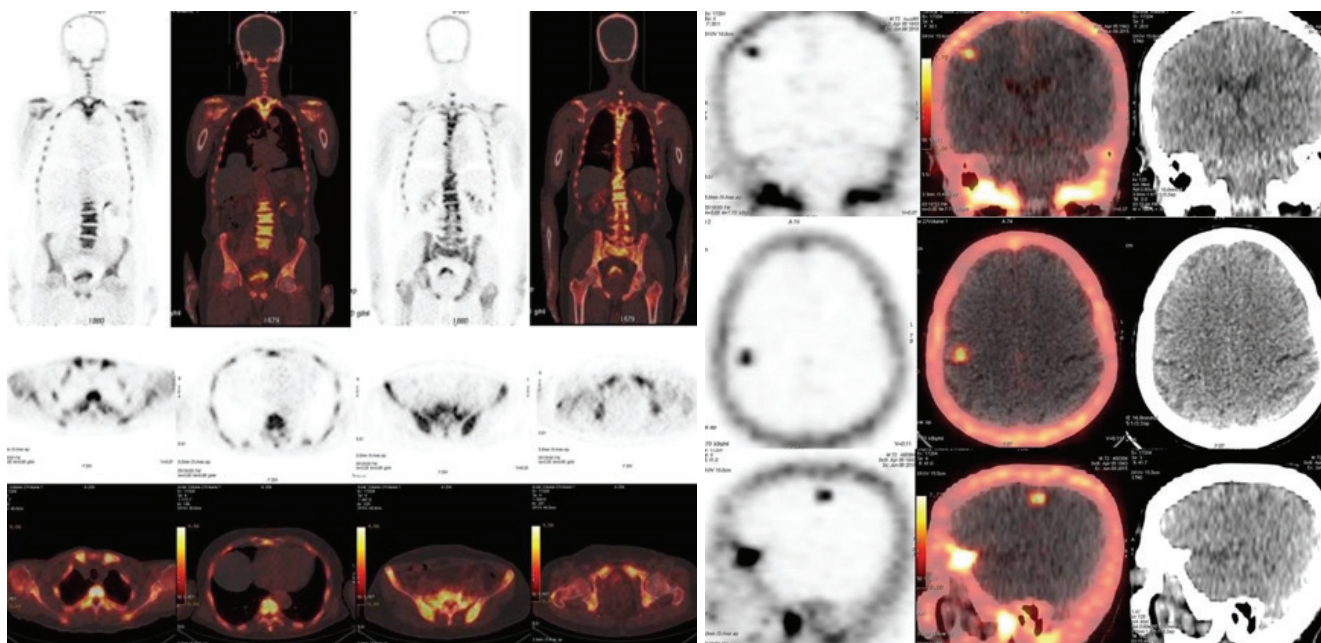


Figure 1. A 74-year-old male was diagnosed as having Gleason 3+7=(10) prostate adenocarcinoma and underwent technetium (Tc) Tc-99m methylene diphosphonate (MDP) whole body bone scintigraphy (WBBS) for staging. There was suspicious metastatic involvement in right 9th rib, right acetabulum and left fibula/proximal tibia in WBBS and sodium fluoride (NaF) positron emission tomography/computed tomography (PET/CT) scan was done for further evaluation.



Figures 2, 3. NaF PET/CT images showed widespread involvement in the skeletal system, including MDP avid lesions. Also NaF involvement was observed in the right parietooccipital field in the cranium (SUV_{max} : 4.8), with no calcification or identifiable lesion in the unenhanced CT counterpart. The patient was evaluated in neurology and radiation oncology clinics and radiotherapy and chemotherapy were initiated for extracranial metastases. The patient was followed up with androgen receptor blocker and did not receive additional treatment for intracranial mass. After three years of follow up for extracranial disease, he was admitted to the emergency room with an epileptic seizure due to intracranial mass on June 2018. The mass was accepted as a metastatic lesion and he is still receiving a treatment for this. (SUV_{max} : Maximum standardized uptake value)

Bone metastasis is a prognostic factor in prostate cancer and the ratio was reported as 70% in autopsy series (1). Recently, the assessment methods have been updated and hybrid metabolic imaging (PET/CT, PET/MR) has gained weight.

The most widely used PET radiopharmaceutical is ^{18}F -FDG. This molecule is a very good metabolic marker for soft tissue and bone marrow, however, it does not reach intended sensitivity and specificity to be accepted as a classical agent for bone imaging, especially in cases with involvement of the cortical bone. While the phosphate groups marked with Tc-99m are used as main method for the detection of bone metastases, technical developments have allowed the spread of ^{18}F -NaF for this purpose (2).

^{18}F -NaF is retained by mineralized bone tissue in proportionally with the osteoblastic activity (3). Tc-99m phosphanats are mostly involved in osteoblastic metastases and fluorodeoxyglucose PET/CT is more associated with bone marrow involvement, ^{18}F -NaF PET/CT shows better involvement in both sclerotic and lytic metastases (4). Whereas ^{18}F -NaF shows high affinity to osseous tissue, it is not retained by normal brain tissue and facilitates the seen of bone structures (4).

Almost all of extra-osseous ^{18}F -NaF involvements are in brain tissue (5). Physiologically, ^{18}F -NaF can not pass the blood-brain barrier. However, if the blood brain barrier is broken down for a reason, the metastatic tumor cells can settle here. The involvement of bone seeking agents in brain metastases, is not just because of deterioration of the blood brain barrier, but also because of the metabolic uptake mechanisms of tumor cells (6). For example, fibril structures and amyloid foci have been reported to exhibit affinity for calcium, physiologically (7). Furthermore, Ca-L, an ion channel, has been shown to be present in pancreatic cancer cells and is effective in tumor pathogenesis (8). A similar mechanism could also be possible for sodium mediated ion channels and ^{18}F -NaF.

As a result, brain metastasis may be detected incidentally in ^{18}F -NaF-images and that unexpected involvement should be carefully evaluated before it is considered as an artifact. This precise approach is necessary to prevent the false staging of the patient.

Ethics

Informed Consent: Written informed consent of the patient was obtained from patient.

Peer-review: Externally peer-reviewed.

Authorship Contributions

Concept: F.U., Design: U.K., F.U., Data collection or processing: U.K., Analysis or interpretation: U.K., F.U., Literature search: U.K., Writing: U.K.

Conflict of Interest: No conflict of interest was declared by the authors.

Financial Disclosure: The authors declared that this study received no financial support.

References

1. Rubens RD: bone metastases incidence and complications. In cancer and the skeleton. Edited by: Rubens RD, Mundy GR. London: Martin Dunitz; 2000:33-42.

2. Cook G, Parker C, Chua S, Johnson B, Aksnes AK, Lewington VJ. ¹⁸F-fluoride PET: changes in uptake as a method to assess response in bone metastases from castrate-resistant prostate cancer patients treated with ²²³Ra-chloride (Alpharadin), EJNMMI Research 2011; 1:4.
3. Installe J, Nzeusseu A, Bol A, Depresseux G, Devogelaer JP, Lonneux M. ¹⁸F-Fluoride PET for Monitoring Therapeutic Response in Paget's Disease of Bone. J Nucl Med 2005;46:1650-1658.
4. Araz M, Aras G, Küçük ÖN. The role of ¹⁸F-NaF PET/CT in metastatic bone disease. J Bone Oncol 2015;4:92-97.
5. Oldan JD, Hawkins AS, Chin BB. ¹⁸F Sodium Fluoride PET/CT in Patients with Prostate Cancer: Quantification of Normal Tissues, Benign Degenerative Lesions, and Malignant Lesions. World J Nucl Med 2016;15:102-108.
6. Fortin D. The blood-brain barrier: its influence in the treatment of brain tumors metastases. Curr Cancer Drug Targets 2012;12:247-259.
7. Worsley DF, Lentle BC: Uptake of technetium-99mMDP in primary amyloidosis with a view of the mechanisms of soft tissue localization of bone seeking radiopharmaceuticals. J Nucl Med 1993;34:1612-1615.
8. Wissenbach U, Niemeyer BA, Fixemer T, Schneidewind A, Trost C, Cavalieri A, Reus K, Meese E, Bonkhoff H, Flockert V. Expression of CaT-like, a Novel Calcium-selective Channel, Correlates with the Malignancy of Prostate Cancer. J Biol Chem 2011;276:19461-19468.



Increased Bone Marrow ¹⁸F-Choline Uptake in a Patient with Hepatocellular Carcinoma and Thalassemia Intermedia

Hepatosellüler Karsinom ve Talasemi Intermedia Tanılı Bir Hastada Artmış Kemik İliği ¹⁸F-Kolin Tutulumu

Luca Filippi

Santa Maria Goretti Hospital, Clinic of Nuclear Medicine, Latina, Italy

Abstract

A 57-year-old male with history of thalassemia intermedia and hepatocellular carcinoma underwent a positron emission tomography/computed tomography (PET/CT) scan with ¹⁸F-choline before radioembolization procedure with ⁹⁰Y-microspheres. The PET/CT scan with ¹⁸F-choline demonstrated highly increased tracer incorporation within a gross lesion in the hepatic dome coupled with diffuse activity in bone marrow, this latter aspect was probably due to the compensatory hematopoiesis stimulation induced by chronic hemolysis. This pattern of skeletal ¹⁸F-choline uptake should be considered as a peculiar PET/CT finding in thalassemic patients.

Keywords: ¹⁸F-choline, positron emission tomography/computed tomography, hepatocellular carcinoma, thalassemia

Öz

Talasemi intermedia ve hepatosellüler karsinom tanılı bir hastada ⁹⁰Y-mikrosfer ile radyoembolizasyon prosedürü öncesi ¹⁸F-kolin ile pozitron emisyon tomografisi/bilgisayarlı tomografi (PET/BT) taraması yapıldı. ¹⁸F-kolin ile PET/BT taraması karaciğer kubbesindeki büyük bir lezyon içerisinde artmış tracer tutulumu ve muhtemelen kronik hemoliz ile indüklenen kompensatuvar hematopoezise kemik iliğinde artmış aktivite gösterdi. Bu skeletal patterned ¹⁸F-kolin tutulumu talasemik hastalara özgü bir PET/BT bulgusu olarak değerlendirilmelidir.

Anahtar kelimeler: ¹⁸F-kolin, pozitron emisyon tomografisi/bilgisayarlı tomografi, hepatosellüler karsinom, talasemi

Address for Correspondence: Luca Filippi MD, Santa Maria Goretti Hospital, Clinic of Nuclear Medicine, Latina, Italy

Phone: +393921247921 **E-mail:** l.filippi@ausl.latina.it **ORCID ID:** orcid.org/0000-0003-4423-5496

Received: 09.08.2019 **Accepted:** 30.09.2019

©Copyright 2020 by Turkish Society of Nuclear Medicine
Molecular Imaging and Radionuclide Therapy published by Galenos Yayınevi.

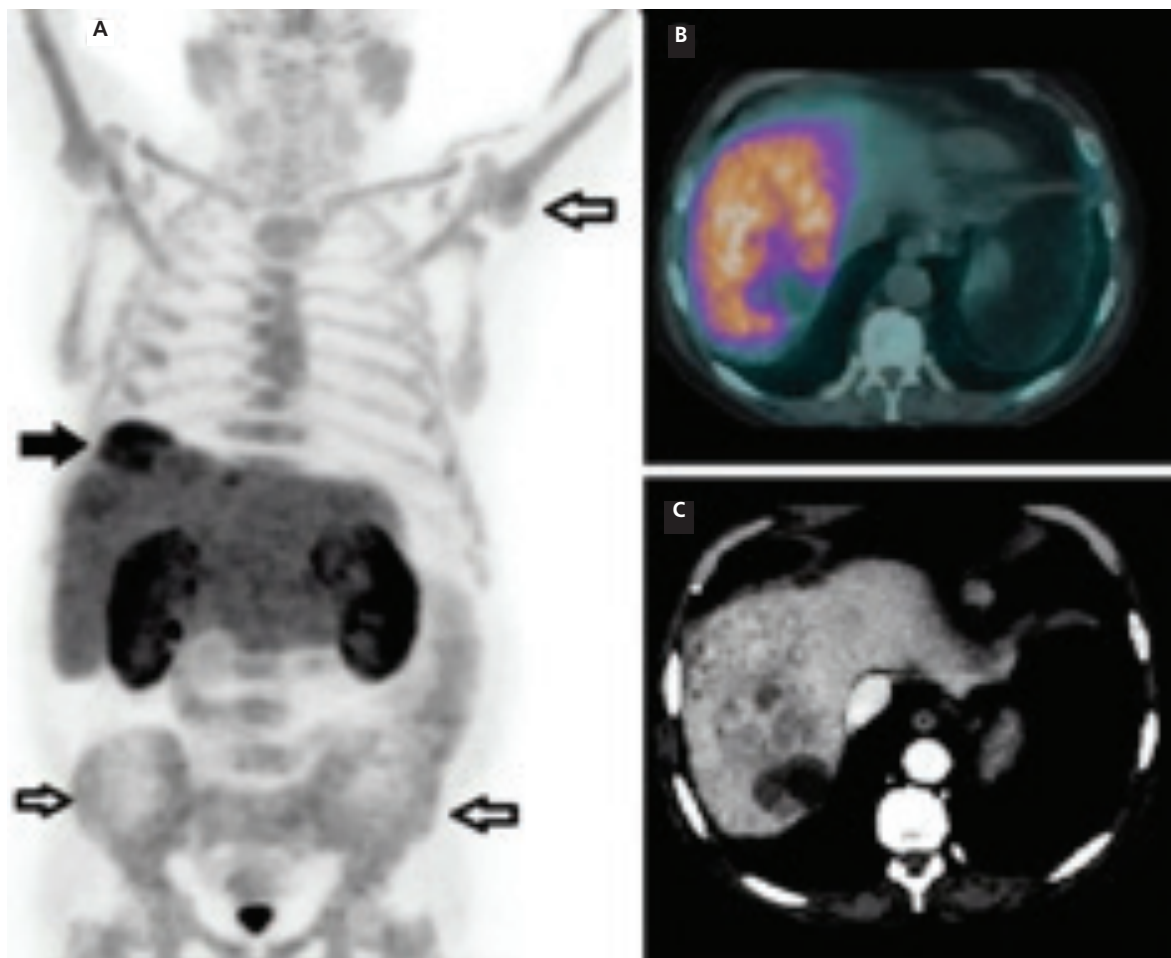


Figure 1. A 57-year-old man was diagnosed as having thalassemia intermedia at the age of 3 years (genotype CD39/IVS 1-6). He received sporadic blood transfusions since childhood and was submitted to splenectomy at the age of 15 years due to giant splenomegaly. Over the years, he developed hemochromatosis secondary to iron overload and was infected by hepatitis C, which was most probably transmitted via blood transfusion before 1990. In April 2018, during a periodical clinical follow-up, an abdominal ultrasound examination revealed multiple lesions in the right hepatic lobe, subsequently confirmed by contrast-enhanced/computed tomography (ce-CT). The patient underwent biopsy which resulted positive for well-differentiated hepatocellular carcinoma (HCC). He received sorafenib until September 2018 when treatment was discontinued due to the onset of cutaneous toxicity and evidence of progressive disease shown by ce-CT. He was enrolled for a loco-regional treatment of the hepatic lesion through radioembolization with ⁹⁰Y-microspheres. Before the radioembolization procedure, he was submitted to positron emission tomography/CT (PET/CT) with ¹⁸F-choline. **(A)** PET maximum intensity projection showed increased tracer uptake in the hepatic dome (black arrow) and diffuse hyperactivity in the axial and appendicular skeleton (black countered arrows). The corresponding fused PET/CT **(B)** and ce-CT **(C)** axial slices demonstrated multiple lesions, with a necrotic peripheral component, in the right hepatic lobe, characterized by intense ¹⁸F-choline incorporation with much higher uptake values (SUV_{max} : 17.0, SUV_{mean} : 6.1) than those calculated in the normal liver parenchyma (SUV_{max} : 7.7, SUV_{mean} : 5.7).

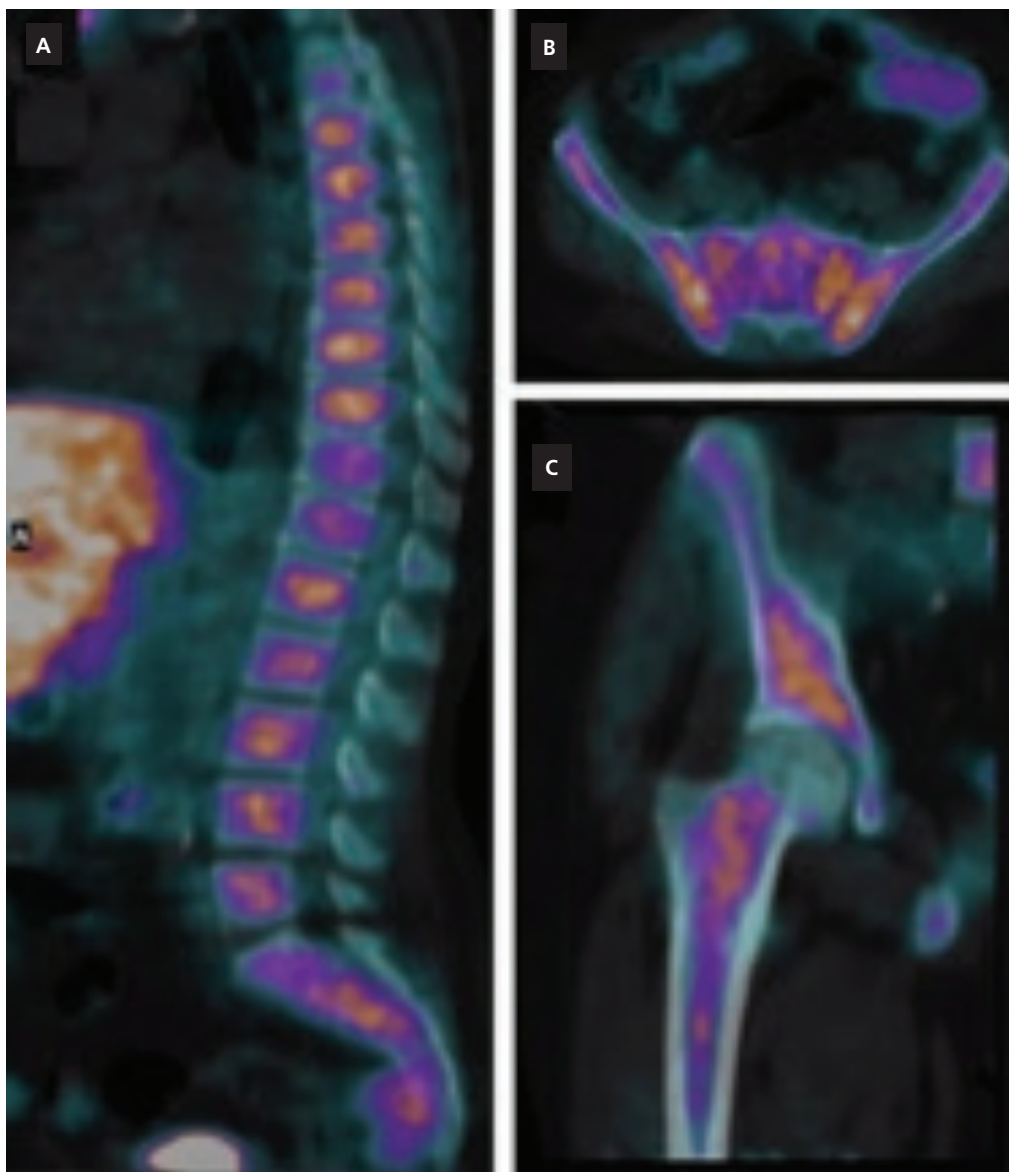


Figure 2. Fused PET/CT well documented tracer incorporation in the endomedullary compartment of the bones, as evident in the sagittal view of vertebrae (**A**), in the axial slice of the pelvic bone (**B**) and in the detailed coronal view of the right femur (**C**). Semiquantitative indices measured in bone marrow, specifically in the pelvic bones, showed significantly increased uptake value (SUV_{max} : 6.2, SUV_{mean} : 4.8) compared with the value reported by Schillaci et al. (1). In a cohort of 80 patients evaluated for assessing the physiological ^{18}F -choline biodistribution (i.e. bone marrow SUV_{mean} : 2.8). Thalassemia intermedia is a rare inherited genetic disease, characterized by a wide spectrum of clinical manifestations (2). Iron overload due to the chronic hemolysis and periodic blood transfusion leads to severe complications, especially at cardiac and hepatic level. Since recent improvements in treatment of thalassemia have led to a significantly prolonged survival, HCC, most probable related to the frequent association of hepatitis C virus-infection and hemochromatosis in thalassemic patients, has emerged as a relatively new complication in long-term survivors (3). Although conventional radiological imaging through CT and magnetic resonance imaging represents the first-line approach for HCC diagnosis, PET/CT with ^{18}F -choline has been introduced as a useful tool for the imaging of HCC, especially before and after loco-regional treatments (4,5). To the best of our knowledge, this is the first report describing the pattern of ^{18}F -choline uptake in a thalassemic patient. It has to be pointed out that diffuse skeletal uptake of ^{18}F -fluciclovine has been recently described in a thalassemic patient affected by prostate cancer with suspicion of bone metastasis (6). Although ^{18}F -fluciclovine and ^{18}F -choline represent different molecular probes in oncology, since the former reflects the upregulation of transmembrane amino-acids transport (7) while the latter is a biomarker of phospholipid synthesis (8), increased uptake of both these 2 tracers in the bone marrow of thalassemic patients are most probably due to hematopoiesis stimulation induced by chronic hemolysis.

Ethics

Informed Consent: This article does not contain any studies with human participants or animals performed by any of the authors.

Peer-review: Externally and internally peer-reviewed.

Financial Disclosure: The author declared that this study received no financial support.

References

1. Schillaci O, Calabria F, Tavolozza M, Ciccio C, Carlini M, Caracciolo CR, Danieli R, Orlacchio A, Simonetti G. ¹⁸F-choline PET/CT physiological distribution and pitfalls in image interpretation: experience in 80 patients with prostate cancer. *Nucl Med Commun* 2010;31:39-45.
2. Aessopos A, Kati M, Farmakis D. Heart disease in thalassemia intermedia: a review of the underlying pathophysiology. *Haematologica* 2007;92:658-665.
3. Mancuso A. Hepatocellular carcinoma in thalassemia: A critical review. *World J Hepatol* 2010;2:171-174.
4. Hartenbach M, Weber S, Albert NL, Hartenbach S, Hirtl A, Zacherl MJ, Paprottka PM, Tiling R, Bartenstein P, Hacker M, Haug AR. Evaluating Treatment Response of Radioembolization in Intermediate-Stage Hepatocellular Carcinoma Patients Using ¹⁸F-Fluoroethylcholine PET/CT. *J Nucl Med* 2015;56:1661-1666.
5. Filippi L, Schillaci O, Bagni O. Recent advances in PET probes for hepatocellular carcinoma characterization. *Expert Rev Med Devices* 2019;16:341-350.
6. Schmitt CR, Schmitt CT, Hinds PR, Sawyer KJ. Use of ¹⁸F-Fluciclovine to Diagnose Recurrent Prostate Carcinoma in a Patient With Beta-Thalassemia. *Clin Nucl Med* 2019;44:544-545.
7. Savir-Baruch B, Zaroni L, Schuster DM. Imaging of Prostate Cancer Using Fluciclovine. *Urol Clin North Am* 2018;45:489-502.
8. Bagni O, Filippi L, Schillaci O. Incidental detection of colorectal cancer via ¹⁸F-choline PET/CT in a patient with recurrent prostate cancer: usefulness of early images. *Clin Nucl Med* 2015;40:328-330.